Title

A PHOTOELECTRON SPECTROSCOPIC STUDY OF BONDING IN INORGANIC AND ORGANOMETALLIC COMPOUNDS

Author

Beach, D.B.

Publication Date

1985-05-01

Lawrence Berkeley Laboratory
UNIVERSITY OF CALIFORNIA

Materials & Molecular Research Division

A PHOTOELECTRON SPECTROSCOPIC STUDY OF BONDING IN INORGANIC AND ORGANOMETALLIC COMPOUNDS

D.B. Beach
(Ph.D. Thesis)

May 1985

Prepared for the U.S. Department of Energy under Contract DE-AC03-76SF00098

DISCLAIMER

A PHOTOELECTRON SPECTROSCOPIC STUDY OF BONDING IN INORGANIC AND ORGANOMETALLIC COMPOUNDS

David Bruce Beach
(Ph.D. Thesis)

Materials and Molecular Research Division
Lawrence Berkeley Laboratory and Department of Chemistry
University of California, Berkeley, California 94720

May 1985

This work was supported by the Director, Office of Energy Research, Office of Basic Energy Sciences, Chemical Sciences Division of the US Department of Energy under Contract Number DE-A003-76SF00098.

A PHOTOELECTRON SPECTROSCOPIC STUDY OF BONDING IN INORGANIC AND ORGANOMETALLIC COMPOUNDS

Table of Contents

List of Tables

List of Figures

Acknowledgement

I would like to thank Professor William Jolly for his guidance and assistance during my time at Berkeley. His enthusiasm, knowlwedge, and dedication served as an example to me through these sometimes puzzling studies.

It is pleasure to acknowledge the contributions of my colleagues to this work. In particular, I wish to thank Dr. Joe Eyermann for many helpful discussions of theoretical inorganic chemistry. I would like to thank Dr. Ken Bomben for instruction in the theory and practice of photoelectron spectroscopy. I would like to thank Dr. Alfred Waterfeld for the synthesis of the compounds studied in Chapter IV, and Dr. Dieter Lentz for providing starting materials and some of the compounds studied in Chapter VII. I would also like to thank Professor Richard Andersen for many helpful discussions, and his careful reading of this thesis.

I am also grateful to the past and present inhabitants of the fifth floor of Latimer Hall, all of whom made graduate school more interesting, and to the members of the famed Dux™ of the Pond softball team, whom I almost managed to their third G. N. Lewis tournament title.

Finally, I would like to thank my parents for their support and patience through these many years of higher education, and my wife, Roxana, for making these last two years the happiest of my life.

This work was supported by the Director, Office of

Energy Research, Office of Basic Energy Sciences, Chemical Sciences Divison of the U.S. Department of Energy under Contract No. DE-A 03-76SF00098.

A PHOTOELECTRON SPECTROSCOPIC STUDY OF BONDING IN INORGANIC AND ORGANOMETALLIC COMPOUNDS

David Bruce Beach

ABSTRACT

The gas-phase X-ray photoelectron spectra of boron trihalides, silyl amines, and thiazyl fluorides were obtained in order to study pi bonding in main-group elements by correcting the valence ionization potentials of these compounds for the effects of charge and electronic relaxation. Using this technique, it was found that the order of pi stabilization in the boron trihalides is $BF_3 > BCl_3 \geq BBr_3 > BI_3$. The nitrogen lone-pair orbitals of trisilylamine and tris(trimethyl)silylamine were found to be approximately 1 eV more stable than a hypothetical nonbonded nitrogen lone pair, thus providing strong experimental evidence for N p pi -> Si d pi bonding. Sulfur d orbital participation was shown to be necessary to rationalize the corrected ionization potentials of NSF and NSF_3. The charge distributions and atomic orbital charater of NSF and NSF_3 obtained from photoelectron spectroscopy provided insight into the observed chemistry of these molecules.

The same technique was used to study sigma and pi interactions in borane adducts of CO and $CNCH_3$, in iron tetracarbonyl olefin complexes, and in transition metal complexes of isocyanides. Borane to carbon monoxide pi bonding was found to be important in BH_3CO, and comparison

of the bonding in BH_3CO and BH_3CNCH_3 suggests that the increase in C-O and C-N bond strength observed when these compounds form borane adducts is due to rehybridization of the sigma orbitals on carbon. The equatorially coordinated ethylene ligand of $Fe(CO)_4C_2H_4$ was found to be a better pi acceptor of electron density from the equatorial metal orbitals than the CO ligand it replaced, but a poorer pi acceptor to the Fe d_{xz}, d_{yz} orbitals, because of the orthogonality of the pi acceptor orbitals of ethylene to these orbitals. By comparing the bonding of $CNCH_3$ to CO in $Fe(CO)_4CNCH_3$, it was shown that $CNCH_3$ is a weaker sigma donor and pi acceptor than CO in this complex, and that filled pi orbital interactions are relatively more important for $CNCH_3$ than for CO.

CHAPTER I. GENERAL INTRODUCTION AND EXPERIMENTAL PROCEDURES

A. General Introduction

This thesis is divided into six main chapters, the first three deal with unusual aspects of bonding in main group inorganic compounds, and the last three are devoted to bonding in organometallic compounds. The unifying theme in this research was the method by which bonding interactions in these compounds were studied. Absolute core binding energies were determined by gas-phase photoelectron spectroscopy and these core binding energies were used to correct valence ionization potentials for the effects of charge and electronic relaxation. The corrected valence ionization potentials convey information on chemical bonding not obtained by either core or valence photoelectron spectroscopy alone.

The first chapter of this thesis is an introduction to the principles of valence and core photoelectron spectroscopy, their interconnection, and the practical aspects of obtaining gas-phase X-ray photoelectron spectra. Chapter II discusses pi interaction between filled halogen "lone pair" orbitals and the vacant boron 2p orbital in the boron trihalides. Chapter III examines pi bonding between the filled nitrogen 2p orbital and the vacant 3d silicon orbitals of silyl amines and alkyl silyl amines. Chapter IV discusses the use of corrected valence ionization potentials to determine the atomic orbital character of the molecular

orbitals of NSF and NSF_3.

The organometallic section of this thesis begins in Chapter V with a study of sigma and pi interactions in the bonding of borane to carbon monoxide, methyl isocyanide, and several other ligands. Chapter VI discusses transition metal-olefin bonding in a series of iron tetracarbonyl-olefin complexes. The final chapter is a study of isocyanides and transition metal-isocyanide complexes.

B. Photoelectron Spectroscopy

Although X-ray photoelectron spectroscopy (XPS) of core electrons and ultraviolet photoelectron spectroscopy (UPS) of valence electrons have developed as separate fields, the underlying principles of both experiments are the same.[1] The fundemental relationship of photoelectron spectroscopy, that energy is conserved in the photoionization process, is an outgrowth of Einstein's explanation of the photoelectric effect in 1905.[2] This relationship is expressed in equation form for gaseous species as:

$$E_B = h\nu - E_{KE}$$

where E_B is the binding energy of the electron being ionized, h is the energy of the ionizing radiation, and E_{KE} is the kinetic energy of the photoelectron. Using monochromatic radiation of known energy, measurement of the kinetic energy of the photoelectrons allows the determination of the binding energy. A photoelectron spectrum consists of a plot of the number of photoelectrons as a function of their kinetic energy, or (as is usually the case) the kinetic

energy may be subtracted from the energy of the ionizing radiation to give a plot of number of photoelectrons versus their binding energy.

As the name implies, UPS uses ultraviolet light produced by an inert gas discharge tube. The majority of the work in the literature has been done with He(I) (21.22 eV) and He(II) (40.81 eV) radiation.[3] Typically, the emitted photoelectrons are sent through an electrostatic analyzer in which an applied electrical field is varied to separated the electrons according to their kinetic energy. The electrons are detected by some form of electron detector, and either counted or converted to a current proportional to the number of electrons. In UPS, the radiation flux from a discharge lamp is sufficiently intense to allow the spectrum to be recorded in a single pass.

The XPS experiment is qualitatively very similar, but with several changes necessitated by experimental difficulties.[4] The relatively low photon flux of X-ray tubes and the lower cross-section for X-ray ionization[3] causes the count rates for XPS to be two to three orders of magnitude less than those in UPS. For this reason, each of the core lines is repetitively scanned, usually under computer control, and the data are summed to give the final spectrum. Also, the resolution of the electrostatic analyzer must be much higher in XPS than in UPS. An analyzer giving a resolution of 20 meV for an electron with a kinetic energy of

10 eV (typical values for UPS), would only be capable of a resolution of 1.6 eV with an electron of kinetic energy 800 eV (typical of XPS).

Photoelectron spectroscopy has been the subject of several books, including those dealing primarily with UPS,[3,5,6] and those dealing primarily with XPS.[7] In addition, review articles have appeared covering specific areas of photoelectron spectroscopy relavent to the material contained in this thesis, including UPS of transition metal[8,9] and transtion metal organometallic compounds,[10] and application of XPS to inorganic compounds.[11]

1. Interpretation of UPS Data

The interpretation of UPS data is generally a two part procedure. First, most UPS spectra of many-atom compounds are complicated by the large number of ionization bands observed, so the first task is the assignment of the bands. The second part of the interpretation process involves evaluating the ionization potentials of a molecule for information about bonding. Before discussing either of these points in detail, it is worthwhile to examine the nature of the ionization process.

When an electron is ejected from a molecule after interaction with a photon, a radical cation is produced in one of possibly many electronic states. A valence ionization potential is therefore the energy of formation of this radical cation:

$$M \xrightarrow{h\nu} M^{+} \cdot$$

In a strict sense, a band of a UPS spectrum should be assigned to the appropriate electronic state of the ion rather than the molecular orbital from which the electron originated, but this approach conveys little useful information to an experimental chemist concerned with the nature of molecular orbtials involved in bonding. For this reason, molecular orbital designations will be used throughout this thesis when discussing ionization potentials. (This approach is essentially a use of Koopmans' theorem[12] which relates ionization potentials to molecular orbitals by stating that ionization potentials are the negative of the self-consistant field (SCF) molecular orbital energies. As will be pointed out later in this chapter, the use of core binding energies to interpret shifts in valence ionization potentials avoids the major reason for the breakdown of Koopmans' theorem: the tendency of electron density to flow to the ionized atom, thus causing the observed ionization potential to be lower than that predicted by Koopmans' theorem.)

i) Assignment of UPS Spectra

The current "standard" method of assignment[8] of UPS spectra is comparison of the observed spectrum to that predicted by some form of molecular orbital calculation. This method has the following drawbacks:

1) With the exception of very small molecules, it is seldom completely reliable.

2) The most accurate calculation method, the ΔSCF method, requires calculation of the eigenvalues of the ground state and ionic states, which requires considerable expenditure of computer time.

3) This procedure reduces UPS to a check of the calculation method, rather than an experimental determination of the electronic structure of a molecule.

To aid in the experimental assignment of UPS bands, several techniques have been developed.[10] These include analysis of line width and vibrational fine structure,[13] use of ionization potential shifts among structurally related compounds,[14] the use of core binding energy data (to be discussed later),[15] and exploitation of the difference in band intensity on going from He(I) to He(II) radiation.[16] Whenever possible, an assignment is most reliably made when based on experimental rather than theoretical grounds.[10]

ii) Valence Ionization Potential Shifts

As far as interpreting the ionization potential data once an assignment has been made, several major problems remain. In some cases, the ionization potetials may be correlated with observed reactivity or a property such as proton affinity,[17] but such correlation is made difficult because ionization potentials are influenced by charge and electronic relaxation energy (the previously mentioned tendency of electron density to flow to the orbital being ionized). A useful method for extracting bonding information from ionization potetials is to study the ionization of

an orbital present in a series of structurally related molecules.[14] This has the advantage of minimizing the effects of electron relaxation, but suffers from the disadvantage that such shifts are often quite small and also reflect changes in charge which may be more significant than changes in bonding. The most reliable method for interpreting valence ionization potentials utilizes core binding energies to correct for changes in charge and electronic relaxation energy, and this method will be discussed in detail in Section C of this chapter.

2. Interpretation of XPS Data

The interpretation of XPS data is generally more straightforward than UPS data because one usually does not have the problem of assignment of the bands. The bands of an XPS spectrum are due to the ionization of atomic core levels which are widely spaced in energy for different elements. Unfortunately, XPS lines tend to be relatively broad, on the order of 1.0 to 2.0 eV fwhm (full width at half-maximum). This is due to the width of the common X-ray sources (0.8 eV fwhm for Mg and 1.0 eV fwhm for Al),[18] and also due to the lifetime of the core ionized state. The widths of XPS lines are sufficiently large that peaks due to atoms of the same element in differing chemical environments often appear as overlapping peaks, which may or may not be deconvolutable into indivdual peaks.

Multiple peaks may also be the result of a final-state

effect.[19] The most common final-state effect is spin-orbit splitting which occurs when an electron is emitted from an orbital with an angular momentum quantum number, l, greater than zero. Coupling of the orbital angular momentum with the electron spin of the final state, either s = 1/2 or s = -1/2, results in two substates, j = l + 1/2 and j = l - 1/2. For example, the 2p line is split into $2p_{1/2}$ and $2p_{3/2}$ lines, and the 4f line is split into $4f_{5/2}$ and $4f_{7/2}$ lines. The degeneracy of the two states, which determines the ratio of their areas, is 2j + 1 (i.e. the area ratio of the $4f_{5/2}$ line to the $4f_{7/2}$ line is 6:8).

Another cause for multiple peaks is shake-up. Shake-up peaks appear as satellite peaks on the high binding energy side of the principal photoelectron peak. Shake-up is caused by the simultaneous ejection of a core electron and the transition of a valence electron to a higher lying bound state. These peaks are often fairly intense, especially in the metal carbonyls of the first transition row elements.[20]

A third type of final state effect which produces multiple lines is multiplet splitting. Multiplet splitting occurs when the the molecule undergoing ionization has unpaired valence electrons. The core ionized final state may couple with the unpaired spins producing multiple lines. All of the compounds studied in this thesis are diamagnetic, so multiplet splitting was not observed.

The interpretation of core binding energy shifts has been the subject of considerable work over the last fifteen

years.[7] Most workers agree that a shift in core binding energy between one compound and another is due to three primary factors:

1) The difference in charge of the atom being ionized.

2) The difference in charge in the other atoms of the molecule.

3) The change in electronic relaxation energy.

These relationships may be expressed in the form of an equation:[21]

$$\Delta E_B = k\Delta Q_A + \Delta V + \Delta E_R$$

Where ΔE_B is the difference in binding energy, k is a constant for the atom being ionized, ΔQ_A is the difference in charge of the atom being ionized, ΔV is the change in potential due to the charges of the other atoms, and ΔE_R is the change in the electronic relaxation energy. The constant, k, is often approximated as $\langle 1/r \rangle$, which may be calculated from the Slater exponent of the valence-shell orbital of the atom being ionized.[22] The potential term, V, is given by the equation:

$$V = \sum_{A \neq B} \frac{Q_B}{r_{AB}}$$

where ΔQ_B are the charge differences in the other atoms of the molecule and r_{AB} is the distance between atom A and atom B. While it is tempting to correlate core binding energy shifts directly with changes in charge on the atom being ionized, there are examples in which potenital effects and

relaxation effects are more significant than the difference in charge.[23]

In order to minimize the effects of electronic relaxation energy and potential, it is generally best, as is also the case in valence spectroscopy, to study a series of structurally related compounds.[24] However, when studying shifts in the binding energy of a small organic molecule coordinated by a metal, a common application of XPS to organometallic chemistry, the effects of potential and relaxation energy differences may make deductions about charge meaningless, even in structurally related compounds. This shortcoming of XPS can be turned to an advantage when binding energies are used to correct valence ionization potentials.

3. Using Core Binding Energies to Interpret Valence Ionization Potentials

In the proceeding sections, it was seen that UPS data are difficult to interpret because of the problem of assignment of the observed bands to molecular orbitals and that an ionization potential alone tells little about the bonding or antibonding character of the orbital that was ionized, and that XPS data are difficult to interpret because core binding energies are affected by factors other than simply the charge on the atom being ionized. The solution to many of the problem besetting the interpretation UPS data, and a new use for XPS data, is to take advantage of the fundamental difference between core and valence spec-

troscopy. Core binding energy data do not contain direct information about chemical bonding, rather only information about charge and electronic relaxation, so that XPS may be used to correct UPS data for the effects of charge and relaxation energy differences.

The first use of combined core and valence spectroscopy to determine the bonding character of a molecular orbital was in 1972 by Hashmall et al.,[25] but it was not until 1981 that the procedure was put on firm practical and theoretical ground by Jolly.[26,27] The approximation made by Jolly which relates shifts in valence ionization potentials to shifts in core binding energies is that "shifts in strictly nonbonding valence orbital ionization potentials are eight-tenths of the corresponding shifts in core binding energy". This approximation has been found to hold on the basis of both theoretical and experimental data. Jolly and Eyermann[28] have determined that a standard deviation of 0.07 is associated with the factor of 0.8. That shifts in nonbonding valence ionization potentials and core binding energies are linearly related is intuitively reasonable when one considers that core orbitals are in fact nonbonding molecular orbitals, so that the theory developed to understand shifts in core levels should apply equally well to nonbonding valence levels.

In order to use Jolly's approximation, it is useful to introduce a "benchmark" for determining the bonding or anti-

bonding character of a molecular orbital. This "benchmark" is called a "localized orbital ionization potential" (LOIP) and is a theoretical nonbonding ionization potential calculated from a nonbonding reference compound and the compound of interest. This calculation is illustrated for the F 2p "lone pair" orbitals of BF_3, a molecule to be considered in detail in Chapter II. The appropriate reference compound is HF, which has a doubly degenerate set of F 2p lone pair orbitals with an ionization potential of 16.06 eV.[29] The F 1s binding energies of HF[30] and BF_3[30] are 694.31 and 694.94 eV, respectively. Eight-tenths of the binding energy difference (E_B(cmpd) - E_B(ref)) is 0.50 eV, and when this correction is applied to the ionization potential of the lone pair orbital of HF, an LOIP of 16.56 eV is obtained.

The significance of this F LOIP of BF_3 is that it corresponds to a hypothetical nonbonding state for the F atoms of BF_3. When this LOIP is compared to the actual F "lone pair" ionization potentials, as is done in the following chapter, the bonding character of each of the molecular orbitals can be determined. If the LOIP is subtracted from the actual ionization potential and a positive difference results, the orbital has bonding character. Conversely, if the difference is negative, the orbital has antibonding character.

The LOIP analysis has been applied to bonding in a variety of inorganic compounds,[27] and the method is also useful in aiding the assignment of valence ionization poten-

tials. For example, Jolly[15] was able to reassign the spectra of the manganese pentacarbonyl halides, $Mn(CO)_5X$, using the hydrogen halides and $Mn(CO)_5H$ as reference compounds. Manganese pentacarbonyl hydride does not have strictly nonbonding orbitals, but it can be used as a reference because the resulting LOIP for the e(Mn) orbitals compares the bonding in $Mn(CO)_5H$ to the bonding in $Mn(CO)_5X$. In this case, it is not possible to have pi type interactions between a hydrogen atom and the e(Mn) orbital of $Mn(CO)_5H$, so that if the LOIP calculated from $Mn(CO)_5H$ for $Mn(CO)_5X$ differs from the actual e(Mn) orbital ionization potential of $Mn(CO)_5X$, the difference is due to a pi interaction between the $Mn(CO)_5$ fragment and the halogen atom. By using the LOIP data and making reasonable assumptions about the nature of pi interactions in $Mn(CO)_5X$, Jolly was able to assign the spectra of $Mn(CO)_5X$.

The use of compounds without strictly nonbonding orbitals as reference compounds is important, because it extends the number of compounds which may be treated using the LOIP approximation. If one were limited to reference compounds with strictly nonbonding lone pair orbitals, only the hydrides of the halogens and chalcogens would be available as references, severely restricting the application of the LOIP approximation. It should be kept in mind that the LOIP calculated when the orbital of the reference compound is not nonbonding corresponds to a hypothetical case were the orbi-

tal in the compound in question has the same bonding character as the reference compound. For example, in the final two chapters of this thesis $Fe(CO)_5$ was used as a reference to study the changes in the metal based orbitals of $Fe(CO)_4L$ (where L is a variety of ligands). The LOIPs of the metal based orbitals calculated from $Fe(CO)_5$ for $Fe(CO)_4L$ represent ionization potentials that the metal based orbitals would have if they had the same bonding character as in $Fe(CO)_5$. If the bonding character of the metal orbitals is changed on going from $Fe(CO)_5$ to $Fe(CO)_4L$, then the change is due to replacing CO by L, and this gives a measure of the donor/acceptor properties of L relative to CO. Using this procedure, it is possible to obtain information on the change in electronic structure of a complex when one ligand is exchanged for another. This information would be useful to a synthetic chemist attempting to change the reactivity of a catalyst, or designing the synthesis of new molecules.

C. Preparation and Handling of Compounds

Essentially all of the compounds studied in this thesis react with oxygen and/or moisture, so that it was necessary to prepare and handle them under inert atmosphere conditions. A general description of the synthesis and handling air-sensitive compounds is given by Shriver.[31]

1. Vacuum Lines

An all-glass preparative high vacuum ($< 10^{-3}$ Torr) line was constructed according to the general design described by Jolly.[32] Mercury manometers were constructed at each end of

a four U-trap fractionation train so that inlet side pressures could be adjusted to allow careful fractionation of volatile mixtures. A pump was connected to the line to pump noncondensable gas. Pressures below 1 Torr were measured with an NRC type 701 thermocouple vacuum gauge. The system was pumped by a high capacity Marvac Model 5BR3 rotary oil pump. Common vacuum line syntheses and manipulations are described by Jolly.[32]

A low vacuum Schlenk type vacuum/inert atmosphere line was constructed for the convienent preparation of organometallic compounds. The construction and use of Schlenk flasks and filter is described by Shriver.[31]

2. Glove Box

Solid transfers, inert atmosphere weighings, and preparation of IR mulls were performed under a nitrogen atmosphere in a Vacuum Atmospheres Company Model HE 43-2 Dri-Lab inert atmosphere glove box equiped with a MO 40-1 Inert Gas Purifier. A 25 watt lamp with a hole in the globe typically burned from 2 weeks to 2 months, indicating that the concentration of oxygen within the box was in the low parts-per-million range.

3. Methods of Characterization

In order to establish the purity of the samples prepared for this study, a variety of analytical techniques were used. One of the more useful criteria of purity is a compound's melting point. The melting points of compounds

with melting points below 20°C were measured by freezing the sample and then allowing it to warm up in an appropriate slush bath in an unsilvered dewar while measuring the temperature. The melting points of compounds with melting points greater than 25°C were measured using a Mel-Temp melting point apparatus. Another reliable indication of the purity of a volatile compound is its vapor pressure. Vapor pressures were measured on the mercury manometer of the vacuum line using a Gaertner cathetometer to measure the height of the mercury column.

Spectroscopic techniques were also used to identify substances and estimate their purity. Infrared spectra were recorded on a Perkin-Elmer 597 Infrared Spectrometer. Proton NMR were obtained on a Varian EM-390 spectrometer.

D. Obtaining X-ray Photoelectron Spectra

This section describes the instrumentation and procedures used to obtain core binding energies of gas phase species.

1. GCA/McPherson ESCA 36 Photoelectron Spectrometer

The instrument used to obtain all of the X-ray photoelectron spectra used in this research was a modified GCA/-McPherson ESCA 36 Photoelectron Spectrometer,[33] shown schematically in Figure I.1. The X-ray source has a water-cooled Mg anode and produces radiation with an energy of 1253.6 eV (Mg K_{α}). (The Mg K_{α} line is actually a spin-orbit split doublet ($K_{\alpha 1,2}$) with a full width at half-maximum of 0.8 eV.) The X-rays pass through an aluminum window (thick-

ness 0.007 mm) on the X-ray tube which blocks electrons from the filament from entering the analyzer. A second window (thickness 0.002 mm) is used on the gas cell to maintain an adequate pressure (10-100 microns) in the gas cell.

Photoelectrons produced in the gas cell pass through a 0.2 mm x 10.0 mm slit into the analyzer. The resolution of the analyzer is adjusted by varying a set of baffles which define the acceptance angle of the analyzer. A narrow setting increases resolution, but cuts down on signal, so that typically the baffle setting is a compromise between resolution and sensitivity. The resolution of the analyzer can be estimated by subtracting the contribution of the source and the natural width of the Ne 1s line from the measured Ne 1s peak width. After careful adjustment, the value obtained for the analyzer's contribution to the observed peak width was only 0.1 eV, indicating a resolution of 0.03%. Baffle adjustment was found to be necessary only after removal of the detector, or cleaning of the analyzer surfaces.

The analyzer itself is a double-focusing hemispherical electrostatic design based on a similar instrument constructed by Siegbahn.[7] The radii of the concentric spheres are 32 cm and 40 cm. A positive potential is applied to the inner sphere and a negative potential 1.25 times that of the inner sphere is applied to the outer sphere. This effectively keeps the center line of the analyzer, radius 36 cm, elec-

trically neutral and prevents electrons from being attracted or repelled by the grounded surfaces at each end of the analyzer. The potentials applied to the spheres are provided by a voltage supply capable of providing voltages in the 10, 100, or 1000 V range, each with an error of less than 0.001%.

The photoelectrons are detected using a single Channeltron (Galileo Electo Optics) electron multiplier operating at 2000 V. The electrons are counted and the count is stored in a Digital Equipment Corporation PDP 8/e minicomputer which also contains the control program for generating sphere voltages and controlling the repetitive scanning of each element. The software supplied by McPherson is described in detail elsewhere.[34]

The entire spectrometer is pumped by a Sargent Welch 3106 DG Turbomolecular pump. Pressure in the analyzer is measured with Granville-Phillips series 270 ionization gauge. The base pressure in the analyzer is 2×10^{-7} Torr and is about $1\text{-}2 \times 10^{-6}$ Torr during data collection. Corrosive vapors are condensed out using an Air Products CSW-202 cryopump.

2. Inlet Systems

Two basic gas inlet systems were used to obtain the spectra in this thesis. An all metal system which could be heated to 200°C to remove adsorbed moisture was used for reactive compounds with high vapor pressures. Flow was regulated using a Whitey 22RS4 micrometer needle valve.

Less volatile compounds were introduced through a large diameter (1.5 cm) inlet system. The sample was held outside the spectrometer in a reservior which could be cooled to regulate the flow of the compound into the spectrometer. To obtain adequate pressures of compounds that do not sublime under high vacuum below 40°C, the entire spectrometer was enclosed in an insulated box and heated. While this prevented material from condensing inside the analyzer, this procedure was not entirely satisfactory. The maximum temperature attained by this procedure was only 75°C, and it required several days for the analyzer to come to thermal equilibrium. Prolonged heating of the spectrometer caused degradation of the Viton seals and of the performance of the detector. To avoid these problems, and to increase the range of temperature to which samples could be heated, a heated gas cell was needed. The design and construction of this heated gas cell is described in Appendix I.

3. Experimental Procedure

Due to the length of time required to obtain a gas-phase X-ray photoelectron spectrum (10 to 24 h), the correction for instrumental drift is critical. Changes in sample pressure, charging on the walls of the spectrometer, and electronic instability all can cause instrumental drift, which shows up as broadening of the peaks and as inaccurate values for the measured binding energies.

To minimize the effects of drift, a microcomputer pro-

gram was developed by A. Bakke called ESCA DRIFT.[35] This program is run on a Commodore 2001 microcomputer interfaced to the PDP 8/e computer which runs the spectrometer. The program collects data over a short period of time (15 to 30 minutes), including a peak due to an inert calibrant gas introduced into the gas cell with the sample. The binding energy of the center of the calibrant peak is determined, and this binding energy is used to adjust the other data collected in the short period for any drift which may have occured. A number of these short scans are summed to give the final spectrum.

The calibration of the peaks that are obtained is done using a program called CALIBRATE.[35] This program uses the Ne 1s line (870.31 eV), the Ne 2s line (48.47 eV), and N_2 N 1s line (409.93 eV) recorded before the start of data collection. The program fits the experimental values and the known values of the binding energies of these lines to a quadratic equation. The intercept of the quadratic line is adjusted to an intercept determined by the binding energy of the inert gas line run with the sample. Using this procedure, the sample is calibrated against the inert gas which was run simultaneously with the sample, and the nonlinearity of the spectrometer is corrected for using the calibrant gases run before the sample.

Once the spectra are obtained, overlapping peaks are deconvoluted using the program CURVY[35] which does an iterative least-squares fit of the spectrum using four parameters

(center, full width at half-maximum, area, Gaussian-Lorentzian line shape mixing ratio) for each peak, and a linear background correction. The program also gives estimates of the standard deviation of each parameter, allows constraints on the parameters during curve fitting, and gives a value of chi-squared as a measure of goodness of fit. Plots of the spectra are done either on a MFE 715 X-Y plotter or Commodore 1520 graphics plotter.

References

(1) Carlson, T. A. "Photoelectron and Auger Spectroscopy"; Plenum Press: New York, 1975.

(2) Einstein, A. Ann. Physik. 1905, 17, 132.

(3) Turner, D. W.; Baker, C.; Baker, A. D.; Brundle, C. R. "Molecular Photoelectron Spectroscopy"; Wiley-Interscience: London, 1970.

(4) Siegbahn, K.; Nordling, C.; Fahlman, A.; Norberg, R.; Hamrin, K.; Hedman, J.; Johansson, G.; Bergmark, T.; Karlsson, S. E.; Lindgren, I.; Lindgren, B. "ESCA: Atomic, Molecular and Solid State Structure by Means of Electron Spectroscopy"; Almqvist and Wiksell: Uppsala, 1967.

(5) Baker, A. D.; Brundle, C. R. "Electron Spectroscopy"; Academic Press: London, 1977.

(6) Eland, J. H. D. "Photoelectron Spectroscopy"; Butterworths: London, 1974.

(7) Siegbahn, K.; Nordling, C.; Johansson, G.; Hedman, J.; Hedan, P.; Hamrin, K.; Gelius, U.; Bergmark, T.; Werme, L.; Manne, R.; Baer, Y. "ESCA: Applied to Free Molecules"; North-Holland, Amsterdam, 1969.

(8) Cowley, A. H. Prog. Inorg. Chem. 1979, 26, 46.

(9) Fenske, R. F. Prog. Inorg. Chem. 1976, 21, 179.

(10) Green, J. C. Structure and Bonding 1981, 43, 37.

(11) Jolly, W. L. Topics in Current Chemistry 1977, 71, 150.

(12) Koopmans, T. Physica 1934, 1, 104.

(13) Rabalis J. W. J. Chem. Phys. 1972, 57, 1185.

(14) Green, J. C.; Jackson, S. E.; Higginson, B. J. Chem. Soc. Dalton 1975, 403.

(15) Jolly, W. L. J. Phys. Chem. 1983, 87, 26.

(16) Higginson, B. R.; Lloyd, D. R.; Connor, J. A.; Hillier, I. H. J. Chem. Soc. Faraday 2 1973, 70, 1418.

(17) DeCock, R. L.; Barbachyn, M. R. J. Am. Chem. Soc. 1979, 102, 2631.

(18) Muilenberg, G. E. "Handbook of X-ray Photoelectron Spectroscopy"; Perkin-Elmer, Eden Prairie, 1978.

(19) Mialki, W. S.; Ph.D. Thesis, Purdue University, 1981.

(20) Bancroft, G. M.; Boyd, D. B.; Creber, D. K. Inorg. Chem. 1978, 17, 1008.

(21) Jolly, W. L.; Bakke, A. A. in "Electron Distributions and the Chemical Bond"; Coppens, P., Hall, M., Eds.; Plenum Press, New York, 1982.

(22) Schwartz, M. E. Chem. Phys. Lett. 1970, 6, 631.

(23) Beach, D. B.; Jolly, W. L. Inorg. Chem. 1983, 22, 2137.

(24) Xiang, S. F.; Bakke, A. A.; Chen, H.; Eyermann, C. J.; Hoskins, J. L.; Lee, T. H.; Seyferth, D.; Withers, H. P.; Jolly, W. L. Organometallics 1982, 1, 699.

(25) Hashmall, J. A.; Mills, B. E.; Shirley, D. A.; Streitwieser, A. J. Am. Chem. Soc. 1972, 94, 4445.

(26) Jolly, W. L. J. Phys. Chem. 1981, 85, 3792.

(27) Jolly, W. L. Accts. Chem. Res. 1983, 16, 370.

(28) Jolly, W. L.; Eyermann, C. J. J. Phys. Chem. 1982, 86, 4834.

(29) Frost, D. C.; McDowell, C. A.; Vroom, D. A. J. Chem. Phys. 1967, 46, 4255.

(30) Jolly, W. L.; Bomben, K. D.; Eyermann, C. J. Atomic Data and Nuclear Data Tables 1984, 31, 433.

(31) Shriver, D. F.; "Manipulation of Air-Sensitive Compounds"; McGraw-Hill, New York, 1969.

(32) Jolly, W. L.; "Synthesis and Characterization of Inorganic Compounds"; Prentice-Hall Inc., Englewood Cliffs, NJ, 1970.

(33) "ESCA 36 Instruction Manual"; GCA Corporation, Acton, MA, 1974.

(34) "ESCA 36 Software System Description"; GCA Corporation, Acton, MA, 1974.

(35) Bakke, A. A.; Ph.D. Thesis, University of California, 1985.

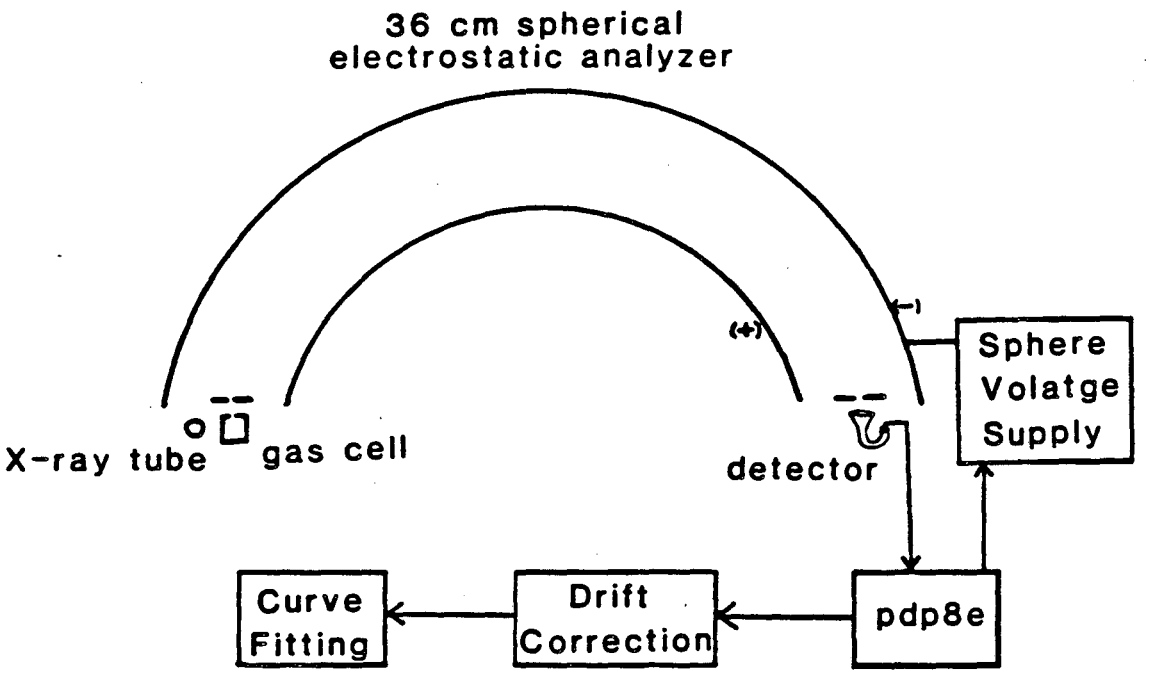

Figure 1.1. Schematic diagram of a McPherson ESCA-36 photoelectron spectrometer.

CHAPTER II. PI BONDING IN THE BORON TRIHALIDES

A. Introduction

The formation of dative pi bonds in the boron trihalides between the vacant p orbital of boron and the filled p orbitals of the halogen atoms has often been invoked[1] to explain the observed trends in bonding and reactivity. For example, the B-Cl and B-F distances in the respective trihalides are considerably shorter (0.2 A) than would be predicted by estimates based on covalent radii, indicating partial multiple bond character in these compounds. More significantly, the Lewis acidities of the boron trihalides are in the order $BBr_3 \geq BCl_3 >> BF_3$,[2] an ordering opposite to that predicted on the basis of electronegativity and steric considerations.

To rationalize the observed Lewis acidity trend, most workers[3-5] have suggested that the energy required to convert the planar boron trihalide to a pyramidal configuration determines the acceptor strength of the trihalide. That is, the weakest acceptor, BF_3, has the highest barrier to reorganization. Experimental evidence for this includes out-of-plane bending force constant measurements[3] which have shown that BCl_3 is more easily distorted than BF_3, and structural studies of BF_3 and BCl_3 adducts of acetonitrile[5] indicate a greater distortion of the boron trihalide fragment in the BCl_3 adduct than in the BF_3 adduct. Semiempirical molecular orbital calculations[5-7] have indicated that origin of the differences in planar-pyramidal reorganization barrier among

the boron trihalides is differences in internal pi bonding, with the order of increasing internal pi bonding interaction being $BF_3 > BCl_3 > BBr_3 > BI_3$. Halogen to boron pi bonding would also reduce the Lewis acidity of the boron trihalides by making it more difficult to transfer electron density to the boron atom when forming an adduct.

Perhaps the most direct experimental measurement of the degree of pi interaction in the boron trihalides is the ionization potentials of the halogen donor orbitals involved in bonding. As discussed in the previous chapter, UPS data alone do not allow direct determination of the degree of bonding interaction, because shifts in valence ionization potentials are due to differences in charge and electronic relaxation energy. Valence ionization potentials are best interpreted after appropriate corrections have been made based on XPS data. The only previous XPS study was done by Allison et al.[8] in 1972, with absolute uncertainties of the core binding energies on the order of $\pm$0.1-0.2 eV. In order to confidently examine the subject of pi bonding in the boron trihalides, it was necessary to redetermine the core binding energies.

B. Experimental

1. Preparation of Compounds

All of the compounds used in this study were obtained commercially. Boron trifluoride and boron trichloride (Matheson) were used without further purification. Boron tri-

bromide (Alfa, stated purity 99.99%) was distilled into a -111°C (CS_2 slush) trap to remove traces of HBr and then into a stainless steel cylinder for storage. Bassett and Lloyd,[9] in their UPS study of the boron trihalides, stated that the vapor of several commercial samples of BBr_3, even those of high stated purity, were contaminated with large amounts (30%) of BBr_2Cl. This was checked using ESCA by scanning the region of 211 to 205 eV for a peak characteristic of a Cl 2p signal. To our limit of detection (in this case, < 1%), no Cl was detected in the sample of BBr_3. Boron triiodide (Columbia Organics) was grossly contaminated with I_2, and was purified by repeated vacuum sublimation until a colorless compound was obtained. The melting point of the sublimed BI_3 was 49°C (lit.[10] 49.9°C).

2. Procedure for Obtaining Spectra

Spectra were obtained by the general method descibed in Chapter I, but with modifications due to the high reactivity of all of the boron trihalides. The boron trihalides, with the exception BF_3, are readily hydrolyzed to form hydrogen halides. To minimize hydrolysis, the inlet systems were heated to 200°C under high vacuum. In addition, the valves leading into the gas cell were closed and the sample valve was opened to allow the gas, at its room temperature vapor pressure, to react with the walls of the inlet system. After several minutes, the gas trapped in the inlet system was pumped off through the rough vacuum system.

Boron trifluoride, trichloride, and tribromide were

connected to the all-metal gas inlet system of the spectrometer, and their flow into the gas cell was controlled with a grease-free micrometer-type needle valve. Boron triiodide does not have sufficent vapor pressure to allow the use of this procedure and was introduced into the spectrometer from a sample reservior through large diameter (>1.5 cm) glass and metal tubing. An appropriate vapor pressure in the gas cell was achieved by holding the sample chamber at -20°C.

Although the presence of hydrogen halide does not affect the boron signal, the peak or peaks due to the halogen atoms of the boron trihalide will be broadened and shifted to higher binding energy. Therefore, the halogen spectra were collected only after boron signals were observed. As a further check, the integrated intensities of the boron and halogen peaks, after correction for differing counting times, were compared with atomic sensitivity factors in the literature.[11] In all cases, reasonable agreement was obtained, thus ruling out gross contamination by hydrogen halide, but not ruling out some uncertainty in the halogen peak position due to hydrogen halide.

C. Results and Discussion

1. Core Binding Energies

The experimental data collected in this study are presented in Table II.1, along with the data of Allison et al.[8] for comparison. The average absolute deviation from the values reported by Allison et al., when such a comparison is

possible, is 0.13 eV.

In the case of BBr_3, we were unable to obtain a satisfactory B 1s spectrum, because the peak due to boron appears only as a shoulder on the high binding side of the Br $3p_{1/2}$ peak. Atomic sensitivity factors[12], the area ratio of the Br $3d_{5/2}$ to the Br $3p_{3/2}$ peaks, and the statistical 2:1 area ratio for the Br $3p_{3/2}$:$3p_{1/2}$ peaks can be used to estimate that the area ratio for the B 1s peak to the Br $3p_{1/2}$ should be 1:8. This area ratio, the width of Br $3p_{1/2}$ peak, and the closeness of the peaks (~2 eV) did not allow us to ascertain the B 1s peak positions to better than $\pm$0.3 eV. The value we obtained was 198.8 eV, in fair agreement with the value 199.0 eV reported by Allison et al., although we are at a loss to explain there observation that the peaks were "well resolved".

The B 1s spectrum of BCl_3 was complicated by the overlap of the α_3 and α_4 satellite lines[12] of the Cl 2p peaks. The α_3 satellite occurs at 8.4 eV lower binding energy with an intensity 8% of the parent peak, while the α_4 satellite occurs at 10.2 eV lower binding energy with an intensity 4.1% of the parent peak. The B 1s spectrum is shown in Figure 2.1. While it was necessary to include peaks at 198.9 and 197.1 eV in order to obtain a proper fit to the data, the B 1s peak is the most intense peak in the spectrum.

The Cl 2p band of BCl_3 and the Br 3d band of BBr_3 were deconvoluted into their spin-orbit components by using area

ratios of 2:1 and 3:2, respectively. The uncertainties (2) given in Table II.1 represent the uncertainties associated with the least-squares fit, which are sensitive to the parameters chosen for the fit. Although we believe the absolute uncertainties of our binding energies in Table II.1 to be less than $\pm$0.05 eV, we feel a more reasonable value for the uncertainty of the the Cl $2p_{3/2}$ and Br $3d_{5/2}$ binding energies is $\pm$0.1 eV.

2. Localized Orbital Ionization Potentials

The calculation of localized orbital ionization potentials (LOIP) is discussed in detail in the first chapter. The appropriate reference compounds for the lone-pair orbitals of the halogen atoms of the boron trihalides are the corresponding hydrogen halides. The core binding energies and valence ionization potentials of the hydrogen halides, along with the calculated LOIP values are given in Table II.2.

3. Halogen Lone Pair Ionization Potentials

The p "lone pair" orbitals of the halogen atoms of the boron trihalides with their symmetry designations are shown in Figure 2.2. The halogen lone-pair orbital ionization potentials reported by Bassett and Lloyd[9] are shown in Table II.3. On the basis of our LOIP calculations, we have interchanged their assignments of the e' and e'' bands of BBr_3 and BI_3. If we use the original assignment for these orbitals, we get the unreasonable result that the e'' orbital

has significant bonding character. If we interchange the assignments, we get the more reasonable result that the orbital is essentially nonbonding, as it is in BF_3 and BCl_3.

Further justification for this interchange of assignments comes from the ionization potentials of the a_2' and e' orbitals. The a_2' and e' molecular orbitals are combinations of the three halogen valence p orbitals that lie in the plane of the molecule. The a_2' and e' orbitals have slight antibonding and bonding character, respectively, but the degeneracy-weighted-average of the ionization potentials of these orbitals should correspond to the ionization potential of a strictly nonbonding valence orbital, provided that these orbitals are not stabilized by interaction with higher lying vacant molecular orbitals or destabilized by interaction with lower lying filled molecular orbitals. As shown in Table II.2, the averages are in good agreement with the LOIP values, indicating negligible interaction with other orbitals and supporting our reassignment of the e' and e'' ionization potentials of BBr_3 and BI_3.

4. Pi Bonding

The final ionization potential to consider is that of the a_2'' orbital. This orbital is of the proper symmetry to interact with the vacant 2p orbital of boron, resulting in internal pi bonding. Table II.3 gives the stabilization of this orbital relative to a nonbonding standard calculated by subtracting the LOIP from the a_2 ionization potential. The data show that there is strong pi bonding in all of the

boron trihalides, and that the order is $BF_3 > BCl_3 \geq BBr_3 > BI_3$.

In their UPS study of the boron trihalides, Basset and Lloyd[9] assumed that the difference between the e'' and a_2'' ionization potentials was a measure of pi bonding. Our results show that this assumption was well justified, but because of their misassignment of the e' and e'' ionizations of BBr_3 and BI_3, they obtained pi stabilization values for BBr_3 and BI_3 which were significantly low. The assignment which we were able to obtain through the use of the LOIP values also clarifies another anomaly in Basset and Lloyd's study in which they found that the a_2' - e'' separation was 0.73 eV for BF_3, 0.66 eV for BCl_3, 1.06 eV for BBr_3, and 1.06 eV for BI_3. This separation is a measure of halogen-halogen interaction (the e'' ionization potential is an approximately nonbonding reference and the a_2' orbital is destabilized by repulsive interaction with the e' orbital) and would be expected to decrease with the larger halides. Basset and Lloyd explained their anomalous result for BBr_3 and BI_3 in terms of increased pi charge transfer in these compounds. When the assignments used in this study are used to calculate the separartion, the following results are obtained: BF_3 0.73 eV, BCl_3 0.66 eV, BBr_3 0.71 eV, and BI_3 0.65 eV. These results show that the separation is essentially constant and that it is not necessary to invoke an unlikely explanation which would have the largest pi charge transfer in the molecules with the smallest pi stabilization

energies.

Summary

The results of this study have given direct experimental evidence that the trend in pi bonding in the boron trihalides is $BF_3 > BCl_3 \geq BBr_3 > BI_3$. The core binding energies made it possible to reassign and reinterpret the valence ionizations potentials of these compounds based on experimental data.

References

(1) Brown, H. C.; Holmes, R. R. J. Am. Chem. Soc 1956, 78, 2173.

(2) "Advanced Inorganic Chemistry"; Cotton, F. A., Wilkinson, G. A.; 2nd edn., Interscience: New York and London, 1966; p 266-270.

(3) Cotton, F. A.; Leto, J. R. J. Chem. Phys. 1959, 30, 993.

(4) Brown, D. G.; Drago, R. S.; Bolles, T. F. J. Am. Chem. Soc. 1968, 90, 5706.

(5) Swanson, B.; Shriver, D. F.; Ibers, J. A. Inorg. Chem. 1969, 8, 2182.

(6) Armstrong, D. R.; Perkins, P. G. Theor. Chim. Acta, 1969, 15, 413.

(7) Lappert, M. F.; Litzow, M. R.; Pedley, J. B.; Riley, P. N. K.; Tweedale, A. J. Chem. Soc. (A) 1968, 3105.

(8) Allison, D. A.; Johansson, G.; Allan, C. J.; Gelius, U.; Sieghbahn, H.; Allison, J.; Sieghban, K. J. Electron Spectrosc. Relat. Phenom. 1972, 1, 269.

(9) Basset, P. J.; Lloyd, D. R. J. Chem. Soc. (A) 1971, 1551.

(10) "CRC Handbook of Chemistry and Physics"; Weast, R. C., Ed.; CRC Press: Boca Raton, FL, 1976; p B-96.

(11) "Handbook of X-ray Photoelectron Spectroscopy"; Riggs, W. M., Wagner, C. D., Davis, L. E., Moulder, J. F., Muilenberg, G. E., Eds.; Perkin-Elmer Corp., 1978; p 188.

Table II.1. Core Binding Energies (eV) of the Boron Trihalides

(This work)

	B 1s		halogen core	
	E_B	fwhm[a]	E_B	fwhm
BF_3	202.85(3)	1.47(9)	694.94(2)[b]	1.61(4)
BCl_3	199.98(6)	1.71(20)	206.84(3)[c]	1.34(6)
BBr_3	198.8(3)[d]		76.57(3)[e]	1.48(8)
BI_3	197.92(5)	1.21(18)	626.82(2)[f]	1.32(7)

(Allison et al.)[g]

BF_3	202.8	694.8[b]
BCl_3	199.8	207.0[c]
BBr_3	199.0	77.0[h]
BI_3	197.8	193.9[i]

[a]Full width at half-maximum. [b]F 1s. [c]Cl $2p_{3/2}$. [d]See text. [e]Br $3d_{5/2}$. [f]I $3d_{5/2}$. [g]Ref. 8. [h]Br 3d. [i]I $4p_{3/2}$.

Table II.2 Core Binding Energies (eV) and Valence Ionization Potentials (eV) of the Hydrogen Halides, and Calculated Localized Orbital Ionization Potentials (LOIPs, eV) for the Boron Trihalides

	E_B[a]	IP[b]
HF	694.31[c]	16.06
HCl	207.39[d]	12.78
HBr	77.36[e]	11.82
HI	627.56[f]	10.64

	LOIP[g]
BF_3	16.56
BCl_3	12.34
BBr_3	11.19
BI_3	10.05

[a] Core binding energies are from Jolly, W. L.; Bomben, K. D; Eyermann, C. J. Atomic Data and Nuclear Data Tables 1984, 31, 433. [b] Frost, D. C.; McDowell, C. A.; Vroom, D. A. J. Chem. Phys. 1967, 46, 4255. [c] F 1s. [d] Cl $2p_{3/2}$. [e] Br $3d_{5/2}$. [f] I $3d_{5/2}$. [g] Calculated using data in Table II.1

Table II.3. Valence Ionization Potential Data (eV) for the Boron Trihalides

	LOIP	IP[a] a_2	IP[a] e'	IP[a] e''	IP[a] a_2''	MWA[b] (a_2 & e')	a_2'' - LOIP
BF_3	16.56	15.95	17.14	16.67	19.13	16.74	2.57
BCl_3	12.34	11.73	12.66	12.39	14.42	12.35	2.08
BBr_3	11.19	10.65	11.71	11.36	13.18	11.36	1.99
BI_3	10.05	9.36	10.42	10.01	11.74	10.06	1.69

[a] Ref. 9. [b] Multiplicity-weighted average.

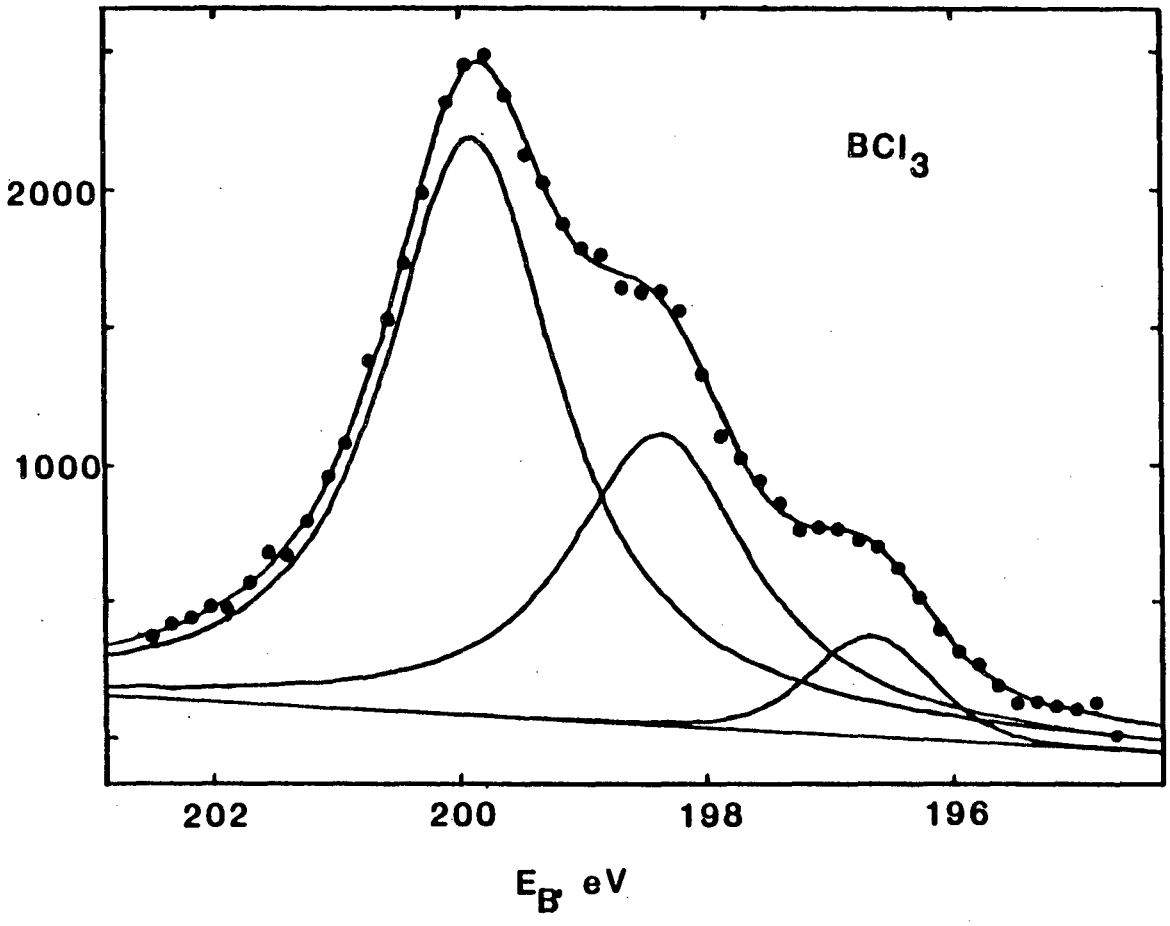

Figure 2.1. Boron 1s spectrum of boron trichloride. The peaks at lower binding energy are the satellite peaks of the Cl 2p peak.

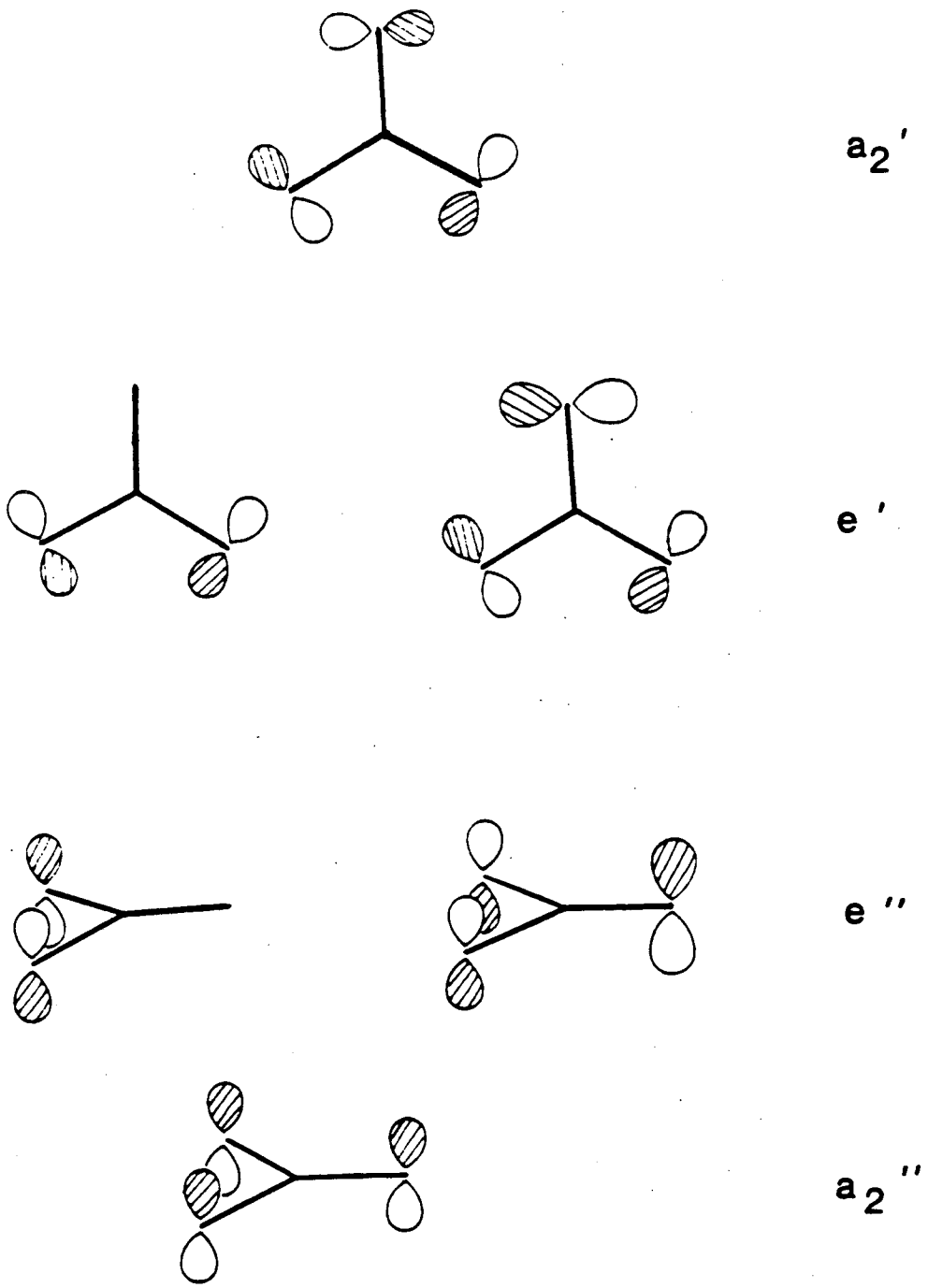

Figure 2.2. Halogen lone-pair orbitals of the boron trihalides.

CHAPTER III. PI BONDING IN TRISILYLAMINE AND RELATED COMPOUNDS

A. Introduction

The use of d orbitals by main group elements has long been debated by inorganic chemists.[1] One of the "textbook"[2-4] examples often cited as providing evidence of d orbital bonding by a main group element is the geometry of the heavy atoms of trisilylamine. On the basis of valence shell electron pair repulsion (VSEPR) theory, a pyramidal structure similar to NH_3 and $N(CH_3)_3$ would have been predicted; however, trisilylamine has been found to be planar.[5] The anomalous planar geometry of trisilylamine and its weak Lewis basicity have usually been interpreted in terms of $N(p\pi)\text{->}Si(d\pi)$ bonding.[6] A planar geometry provides the best overlap of the lone-pair p orbital of the N atom with the vacant d orbitals on the Si atoms. Removal of electron density from the nitrogen atom by the silicon atoms decreases the basicity of the nitrogen atom.

Alternate explanations for the planarity of trisilylamine have been proposed by Noodleman and Paddock[7] and by Glidewell.[8] Noodleman and Paddock concluded, on the basis of $X\alpha$ scattered wave self consistent field molecular orbital calculations, that while d orbital interactions are significant in $N(SiH_3)_3$, repulsion of the positively charged SiH_3 groups is responsible for the planarity of $N(SiH_3)_3$. Glidewell also suggests that repulsion of nonbonded silyl groups was resposible for determining the geometry of trisilyl-

amine, because a pyramidal geometry would lead to significant steric crowding. Glidewell further suggests that steric crowding caused by going from a trigonal planar geometry to a tetrahedral geometry is the reason for the weak Lewis acidity of trisilylamine.

In order to determine the stabilization energy of the N lone pair of trisilylamine, we undertook a photoelectron spectroscopic study of trisilylamine, and structurally related tris(trimethylsilyl)amine. The low resolution UPS spectrum of trisilylamine was recorded by Cradock et al.[9] in 1972. Fortunately, the band corresponding to the ionization of the lone pair is separated by several eV from the other bands of the spectrum and is readily assigned. The UPS spectrum of tris(trimethylsilyl)amine has also been reported.[10]

In order to use the LOIP method to study the stabilization of the N atom p orbital, it is desirable to have a N containing compound with a strictly nonbonding lone pair; however, no such compound exists. Eyermann and Jolly[11] have calculated the valence ionization potential shift and binding energy shift on going from pyramidal to planar ammonia using an extended basis set SCF calculation, and the values calculated for planar ammonia can be used to determine the orbital interaction in trisilylamine.

B. Experimental

1. Preparation of Compounds

Trisilylamine was prepared by the reaction of SiH_3Br and NH_3:[12]

$$3\ SiH_3Br + 4\ NH_3 \longrightarrow N(SiH_3)_3 + 3\ NH_4Br$$

Bromosilane was prepared on the vacuum line by the reaction of HBr (Matheson) and phenylsilane (Petrarch). The low temperature distillation apparatus described by Ward[13] was used to remove traces of HBr from the semi-pure bromosilane. The vapor pressure of the purified bromosilane was 707 mm at 0 °C (lit. 710 mm).[13] Ammonia (Matheson) was dried over sodium prior to use. The vapor pressure of the trisilylamine used in this study was 109 mm at 0 °C (lit. 109 mm).[12] (Note: On two occasions, the residue from the fractionation of the crude bromosilane exploded violently on being exposed to the atmosphere, even though the traps containing the residue had been filled with argon before allowing them to warm to room temperature. On other occasions, the residue inflamed without explosion. Ward[13] describes bromosilane as being spontaneously flammable, but it would appear that certain air/bromosilane mixtures are also explosive.)

Tris(trimethylsilyl)amine was obtained commercially (Petrarch) and was sublimed before use. The melting point of the sublimed material was 70 °C (lit. 70-71 °C).[14]

2. Obtaining X-ray Photoelectron Spectra

The flow of trisilylamine into the spectrometer was regulated with a needle valve. Tris(trimethylsilyl)amine was not sufficiently volatile to flow through the needle valve and was introduced into the spectrometer through a

large-diameter (1.5 cm) inlet system from a reservoir held at -20°C.

C. Results and Discussion

1. Core Binding Energies

The core binding energies of trisilylamine and tris-(trimethylsilyl)amine are tabulated in Table III.1. The N 1s peak of both compounds overlapped with a small peak at 401.5 eV which was due to the α_3 satellite line of the N_2 calibrant gas, but it was possible to deconvolute the two bands to obtain accurate N 1s binding energies.

2. Pi Bonding in Trisilylamine

Using planar ammonia as a nonbonding reference, LOIP values can be calculated for trisilylamine and related nitrogen containing compounds. The calculated LOIP values and experimental ionization potentials are given in Table III.2.

It can be seen that the N lone-pair orbital of trisilylamine is 1 eV more stable than a hypothetical nonbonding N lone pair orbital, while the lone pair orbital of trimethylamine is 0.9 eV less stable than a strictly nonbonding N lone pair. The destabilization of the lone pair of trimethylamine is due to a repulsive interaction between the C-H bonding orbitals and the N lone pair. The same destabilizing interaction between Si-H bonding orbitals and the N lone pair should also exist in trisilylamine. The net stabilization of the lone pair indicates significant interaction of higher lying empty orbitals of trisilylamine with

the N lone-pair orbital. Similar calculations for tris(trimethylsilyl)amine and bis(trimethylsilyl)amine show that the N lone-pair orbitals in these molecules are stabilized by 0.9 and 0.5 eV, respectively.

3. Pi Bonding in Disilylether

A compound in which one might expect to have pi interactions similar to silylamine is disilylether. The oxygen atom has a lone-pair orbital which may repulsively interact with Si-H bonding orbitals or may be stabilized by donating electron density in a pi interaction to vacant Si orbitals. The appropriate nonbonding reference compound for the LOIP analysis is water. The O 1s binding energies, LOIP values, lone-pair ionization potentials, and the lone-pair stabilization energies of H_2O, $(CH_3)_2O$, and $(SiH_3)_2O$ are given in Table III.3.

It can be seen that both dimethylether and disilylether have negative lone-pair stabilization energies, indicating a repulsive interaction between the O lone pair and the MH_3 orbital with the same b_1 symmetry. If the lone-pair orbital is destabilized by interaction with the b_1 MH_3 orbital, then the b_1 MH_3 orbital should be stabilized. It is possible to use the t_2 ionization potentials of CH_4 and SiH_4 to calculate reference ionization potentials corresponding to a noninteracting MH_3 group. These hypothetical noninteracting valence ionization potentials are actually LOIPs which are not based on nonbonding references, but they are useful in comparing the bonding character of an orbital present in two

compounds. In this case, C-H bonding orbitals of CH_4 and the Si-H bonding orbitals of SiH_4 are compared with the experimental b_1 MH_3 ionization potentials in $(CH_3)_2O$ and $(SiH_3)_2O$ to determine the stabilization of b_1 MH_3 orbitals.

Unlike trisilylamine and trimethylamine, the UPS spectra of dimethylether and trisilylether[15,16] were recorded under high resolution conditions, but unfortunately there is no consensus on the assignment of the b_1 MH_3 ionization potential in either compound. The calculated LOIP for the b_1 CH_3 orbital of $(CH_3)_2O$ is 15.4 eV, and it is likely that the band corresponding to the ionization of this orbital lies in a peak at 16.2 eV, indicating a stabilization of 0.8 eV. The calculated LOIP for the b_1 SiH_3 orbital of $(SiH_3)_2O$ is 13.2 eV. This band probably lies in a peak at 14.5 eV, indicating a stabilization of 1.3 eV. The greater stabilization of the b_1 MH_3 orbital of $(SiH_3)_2O$ relative to $(CH_3)_2O$ is reasonable because the b_1 SiH_3 orbital of $(SiH_3)_2O$ is closer in energy to the O lone-pair orbital than is the CH_3 b_1 orbital of $(CH_3)_2O$. The small net destabilization of the O lone pair in disilylether indicates that stabilizing interaction of higher-lying empty Si orbitals is less than the destabilizing repulsion of the b_1 SiH_3 orbital.

In comparing the lone-pair stabilization energies of $(SiH_3)_2O$ and $(SiH_3)_3N$ it is important to point out that both Si-H bonding orbital repulsion and pi bonding would be expected to cause the lone-pair stabilization energy of

$(SiH_3)_3N$ to be greater than $(SiH_3)_2O$. The nitrogen lone-pair orbital lies higher in energy than does the oxygen lone-pair orbital, thus decreasing the repulsion of the Si-H bonding orbitals with the lone-pair orbital, and increasing the overlap with the vacant Si based acceptor orbitals which are high lying in energy.

4. Silicon d Orbital Participation

Silylamine, tris(trimethylsilyl)amine, bis(trimethylsilyl)amine, and probably disilylether all have lone-pair orbitals which are stabilized by pi bonding to higher lying empty Si based orbitals. The traditional opinion, to which we are inclined, is that the empty $d\pi$ orbitals of the silicon atoms interact with the $p\pi$ lone-pair orbital. However, it has been suggested[17] that the lone-pair stabilization in compounds of the type R_2N-SiX_3 and $RO-SiX_3$ is due to the interaction of the lone-pair with the σ^* orbitals of the Si-X bonds. It is argued that the polarity of the Si-X bond causes the σ^* orbital to have considerable Si p orbital character which overlaps with lone-pair orbital. However, in the case of Si-H and Si-C bonds, as in trisilylamine and tris(trimethylsilyl)amine, the small Pauling electronegativity differences between silicon and hydrogen ($\Delta\chi = 0.3$) and silicon and carbon ($\Delta\chi = 0.7$) would suggest that the and σ^* orbitals would have similar p orbital character, making this argument less plausible. We therefore conclude that Si d orbitals are responsible for pi bonding in these compounds.

Summary

The LOIP method has been used to determine that the lone-pair orbital stabilization energies of trisilylamine and tris(trimethylsilyl)amine are 1.0 an 0.9 eV, respectively. It is our conclusion that that d orbitals on Si are responsible for these lone-pair orbital stabilizations.

References

(1) Brill, T. B. J. Chem. Ed. 1973, 50, 393.

(2) Jolly, W. L.; "Modern Inorganic Chemistry"; McGraw-Hill: New York, 1984; p 128-129.

(3) Huheey, J. "Inorganic Chemistry"; 2nd edn., Harper & Row: New York, 1978; p 712-713.

(4) Purcell, K. F.; Kotz, J. C. "Inorganic Chemistry"; Saunders: Philadelphia, 1977.

(5) Hedberg, K. J. Am. Chem. Soc. 1955, 77, 4631.

(6) Burg, A. B.; Kulijian, E. S. J. Am. Chem. Soc. 1950, 72, 3103.

(7) Noodleman, L.; Paddock, N. L. Inorg. Chem. 1979, 18, 354.

(8) Glidewell, C. Inorg. Chim. Acta 1975, 12, 219.

(9) Cradock, S.; Ebsworth, E. A. V.; Savage, W. J.; Whiteford, R. A. J. Chem. Soc. Faraday Trans. 2 1972, 68, 934.

(10) Starzewski, K. A.; tom Dieck, H.; Bock, H. J. Organomet. Chem. 1974, 65, 311.

(11) Eyermann, C. J.; Jolly, W. L. J. Phys. Chem. 1982, 87, 3080.

(12) Ward, G. L. Inorg. Syn. 1968 11, 168.

(13) Ward, G. L. Ibid. 1968, 11, 159.

(14) "Silicon Compounds Register and Review", Petrarch Systems: Bristol, PA, 1982; p 122.

(15) Cradock, S.; Whiteford, R. A J. Chem. Soc. Faraday Trans. 2 1972, 68, 281.

(16) Bock, H.; Mollere, P.; Becker, G.; Fritz, G. J. Organomet. Chem. 1973, 61, 113.

(17) Pitt, C. G. Ibid. 1973, 61, 49.

Table III.1. Core Binding Energies (eV) of Trisilylamine and Tris(trimethylsilyl)amine

	N 1s		Si 2p		C 1s	
	E_B	fwhm[a]	E_B	fwhm	E_B	fwhm
$N(SiH_3)_3$	403.91(2)[b]	1.33(9)	107.47(3)	1.63(7)		
$N[Si(CH_3)_3]_3$	402.72(2)	1.47(9)	106.35(3)	1.66(8)	289.60(3)	1.61(9)

[a] Full width at half-maximum. [b] Uncertainty indicated parenthetically.

Table III.2. Calculated LOIPs and Experimental Ionization Potentials (eV) of Amines and Silylamines

	LOIP	IP	Lone-Pair Stabilization Energy (IP - LOIP)
planar NH_3[a]	9.8	(9.8)	0.0
$N(CH_3)_3$	9.4[b]	8.54[c]	-0.9
$N(SiH_3)_3$	8.7	9.7[d]	1.0
$N[Si(CH_3)_3]_3$	7.7	8.60[e]	0.9
$NH[Si(CH_3)_3]_2$	8.2[b]	8.66[e]	0.5

[a] Reference 11. [b] Calculated using binding energy data from: Jolly, W. L; Bomben, K. D.; Eyermann, C. J. At. Data Nuc. Data. Tables 1984, 31, 433. [c] Elbel, S.; Bergmann, H.; Ensslin, W. J. Chem. Soc. Faraday Trans. 2 1974, 70, 555. [d] Reference 9. [e] Reference 10.

Table III.3. Lone-Pair Stabilization Energies (eV) of Disilylether and Related Compounds

	E_B, O 1s	LOIP	IP	Lone-Pair Stabilization Energy (IP - LOIP)
H_2O	539.90	(12.62)[a]	12.62[b]	0.0
$(CH_3)_2O$	538.6	11.6	10.0[c]	-1.6
$(SiH_3)_2O$	538.60	11.58	11.17[c]	-0.4

[a] Calculated using binding energy data from: Jolly, W. L.; Bomben, K. D.; Eyermann, C. J. At. Data Nuc. Data Tables 1984, 31, 433. [b] Rosenstock, H. M.; Sims, D.; Schroyer, S. S.; Webb, W. J. Natl. Stand. Ref. Data Ser. (U. S. Natl. Bur. Stand.) 1980, NSRDS-NBS 66, part 1. [c] Reference 15.

CHAPTER IV. X-RAY PHOTOELECTRON SPECTROSCOPIC STUDY OF THIAZYL FLUORIDE AND THIAZYL TRIFLUORIDE

A. Introduction

The chemistry of sulfur-nitrogen-fluorine compounds has been the subject of considerable research since their discovery thirty years ago by Glemser and co-workers.[1] The physical properties and reaction chemistry of the simplest of these compounds, thiazyl fluoride and thiazyl trifluoride, was the subject of a recent review by Glemser and Mews.[2]

Thiazyl fluoride (NSF) was orginally thought[3] to have the structure SNF by analogy to isoelectronic ONF, but was shown to have the structue NSF with a short (1.45 A) NS bond and a long (1.64 A) SF bond. The shortness of the NS bond has often been explained in terms of a NS triple bond, implying sulfur hypervalency.[4] The NSF bond angle in thiazyl fluoride is 117°, consistent with the structure predicted by VSPER theory and similar to the isoelectronic molecule SO_2.

The chemistry[2] of thiazyl fluoride is quite varied. The pi-system undergoes both oligomerization reactions and cycloadditions. Fluorine-containing Lewis acids abstract the fluorine atom of thiazyl fluoride to give thiazyl salts. Electrophilic transition metal ions form nitrogen-bound coordination complexes such as $[Ni(NSF)_6]^{2+}$, while nucleophiles attack the electropositive sulfur atom to displace fluoride.

The UPS spectrum of thiazyl fluoride has been recorded by Cowan et al.[5] and by Dixon et al.[6] The spectra were assigned by analogy to SO_2, and both groups concluded that the HOMO was a lone-pair orbital on sulfur. Theoretical studies[7,8] of the electronic structure of thiazyl fluoride have recently suggested that the HOMO was principally nitrogen in character, and that the use of sulfur d orbitals was necessary to accurately describe the bonding.

Thiazyl trifluoride, NSF_3, has a distorted tetrahedral geometry with the sulfur atom at the center. The NS bond distance (1.42 A) in thiazyl trifluoride is even shorter than in thiazyl fluoride, and the S-F bond distances (1.55A) are also considerably shorter. Both of these facts have been explained in terms of S d pi bonding to both N and F.[9]

The reaction chemistry[2] of NSF_3 is also very interesting. The molecule does not react with sodium below 200°C, and unlike NSF, NSF_3 is stable both as a gas and liquid and can be stored at room temperature. Thiazyl trifluoride undergoes addition reactions of the S-N bond, but does not trimerize like NSF. Fluoro-Lewis acids form adducts without abstracting fluoride. Transition metal complexes such as $[Mn(NSF_3)_4]^{2+}$ and $[Re(CO)_5NSF_3]^{+}$ have been synthesized. Thiazyl trifluoride undergoes a variety of nucleophilic substitution reactions, both with and without retention of the N-S triple bond.

The UPS spectrum of NSF_3 has been recorded by Cowan et

al.[5] These workers concluded that the HOMO of NSF_3 is a NS pi level which is significantly stabilized by sulfur d orbitals. The core binding energies have previously been measured by Avanzino et al. in 1975.[10]

In order to use the LOIP method to analyze the bonding in thiazyl fluoride and thiazyl trifluoride, it was necessary to measure their core binding energies. The core binding energies of NSF_3 were remeasured because our present instrumentation allows for much more accurate binding energy measurements.

B. Experimental

1. Preparation of Compounds

Thiazyl fluoride and thiazyl trifluoride were prepared by Dr. A. Waterfeld with materials provided from the laboratory of Prof. R. Mews.

Thiazyl fluoride was prepared by the thermal decomposition of $Hg(NSF_2)_2$ at 110 ^oC in high vacuum.[11] The material was collected in a -196 ^oC glass trap and was immediately tranfered to a Monel vessel. Vapor-phase infrared spectroscopy showed a trace ammount of SiF_4, presumably formed by reaction with the glass walls of the vacuum system. Silicon tetrafluoride is sufficiently volatile (bp -86 ^oC) that it was possible to pump the SiF_4 out of the sample while holding the sample resorvior at -110 ^oC.

Thiazyl trifluoride was prepared by the reaction of SbF_5-NSF_3 with KF[12] at 20 ^oC on an all-metal vacuum line. The infrared spectrum agreed with the literature.[13]

2. Obtaining of Spectra

Thiazyl fluoride and thiazyl trifluoride were introduced in the spectrometer through an all-metal inlet system. The flow of vapor into the spectrometer was regulated using a micrometer needle valve. The inlet system was heated to 200°C under vacuum before obtaining spectra to remove adsorbed water. Thiazyl fluoride was held at -78°C (dry ice-acetone) and thiazyltrifluoride was held at -45°C (chlorobenzene slush) during data collection.

C. Results and Discussion

The core binding energies of NSF and NSF_3 are shown in Table IV.1. The binding energy data for NSF_3 replaces less accurate data reported by Avanzino et al.[10] from this laboratory.

1. Charge Estimates from Core Binding Energies

Recently, Larson and Folkesson[14] have described a method of calculating atomic charges of free molecules using gaseous core binding energy data and empirical charge/binding energy correlations obtained from solid state ESCA. This method is currently applicable only to second and third row elements, but has been shown to give estimates of atomic charge which agree fairly well with those obtained by ab initio calculation.

Perhaps the simplest way of explaining the charge calculation method of Larson and Folkesson is to use the calculation of the atomic charges of NSF as an example. Larson

and Folkesson have published a series of empirically determined equations which linearly relate binding energy data with atomic charge in the solid state. On going from the solid state to the gaseous species, it is necessary to introduce a constant a which accounts for the difference in reference level in solid and gas-phase ESCA (Fermi level of the spectrometer material versus the vacuum level). The three equations for the charge on the nitrogen, sulfur and fluorine atoms of NSF using the data from Table IV.1 are:

$$406.88 = a + 7.00q_N + 401.4 \quad (N\ 1s)$$

$$174.14 = a + 3.38q_S + 163.8 \quad (S\ 2p_{3/2})$$

$$692.74 = a + 4.28q_F + 688.8 \quad (F\ 1s)$$

A fourth equation is obtained by requiring that the sum of the atomic charge in NSF to be zero:

$$0 = q_N + q_S + q_F$$

The charges are obtianed by solution of simultaneous equations. The results for NSF and NSF_3 are given in Table IV.2, along with the charges calculated by ab initio methods,[7] and by semi-empirical CNDO/2 calulations.

It can be seen that the ESCA results differ from the ab initio results primarily in describing the polarity of the N-S bond. The ab initio results of Zirz and Aldrichs[7] for NSF give the suspicious result that the N atom bears approximately the same charge as the F atom. The most likely reason for this result is the limited basis set used by Zirz and Aldrichs which fails to adequately describe the contribution of S 3d orbitals. Sulfur d orbital pi bonding would

decrease the positive charge on sulfur and the negative charge on nitrogen. In the ab initio calculation of NSF by Seeger et al.,[8] the authors found it necessary to include two sets of d functions to obtain the lowest total energy, while Zirz and Aldrich used only one set of d orbitals in their calculation.

In rationalyzing atomic charge distributions in terms of chemical bonding, it is often useful to explain the results in terms of a valence bond structure or mixtures of valence bond structures. For NSF, the ESCA charge distribution is consistent with a 3:1 mixture of the resonance forms:

The calculated results of Zirz and Aldrich are consistent with a roughly 1:1 mixture. Again, we feel that their calculation overestimates the polarity of the N-S bond, but we agree that the charge data suggests that it is not necessary to invoke hypervalent sulfur to explain the observed bonding.

A similar analysis of the ESCA charge data for NSF_3 indicates that approximately equal mixtures of the following four resonance structures are necessary to rationalize the observed charges:

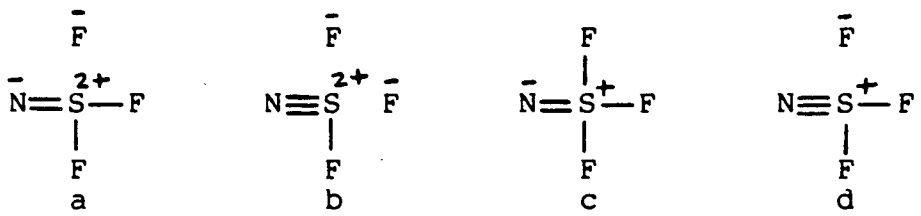

Structures a, b and d imply hyperconjugation, and structures

c and d imply d orbital sulfur hypervalency. Zirz and Aldrichs concluded that their calculations were consistent with a 3:1 mixture of structures a and b, and that structures such as c and d were of only minor importance in the bonding of NSF_3. Once again, we believe that calculations using a larger basis set would decrease the polarity of the N-S bond, and increase the importance of hypervalent resonance structures such as c and d.

One final result merits discussion. The naive interpretaton of the N 1s core binding energy, the ESCA charge calculation, and the ab initio study of Zirz and Aldrichs all indicate that the nitrogen atom of NSF_3 is more negatively charged than the nitrogen atom of NSF. This increase in negative charge is surprising in view of the gain of two electronegative fluorine atoms, and has important implications when one considers the reactivity differences between the two molecules (see Section IV C.3). Because of the importance of the interpretation of this result, we wished to be assured of the validity of the assumption that a decrease in binding energy corresponds to an increase in negative charge. Therefore, we estimated the effect of the the changes in relaxation energy and potential associated with this binding energy shift.

The change in charge of the nitrogen atom (Δq_N) on going from NSF to NSF_3 may be calculated from:[15]

$$q_N = (1/k)(\Delta E_B - \Delta V + \Delta E_R)$$

where ΔE_B is the change in the N 1s binding energy, k is 26.53 eV/charge,[16] ΔV is the change in potential due to the charges of the other atoms, and ΔE_R is the change in relaxation energy. The E_R values were calculated by the transition state method,[17] using CNDO/2[18] wave functions and the equivalent cores approximation.[19] The experimental geometries of NSF and NSF_3 were used.[2] Straightforward application of the method involves the relation:

$$E_R = 0.5[\Phi_{val}(N) - \Phi_{val}(O^+)]$$

where $\Phi_{val}(N)$ is the valence potential in the ground-state molecule and $\Phi_{val}(O^+)$ is the valence potential in the ion, approximated by replacing the N nucleus by the O nucleus. Calculations based on this relation yield $\Delta E_R = 0.8$ eV, a value almost exactly equal to $-\Delta E_B$. Previous studies[20] have shown that ΔE_R values calculated by this method are usually too large and must be reduced by a factor of about half to give satisfactory correlations with binding energy data. Thus, we conclude in this case that $\Delta E_R + \Delta E_B \leq 0$. The sulfur atom of NSF_3 is significantly more positivley charged than that of NSF, and therfore $\Delta V > 0$. Hence, the calculations, even allowing for uncertainty in ΔE_R, indicate that $\Delta q_N < 0$ and confirming our assumption that the nitrogen atom of NSF_3 is more negatively charged than the nitrogen atom of NSF.

2. LOIP Analysis

The LOIP method may be used to quantify the bonding or antibonding character of the molecular orbitals of thiazyl

fluoride and thiazyl trifluoride and to ascertain the atomic orbital character of those molecular orbitals. The LOIPs of thiazyl fluoride and thiazyl trifluoride were calculated using planar ammonia, hydrogen sulfide, and hydrogen fluoride as nonbonding reference compounds. The results are given in Table IV.3.

The LOIPs from Table IV.3 are the ionization potentials that the p orbitals of the nitrogen, sulfur and fluorine atoms would have if these orbitals were strictly nonbonding. Since the valence orbitals accessable by He(I) spectroscopy are principally composed of p orbitals, comparison of the actual ionization potentials of the thiazyl fluorides with the LOIP values should indicate how the atomic orbitals combine to form molecular orbitals.

i) NSF

The first five bands in the UPS spectrum of NSF lie at 11.82, 13.50, 13.87, 15.61, and 16.47 eV.[5] The corresponding molecular orbitals have been characterized as pi or quasi-pi orbitals. The LOIP data strongly suggests that the 11.82 eV band corresponds to a molecular orbital derived mainly from a nitrogen 2p orbital (LOIP = 11.1) eV, with 0.7 eV bonding character. The data indicate that the bands at 13.50 eV and 13.87 eV correspond to molecular orbitals derived mainly from sulfur 3p orbitals (LOIP = 13.62 eV), with very slight antibonding and bonding character, respectively. The bands at 15.61 and 16.47 eV appear to corres-

pond to bonding orbitals derived mainly from the fluorine 2p orbitals (LOIP = 14.80 eV). We believe that the molecular orbital assignments and qualitative molecular orbital pictures shown in the energy level diagram of Figure 4.1 are logical deductions from the data. The symmetry assignments are largely in agreement with those of the UPS investigators,[5,6] but in most cases the indicated atomic orbital contributions to the molecular orbitals are substantially different from those given by the UPS investigators. The differences are mainly due to the LOIP values, which show that the nonbonding nitrogen 2p level lies well above the nonbonding sulfur 3p level. The earlier workers assumed an ordering consistent with the electronegativities of the neutral atoms, i.e., the reverse order.

The HOMO, which we characterize as a sulfur-nitrogen bonding orbital located mainly on the nitrogen atom, has been described variously as a sulfur lone pair[6] and as an orbital centered mainly on nitrogen and fluorine.[8] The bonding character of the orbital is inconsistent with the involvement of only valence p orbitals in the bonding. If we restrict the bonding to p orbitals, the HOMO would be expected to look something like this:

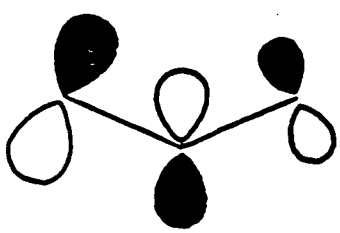

The orbital picture implies a net antibonding interaction.

Hence, the LOIP data indicate that the HOMO has been stabilized by interaction with a higher lying orbital, presumably a sulfur d orbital, and therefore the HOMO has considerable N($p\pi$) -->S($d\pi$) character, as indicated crudely in Figure 4.1. The electron density contour plot of the HOMO of NSF by Seeger et al.[8] shows the greatest electron density in the region of the nitrogen atom, with the general shape of the in-plane nitrogen 2p orbital, thus supporting our conclusions about the character of this orbital.

ii) NSF_3

The first four bands in the UPS spectrum of NSF_3 [5] lie at 12.50, 14.15, 16.65, and 18.35 eV, and the corresponding molecular orbitals have been characterized as derived mainly from combinations of valence p orbitals of the atoms of the molecule. The first band has been assigned to the 7e(π) orbitals, corresponding to pi bonding between the nitrogen and sulfur atoms. However, the LOIP data are not at all consistent with a description of this pi bonding, based only on valence p orbitals. If only p orbitals were involved in the S-N pi bonding, the first ionization potential would be lower than the nitrogen atom LOIP, 10.4 eV. It is clear that the the 7e orbitals have been strongly stabilized by interaction with higher lying orbitals, presumably a pair of sulfur d orbitals.

The second band has been assigned to the $10a_1(\sigma)$ orbital which has been described as a "nitrogen lone pair". The

ionization potential and LOIP values are consistent with this interpretation if the orbital is described as having strong S-F antibonding character, and weak S-N bonding character. The S-N bonding character of this orbital is probably further weakened by mixing with the $8a_1(\sigma)$ orbital which would have considerable out-of-phase N-S s character, principally on nitrogen. This mixing of s and p orbitals would be analogous to the mixing of the 4σ and 5σ orbitals of CO (see Chapter V).

The third band is intense and broad and has an ionization potential close to the fluorine atom LOIP value. Therefore, we believe the band is a composite, assignable to the fluorine lone pair orbitals, 6e, $1a_2$, 5e, and $9a_1$. Cowan et al. assign this band to 6e alone, without comment.

The ionization potential of the fourth, weak band (18.35 eV) could be either the previously mentioned $8a_1$ orbital (principally N 2s in character), or it could be a S-F bonding sigma bonding orbital. Cowan et al. tentatively assign this band to $1a_2$, a nonbonding fluorine orbital that we have included in the composite third band.

3. Correlation of Electronic Structure with Chemical Reactivity

Knowledge of the electronic structure of NSF and NSF_3 gained in this study can be used to explain the observed chemistry of these molecules. The charge distributions obtained by ESCA explain why fluoro-Lewis acids attack the highly negatively charged fluorine atom of NSF, while form-

ing nitrogen bound adducts with NSF_3. The surpising result that the nitrogen atom of NSF_3 is more negatively charged than the nitrogen atom of NSF explains the better sigma donor properties of NSF_3. The charge distributions also show that the sulfur atom of both molecules bears a high positive charge, indicating that the sulfur atom would be the site of nucleophilic attack.

The final question to be considered is the bonding of NSF and NSF_3 to transition metal ions. The situation is somewhat simplier for NSF_3. The $10a_1$ orbital of NSF_3 was shown by the LOIP analysis to be strongly S-F antibonding and weakly S-N bonding in character. When NSF_3 forms a bond to a transition metal ion, the electron density from this orbital flows towards the metal. Because of depopulation of the S-F antibonding region of the orbital, the S-F bonds are strengthened, and because of rehybridization at the nitrogen atom (in which the s character of the N-S sigma bond increases), the N-S bond is also strengthened.

The situation is not so clear cut for NSF. The HOMO depicted in Figure 4.1 and the electron density contour plot of Seeger et al.[8] both have no electron density along what would be the metal-nitrogen-sulfur bond axis. An explanation of the bonding in compounds such as $[M(NSF)_6]^{2+}$ (where M = Co, Ni) must account for the following structural properties:[2]

1) The compounds are octahedrally coordinated via the N

atoms of the NSF ligands.

2) The N-S and S-F bond distances in the NSF ligand both decrease on complex formation.

3) The M-N bond distance is similar to a typical metal-amine bond distance.

Point 3 would indicate that the M-N bond is reasonably stong, that is, not unusually weak. This means either strong sigma bonding or weak sigma and strong pi bonding. Point 2 would indicate that pi back-bonding was not significant in these compounds and this is also supported by the fact that the metals are in high oxidation states, making them poor pi donors. The ligand could potentially act as a pi donor to the metal, but the t_{2g} acceptor level in these molecules is filled, meaning that the metal would be forced to use the next higher set of empty orbitals, the 4p orbitals, clearly an unlikely situation. We are left with having to form a sigma donor orbital largely on nitrogen.

The most likely explanation for the bonding in these transition metal-thiazyl fluoride complexes is that the nitrogen based HOMO changes its atomic orbital character in forming a sigma bond to the metal. If one is restricted to pure p orbitals and does not allowing mixing of the orbitals of the same symmetry, the HOMO and the two lowest lying unoccupied molecular orbitals of NSF are:

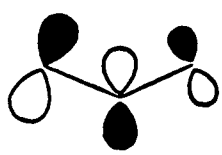

13a'

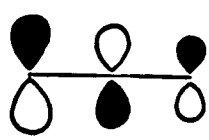

4a''

14a'

When a transition metal cation with a low lying filled t_{2g} metal orbital interacts with the 13a' and 4a'' orbitals (pi and quasi-pi symmetry), these orbitals are destabilized. On the other hand, the 14a' orbital is stabilized by interaction with the partially filled e_g metal orbital. The 14a' orbital then becomes the sigma donor orbital in these complexes. Of course, the 13a' and 14a' orbitals are of the same symmetry, so essentially all that happens is that the 13 a'orbital gains N p character along the M-N bond axis, while the 14a' orbital gains N p character in the NSF plane.

This explanation of the bonding also accounts for the observed bond shortening in the NSF ligand. Both 13a' and 14a' are S-F antibonding orbitals, so that flow of electrons from the orbital formed by mixing these two orbitals would be expected to strengthen the S-F bond. The 13a' orbital is S-N antibonding while the 14a' orbital is S-N bonding, so that increased mixing of the two orbitals would strengthen the N-S bond (as would the rehybridization described previously for NSF_3 which should also occur in metal-NSF complexes).

Summary

X-ray photoelectron spectroscopy has been used to determine the charge distribution in NSF and NSF_3. The nitrogen atom of NSF_3 was shown to be more negatively charged than the nitrogen atom of NSF. Binding energy data were

used with valence ionization potentials to obtain the atomic orbital character of the molecular orbitals of NSF and NSF_3. The HOMO of NSF was found to be mostly N 2p in character, and not a sulfur lone pair as previously suggested. The electronic structure deduced in this study was then used to discuss the observed chemistry of thiazyl fluoride and thiazyl trifluoride, and a scheme for bonding in transition metal-NSF complexes was proposed.

References

(1) Glemser, O.; Schröder, H.; Haesler, H. Z. Z. Anorg. Allg. Chem. 1955, 279, 28.

(2) Glemser, O.; Mews, R. Angew. Chem. Int. Ed. Engl. 1980, 19, 883.

(3) Glemser, O.; Richert, H.; Rogowski, F. Natruwissenshaften 1960, 47, 94.

(4) Cook, R. L.; Kirchoff, W. H. J. Chem. Phys. 1967, 47, 4521.

(5) Cowan, D. O.; Gleiter, R.; Glemser, O.; Heilbronner, E. Helv. Chim. Acta 1972, 55, 2418.

(6) Dixon, R. N.; Duxbury, G.; Fleming, G. R.; Hugo, J. M. V. Chem. Phys. Lett. 1972, 14, 60.

(7) Zirz, C.; Aldrichs, R. Inorg. Chem. 1984, 23, 26.

(8) Seeger, R.; Seeger, U.; Bartetzko, R.; Gleiter, R. Inorg. Chem., 1982, 21, 3473.

(9) Glemser, O.; Mews, R. Adv. Inorg. Radiochem. 1970, 14, 33.

(10) Avanzino, S. C.; Jolly, W. L.; Lazarus, M. S.; Perry, W. B.; Rietz, R. R.; Schaaf, T. F. Inorg. Chem. 1975, 14, 1595.

(11) Glemser, O; Mews, R.; Roesky, H. W. Chem. Ber. 1969, 102, 1523.

(12) Waterfeld, A.; Mews, R., unpublished results.

(13) Waterfeld, A.; Ph.D. Thesis, Göttingen, 1981.

(14) Larsson, R., private communication. See Larson, R.; Folkesson, B. Phys. Scr. 1977, 16, 357.

(15) Gelius, U. Phys. Scr. 1974, 9, 133.

(16) The <1/r> value calculated from the Slater exponent of the valence-shell orbital of nitrogen is 26.53 eV/charge.

(17) Davis, D. W.; Shirley, D. A. J. Electron Spectrosc. Relat. Phenom. 1974, 3, 137.

(18) Sherwood, P. M. A. J. Chem. Soc. Faraday Trans. 2 1976, 72, 1791, 1805.

(19) Jolly, W. L. In "Electron Spectroscopy: Theory, Techniques and Applications; Brundle, C. R.; Baker, A. D., Eds.; Academic Press: London, 1977; Vol. I, pp 119-149.

(20) Avanzino, S. C.; Chen, H. W.; Donahue, C. J.; Jolly, W. L. Inorg. Chem. 1980, 19, 2201.

Table IV.1. Core Binding Energies (eV) of Thiazyl Fluoride and Thiazyl Trifluoride

	S $2p_{3/2}$		N 1s		F 1s	
	E_B	fwhm[a]	E_B	fwhm	E_B	fwhm
NSF	174.14(4)[b]	1.24(15)	406.88(2)	1.31(6)	692.74(2)	1.79(10)
NSF_3	177.10(4)	1.08(16)	406.10(3)	1.53(19)	695.32(2)	1.76(7)

[a] Full width at half maximum. [b] Uncertainty in last digit indicated in parentheses.

Table IV.2 Calculated Atomic Charges of Thiazyl Fluoride and Thiazyl Trifluoride

	ESCA[a]	Ab Initio[b]	CNDO/2[c]
NSF:			
q_N	-0.23	-0.59	-0.20
q_S	0.96	1.12	0.42
q_F	-0.73	-0.61	-0.22
NSF_3:			
q_N	-0.48	-0.73	-0.18
q_S	1.55	1.85	0.65
q_F	-0.36	-0.44	-0.16

[a] See text for computational details. [b] Reference 7.
[c] Includes d orbital functions on sulfur, based on methods described in reference 18.

Table IV.3 Localized Orbital Ionization Potentials (eV) for Thiazyl Fluoride and Thiazyl Trifluoride.

	N 2p	F 2p	S 3p
NSF	11.1	14.80	13.62
NSF_3	10.4	16.87	15.99

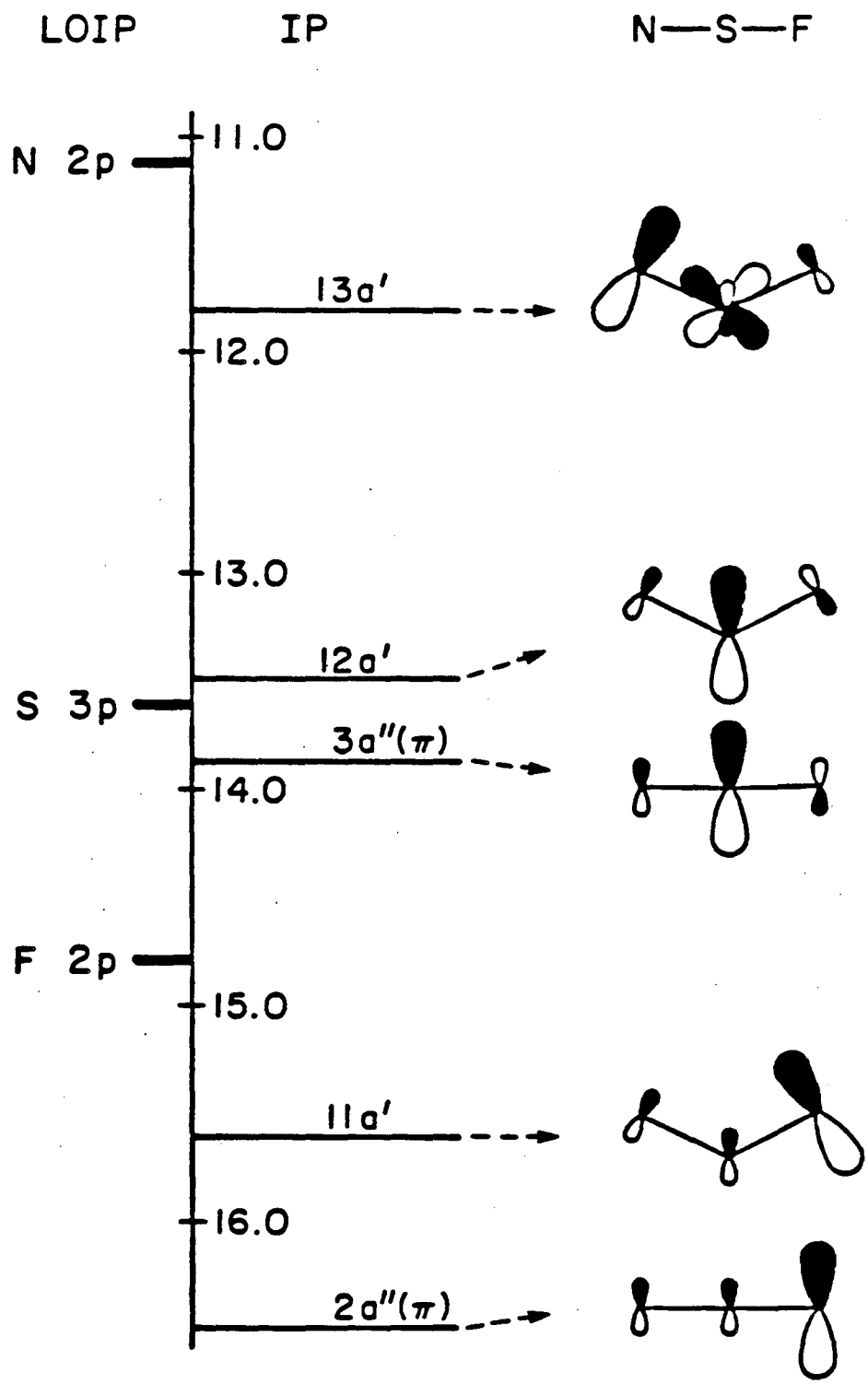

Figure 4.1. Molecular orbital energy level diagram for NSF, showing the LOIP values for the N 2p, S 3p, and F 2p orbitals.

CHAPTER V. BONDING IN BORANE CARBONYL AND RELATED BORANE ADDUCTS

A. Introduction

The bonding of carbon monoxide to transition metals has long been the subject of spectroscopic investigations[1] and theoretical studies.[2] Most studies have shown that the metal-carbon bond is best described terms of a synergistic sigma/pi interaction, in which there is sigma donation of electron density to the metal from the "lone-pair" carbon orbital, and pi back donation of electron density from the filled metal orbitals to the antibonding C-O pi orbitals. The extent to which each of the interactions contributes to the bond is a subject of continuing debate.[3]

A relativlely simple molecule in which similar sigma/pi type bonding might be expected is borane carbonyl, BH_3CO. The boron-carbon bonding in borane carbonyl has often been described[4] as a sigma bond formed between the filled "lone-pair" orbital of CO and the empty B 2p orbital of BH_3, and as a pi bond formed between the filled B-H bonding orbitals of BH_3 and the pi^* orbitals of CO. A study of bonding in a relatively simple adduct of CO such as borane carbonyl should provide insight into the more complex interactions that occur when CO forms a bond to a transition metal.

A spectroscopic tool which has often been used to study the bonding of CO in a variety of compounds is infrared spectroscopy.[5] The C-O stretching force constant decreases substantially when CO is coordinated by a transition metal,

providing evidence of for $d_\pi \longrightarrow \pi^*$ bonding. When CO is coordinated by non-transition element complexes or adsorbed on the surface of non-transition metal solids, the C-O stretching force constant increases.[6] In these compounds in which only sigma bonding is thought to be significant, the increase in force constant has generally been ascribed to the depopulation of a slightly antibonding carbon "lone-pair" orbital of CO.[7] In BH_3CO, the C-O stretching force constant is only slightly higher than in free CO, and this has been interpreted as indicating that some of the strengthening of the C-O bond caused by sigma bonding is being counteracted by weakening of the C-O bond through pi bonding. Unfortunately, infrared spectroscopy cannot separate pi and sigma contributions to the bonding.

On the other hand, the UPS spectrum of BH_3CO should provide a method for distinguishing between sigma and pi contributions, because the shift in ionization potential of each of the sigma and pi orbitals of CO on forming a borane adduct can be measured individually. This is due to the fact that on going from $C_{\infty v}$ (CO) to C_{3v} (BH_3CO) symmetry, the sigma and pi orbitals remain orthogonal. The UPS spectra of several borane adducts, including BH_3CO, have been measured by Lloyd and Lynaugh.[8] The UPS data for BH_3CO indicate that the carbon "lone-pair" orbital of CO has been stabilized by only 0.1 eV by the formation of the borane adduct. This has been interpreted[9] as evidence for an ex-

ceedingly weak sigma interaction, implying that the not negligible dissociation energy of BH_3CO is due mainly to pi bonding, a conclusion seemingly at odds with those based on IR data.

A molecule with an electronic structure similar to CO is methyl isocyanide, $CNCH_3$. By comparing the shifts in ionization potential of methyl isocyanide on forming BH_3CNCH_3 to the shifts in ionization potential of CO on forming BH_3CO, it should be possible to make reasonable deductions about the relative pi/sigma donor/acceptor properties of methyl isocyanide and carbon monoxide.

Again, UPS data are best interpreted with corrections based on core binding energies. Therefore, this chapter will describe the determination of the core binding energies of several borane adducts, the interpretaion of sigma and pi bonding trends among borane adducts based on the use of the LOIP method, and analysis of the bonding in BH_3CO in comparison to BH_3CNCH_3.

B. Experimental

Diborane was prepared by the reaction of $NaBH_4$ and H_3PO_4.[10] Methyl isocyanide was prepared by the dehydration of N-methyl-formamide.[11] Borane-methyl isocyanide[12] can be prepared simply by condensing stoichiometric quantities of diborane and methyl isocyanide in a flask on the vacuum line and allowing the flask to warm to room temperature. However, the product is relatively nonvolatile and was found to form oligomers when heated, so that it was not possible to

heated the sample to increase the flow of vapor into the spectrometer. In order to obtain an adequate flow of vapor into the spectrometer gas cell, the compound was prepared in a 2-l bulb equipped with a 2.5-cm valve that led directly into the spectrometer inlet system. Excess methyl isocyanide was condensed over most of the interior surface of the bulb by slowly raising a liquid-nitrogen-filled Dewar around the bulb as the methyl isocyanide was admitted. Diborane was condensed into the flask, and the flask was allowed to warm to room temperature. The volatile residue was pumped off, leaving the adduct. Sufficient vapor evolved from the solid distributed over this large surface area to obtain spectra of the adduct at room temperature. The infrared spectrum of the solid in the sample flask agreed with that in the literature.[12]

Borane-phosphorus trifluoride was prepared by the method of Perry and Bissot,[13] in which B_2H_6 is reacted with excess PF_3 (8 atm) for three days. The product was purified by fractional condensation, and its vapor pressure (23 mm at -111.8 ^{o}C) agreed with that in the literature.[13] To minimize dissociation of BH_3PF_3, the sample was stored at -196^{o}C, fractionated immediately prior to use, and held at -111.8 ^{o}C during collection of the spectra. The B 1s peak of B_2H_6 is separated from the B 1s peak of the adduct by more than 2 eV and was not observed. The measured phosphorus and fluorine binding energies of BH_3PF_3 are very

similar to those of PF_3, so that free PF_3 would not be readily observed. The absence of a peak attributable to diborane is our principal evidence that the compound does not dissociate under the conditions of measurement.

Borane-ammonia was obtained commercially (Alfa) and was sublimed before use. The spectrometer was heated to 50°C, at which temperature a very weak signal was obtained. Attempts to use higher temperatures resulted in decomposition. The half-widths of the B 1s and N 1s lines were unusually broad, probably because of spectrometer drift during the 20 h necessary to obtain the spectra, even though a drift correction was applied every 30 min.

C. Results and Discussion

1. Core Binding Energies

The core binding energies of BH_3PF_3, BH_3CNCH_3, and BH_3NH_3 obtained in this study are given in Table V.1, along with the core binding energies of BH_3CO, $BH_3N(CH_3)_3$, and $BH_3P(CH_3)_3$ which are taken from the literature.[14]

The core binding energies of the free Lewis bases are given in Table V.2.

2. Pi Bonding.

In all of the borane adducts, the HOMO is the BH_3 bonding molecular orbital of e symmetry, which shall be refered to as $e(BH_3)$. The only borane adduct in which the $e(BH_3)$ orbital cannot conceivably interact with another molecular orbital is BH_4^- ion, for which the gas-phase core binding energy is unknown. In the absence of an ideal

$e(BH_3)$ reference, we have chosen the $e(BH_3)$ orbital of BH_3NH_3 as a reference to measure the relative bonding or antibonding character to the $e(BH_3)$ orbitals of the other borane adducts, i.e., our reference for the LOIP analysis will be the $e(BH_3)$ orbital of BH_3NH_3, and the B 1s binding energies will used to correct the valence ionization potentials. The results of this analysis are given in Table V.3.

It can be seen that only in the cases of BH_3CO and BH_3PF_3 is there a stabilization of the $e(BH_3)$ orbital relative to the $e(BH_3)$ orbital of BH_3NH_3. In all other cases, the $e(BH_3)$ LOIP value exactly predicts the ionization potential of the $e(BH_3)$ orbital of the adduct. If one reasonably assumes that NH_3 is not a pi acceptor, then the results indicate that there is little or no pi acceptance by $N(CH_3)_3$, $P(CH_3)_3$, and $CNCH_3$ when these ligands form borane adducts.

The origin of the stabilization in BH_3CO is probably back-bonding to the π^* orbital of CO. The subject of pi bonding in BH_3CO and BH_3CNCH_3 will be treated in more detail in a subsequent section.

The stabilization of the $e(BH_3)$ orbital in BH_3PF_3 could arise from back-bonding to either the $\sigma^*(P-F)$ or the P $d\pi$ orbitals of PF_3. We believe that our data strongly suggest that P $d\pi$ bonding is far more important than $\sigma^*(P-F)$ bonding. Pi acceptance by the $\sigma^*(P-F)$ orbitals should lead to an increase in negative charge on the fluorine atoms of PF_3,

which should result in a lowering of the F 1s binding energy on going from PF_3 to BH_3PF_3. In fact, the F 1s binding energy increases slighlty on complex formation, indicating a net flow of electron density in the opposite direction. Further evidence for an increase in positive charge on the fluorine atoms comes from the multiplicity weighted average fluorine lone pair ionization potential of PF_3, which increases from 17.0 to 17.3 eV on complex formation.[15] The P-F bond of PF_3 also becomes slightly shorter[16] on adduct formation, also indicating negligible pi acceptance by the σ^*(P-F) orbitals.

The phosphorus $2p_{3/2}$ binding energy is unchanged on complex formation, indicating that the flow of electron density from the phosphorus lone pair is balanced by an increase in relaxation energy on complex formation and by the flow of electron density back into the empty P dπ orbitals.

3. Sigma Bonding

The core binding energies of the donor atoms in the free Lewis base and in the borane adduct may be used to calculate the expected shift in the Lewis base lone pair ionization potential upon formation of the borane adduct, assuming no sigma interaction between the base and the BH_3 group. Addition of this shift to the free-base lone pair ionization potential (column 2 of Table V.4) gives the LOIP (column 3 of Table V.4), which corresponds to a hypothetical ionization potential that the lone-pair orbital would have

if there were no sigma bonding in the complex. In the last column of Table V.4 are listed the differences between the actual $\sigma(BH_3L)$ ionization potentials and the reference value. These values represent the stabilization of the base lone pair due to sigma donor interaction with the borane group. Fortuitously, the lone pair stabilization energies in BH_3CO and BH_3PF_3 are approximately the same as would be calculated from the uncorrected ionization potentials of the free Lewis bases. However, this is not true for the other adducts, where errors as great as 2.2 eV would be made by using the uncorrected ionization potentials.

The results shown in Table V.4 indicate that $N(CH_3)_3$ is a better sigma donor than NH_3, presumably because a methyl group is more electron releasing than a hydrogen atom. A similar inductive effect is shown by the phosphorus bases. Electron-releasing methyl groups make trimethylphosphine a better sigma donor than trifluorophosphine with its electron withdrawing fluorine atoms. Sigma donor properties of CO and $CNCH_3$ will be discussed in the next section.

4. Bonding in BH_3CO and BH_3CNCH_3

Using core binding energies, one can calculate the changes in the ionization potentials of CO and $CNCH_3$ due to changes in charge and relaxation energy that occur when these molecules form borane adducts. These corrected ionization potentials may then be used to construct energy level diagrams that illustrate the changes in the bonding charac-

ter of the orbitals of CO and $CNCH_3$ when coordinated by a BH_3 group.

There are three bands in the He(I) photoelectron spectrum of CO.[17] These ionization potentials correspond to the 5σ carbon lone pair orbital, the 1π C-O pi orbital, and the 4σ C-O sigma bonding orbital, which is largely oxygen in character. The carbon core binding energy difference between CO and BH_3CO is used to correct the 5σ ionization potential; the average of the carbon and oxygen binding energy differences is used to correct the 1π ionization potential, and the oxygen binding energy difference is used to correct the 4σ ionization potential. An energy level diagram using these corrected ionization potentials, the ionization potentials of BH_3CO, and the $e(BH_3)$ ionization potential calculated with BH_3NH_3 as a reference is shown in Figure 5.1.

In methyl isocyanide, four ionizations are observed in the He(I) spectrum,[17] corresponding to the $7a_1$ carbon lone pair orbital, the 2e C-N pi orbital, the 1e pseudo-pi C-H sigma orbital, and the $6a_1$ C-N sigma orbital. The $7a_1$, 2e, and $6a_1$ ionization potentials were corrected analogously to their CO counterparts, and the 1e orbital ionization potential was corrected using the methyl carbon binding energy difference between $CNCH_3$ and BH_3CNCH_3. An energy level diagram for BH_3CNCH_3 is shown in Figure 5.2.

The pi bonding interactions in BH_3CO and BH_3CNCH_3 are relatively straightforward. The filled 1π orbital of CO and

the 2e orbital of $CNCH_3$ are both stabilized approximately 0.3 eV by interaction with a filled e(BH_3) orbital. In BH_3CNCH_3, the C-N π^* orbital stabilizes the e(BH_3) by the same amount that it is destabilized by the filled C-N π orbital. The net effect is that the energy of the e(BH_3) orbital is unchanged, although electron density from this orbital has been delocalized into the $CNCH_3$ pi orbitals, contributing to B-C bonding. The 1e level, which is localized on the methyl group, is unchanged in bonding character. In BH_3CO, the CO π^* orbital interacts more strongly with the e(BH_3) orbital, so that the latter orbital is significantly (0.5 eV) stabilized. This flow of negative charge back to the CO group is reflected in the decreased carbon and oxygen binding energies on going from CO to BH_3CO.

The sigma bonding interactions are more complex. The 5σ orbital of CO is only slightly stabilized on coordination by the BH_3 group. If one only considered HOMO-LUMO interactions, one would conclude that sigma bonding in BH_3CO is negligible. However, it is possible that the $7a_1$ lone pair orbital of the complex is energetically poised about midway between the empty $8a_1$ orbital (the BH_3 "acceptor" orbital) and the $6a_1$ B 2s orbital (see Figure 5.3). In such a situation, the $8a_1$ orbital would destabilized about as much as the $6a_1$ orbital would be stabilized, with little net stabilization or destabilization of the $7a_1$ orbital. However, an overall stabilization of the system, corresponding to B-C

sigma bonding, would result because of the occupancy of the $6a_1$ orbital.

Further support for this explanation is found in the shift of the 4σ ionization potential of CO. On formation of the borane adduct, this orbital is significantly destabilized. This destabilization is undoubtedly due to a repulsive interaction with the orbital of mainly B 2s character, which lies just beyond the range of He(I) ionization. In the complexes studied by Lloyd and Lynaugh,[8] the only complex in which the "B 2s" ionization potential could be observed with any certainty (at 18.04 eV) was $BH_3N(CH_3)_3$. In $BH_3N(CH_3)_3$, it would be expected that there would be a very strong repulsive interaction between the "B 2s" and "N 2s" orbitals, causing the "B 2s" orbital ionization to be at significantly lower ionization potential than in BH_3CO. Therefore, it is reasonable to propose that the ionization potential of the $6a_1$ orbital in BH_3CO lies slightly higher than 21 eV.

The sigma bonding interactions in BH_3CNCH_3 are very similar. The $7a_1$ orbital of $CNCH_3$ lies lower in ionization potential than does its CO counterpart, so there is less repulsive interaction with the "B 2s" orbital and a greater net stabilization. Once again, the orbital at higher ionization potential, $6a_1$, is significantly destabilized by interaction with the "B 2s" orbital of BH_3.

5. Rehybridization

The strenghtening of the C-O bond on going from CO to

non-transition metal element adducts such as BH_3CO has usually been ascribed to a withdrawl of electron density from the antibonding carbon lone pair orbital of CO.[18] Unfortunately, whether this lone pair orbital is considered antibonding or bonding depends on whether one uses Mulliken overlap population analysis[7] or orbital contour plots,[19] respectively, to determine the orbital character.

The fact that the vibrational frequency of CO increases[17] from 2143 to 2160 cm^{-1} upon ionization of the lone pair orbital suggests, but does not prove, that the orbital is slightly antibonding. Undoubtedly, the orbital is strongly modified by rehybridization either by removal of an electron from the orbital or by coordination to a Lewis acid. When the carbon lone pair loses an electron, or becomes engaged in bonding, it acquires more p character, and the opposite carbon sigma orbital (4σ) aquires more s character. This increase in s character increases the strength of the C-O bond. Theoretical work by Sherwood and Hall[20] has shown that, even in long-distance interactions of CO with a transition metal, sigma rehybridization occurs, with a shift of lone pair electron density toward the metal and a shortening of the C-O bond.

In the case of BH_3CO, the extent to which the C-O bond is strengthened by such rehybridization cannot be simply determined from the measures of the C-O bond strength (such as the C-O stretching frequency) because pi back-bonding

causes a simultaneous weakening of the bond. However, the situation is simpler in the case of the methyl isocyanide adduct of borane, BH_3CNCH_3, because there is little pi back-bonding in this molecule. The marked increase in the C-N stretching frequency of 150 cm^{-1} on going from $CNCH_3$ to the adduct must be entirely due to rehybridization of the sigma N-C-B system. This conclusion is supported by an ab initio study of $CNCH_3$ that shows that the HOMO has bonding character.[21]

Summary

The sigma and pi bonding properties of NH_3, $N(CH_3)_3$, PF_3, $P(CH_3)_3$, CO, and $CNCH_3$ as borane adducts were studied using combined core and valence photoelectron spectroscopy. The data indicate that pi back-bonding is only significant in BH_3CO and BH_3PF_3. It is proposed that the strengthening of the C-O bond in CO and the C-N bond in $CNCH_3$ upon coordination to BH_3 is a consequence of rehybridization of the carbon sigma orbitals.

References

(1) Cotton, F. A.; Wilkinson, G. "Advanced Inorganic Chemistry"; 3rd edn., Wiley-Interscience: New York, 1972; pp 693-701.

(2) Baerends, E. J.; Ros, P. Mol. Phys. 1975, 30, 1735.

(3) Johnson, J. B.; Klemperer, W. G. J. Am. Chem. Soc. 1977, 99, 7132.

(4) DeKock, R. L.; Gray, H. B. "Chemical Structure and Bonding"; Benjamin/Cummings: Menlo Park, CA, 1980; pp 322-324.

(5) Nakamoto, K. "Infrared Spectra of Inorganic and Coordination Compounds"; 2nd. edn., Wiley: New York, 1970.

(6) Brown, T. L.; Darensbourg, D. J. Inorg. Chem. 1967, 6, 971.

(7) DeKock, R. L.; Sarapu, A. C.; Fenske, R. F. Inorg. Chem. 1971, 10, 38.

(8) Lloyd, D. R.; Lynaugh, N. J. Chem. Soc. Faraday Trans. 2 1972, 68, 947.

(9) Ermler, W. C.; Glasser, F. D.; Kern, C. W. J. Am. Chem. Soc. 1976, 98, 3799.

(10) Norman, A. D.; Jolly, W. L. Inorganic Syntheses 1968, 11, 15.

(11) Cassanova, J. C.; Parry, R. W. J. Am. Chem. Soc. 1963, 85, 4280.

(12) Watari, F. Inorg. Chem. 1982, 21, 1442.

(13) Parry, R. W.; Bissot, T. C. J. Am. Chem. Soc. 1956, 78, 1524.

(14) Jolly, W. L.; Bomben, K. D.; Eyermann, C. J. At. Data Nucl. Data Tables 1984, 31, 433.

(15) Hillier, I. H.; Marriot, J. C.; Saunders, V. R.; Ware, M. J.; Lloyd, D. R.; Lynaugh, N. J. Chem. Soc. Chem. Commun. 1970, 1586.

(16) Bock, H. Pure Appl. Chem. 1975, 44, 343.

(17) Turner, D. W.; Baker, A. D.; Brundle, C. R. "Molecular Photoelectron Spectroscopy"; Wiley-Interscience: London, 1970.

(18) D'Amico, K. L.; Trenary, M.; Shinn, N. D.; Solomon, E. I.; McFeely, F. R. J. Am. Chem. Soc. 1982, 104, 5102.

(19) Streitwieser, A.; Owens, P. H. "Orbital and Electron Density Diagrams"; Macmillan: New York, 1973; pp 92-96.

(20) Sherwood, D. E.; Hall, M. B. Inorg. Chem. 1983, 22, 93.

(21) Bevan, J. W.; Sandorfy, C.; Pang, F.; Boggs, J. E. Spectrochim. Acta, Part A 1981, 37A, 601.

Table V.1 Core Binding Energies of Borane Adducts

	B 1s		Lewis base donor atom		other levels	
	E_B	fwhm	E_B	fwhm	E_B	fwhm
BH_3NH_3	193.73(4)	1.64(10)	408.41(2)[a]	1.61(6)		
$BH_3N(CH_3)_3$[b]	193.73		406.68[a]			
BH_3CO[c]	195.10(6)	1.73(16)	296.18(4)[d]	1.25(17)	542.05(2)[e]	1.50(8)
BH_3CNCH_3	193.60(3)	1.63(10)	293.43(3)[d]	1.07(7)	294.06(7)[f] 407.13(2)[a]	1.23(15) 1.29(8)
BH_3PF_3	194.69(5)	1.49(14)	141.79(3)[g]	1.37(5)	694.30(2)[h]	1.69(6)
$BH_3P(CH_3)_3$[b]	192.93		137.17[g]			

[a] N 1s. [b] Data from Ref. 14. [c] Beach, D. B.; Eyermann, C. J.; Smit, S. P.; Xiang, S. F.; Jolly, W. L. J. Am. Chem. Soc. 1984, 106, 536. [d] C 1s. [e] O 1s. [f] Methyl carbon. [g] P $2p_{3/2}$. [h] F 1s.

Table V.2 Core Binding Energies (eV) of Free Lewis Bases

	Donor atom level	Other levels
	E_B	E_B
NH_3[a]	405.52[b]	
$N(CH_3)_3$	404.82[b]	291.26[c]
CO	296.19[d]	542.57[e]
$CNCH_3$	292.37[d]	293.35[c] 406.68[b]
PF_3	141.78[f]	694.09[g]
$P(CH_3)_3$	135.93[f]	290.30[c]

[a] All data from Ref. 14. [b] N 1s. [c] Methyl C 1s. [d] C 1s. [e] O 1s. [f] P $2p_{3/2}$. [g] F 1s.

Table V.3. Stabilization (eV) of the e(BH_3) Orbital of BH_3L, Relative to BH_3NH_3.

	IP[e(BH_3)][a]	LOIP	IP - LOIP
BH_3NH_3	10.61[b]	(10.61)	(0.0)
$BH_3N(CH_3)_3$	10.32[b]	10.32	0.0
BH_3CO	12.22[b]	11.71	0.5
BH_3CNCH_3	10.52[c]	10.51	0.0
BH_3PF_3	12.0[d]	11.38	0.6
$BH_3P(CH_3)_3$	10.0[d]	10.0	0.0

[a] Average of Jahn-Teller split bands. [b] Ref. 8. [c] Ref. 21 [d] Ref. 16.

Table V.4. Stabilization (eV) of the Lewis Base Lone Pair Orbital in Borane Adducts

	IP(:L)	LOIP	IP[BH_3-L]	IP[BH_3-L] -LOIP
BH_3NH_3	10.84[a]	13.09	13.92[b]	0.83
$BH_3N(CH_3)_3$	8.45[b]	9.95	11.51[b]	1.56
BH_3CO	14.01[a]	13.96	14.13[b]	0.17
BH_3CNCH_3	11.24[a]	12.09	12.70[c]	0.61
BH_3PF_3	12.29[d]	12.30	12.9[e]	0.6
$BH_3P(CH_3)_3$	8.6[f]	9.6	10.9[e]	1.3

[a] Ref. 17. [b] Ref. 8. [c] Ref. 21. [d] Basset, P. J.; Lloyd, D. R. J. Chem. Soc. Dalton 1972, 248. [e] Ref. 16. [f] Cradock, S.; Ebsworth, E. A. V.; Savage, W. J.; Whiteford, R. A. J. Chem. Soc. Faraday 2 1972, 68, 934.

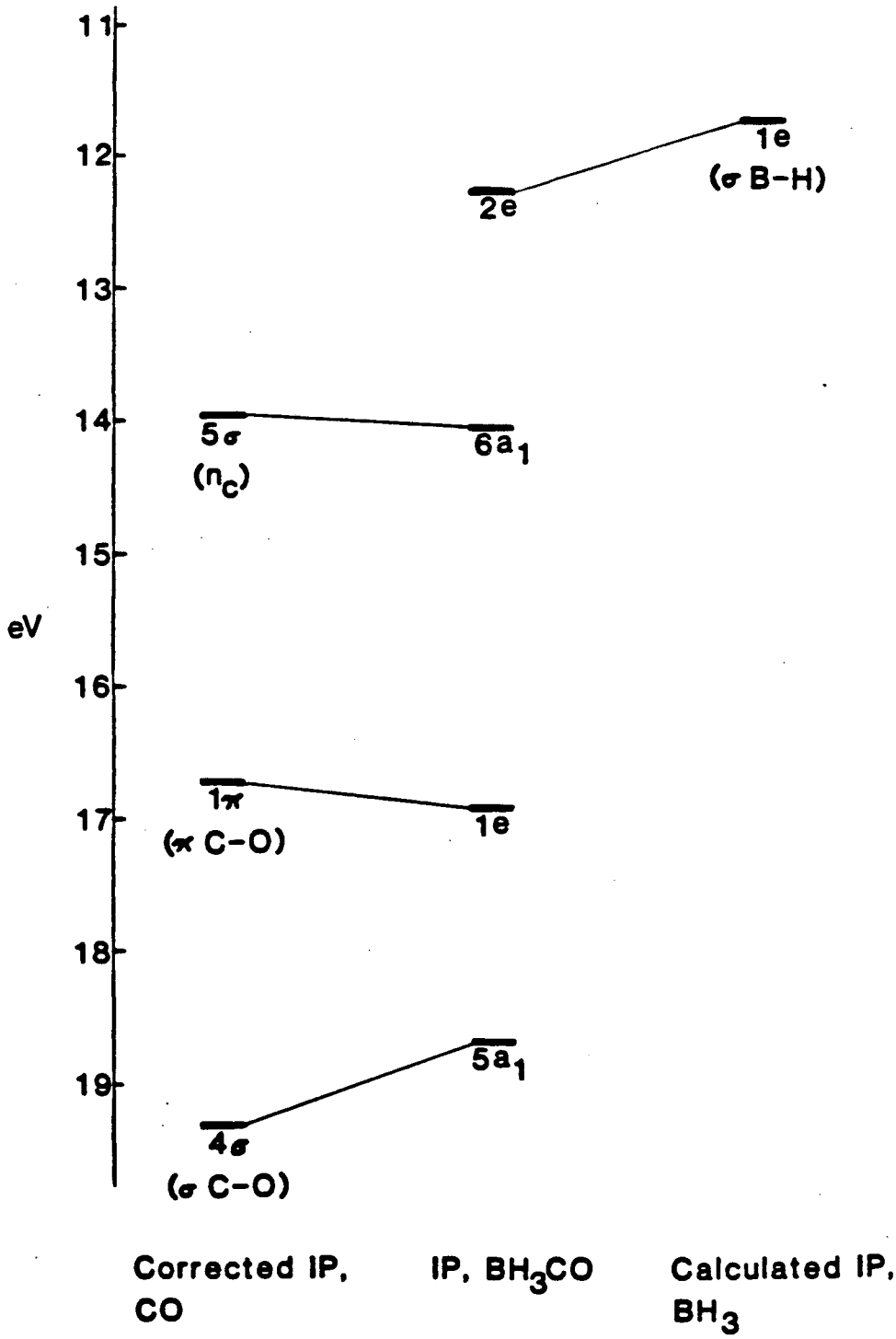

Figure 5.1. Energy level diagram for borane carbonyl.

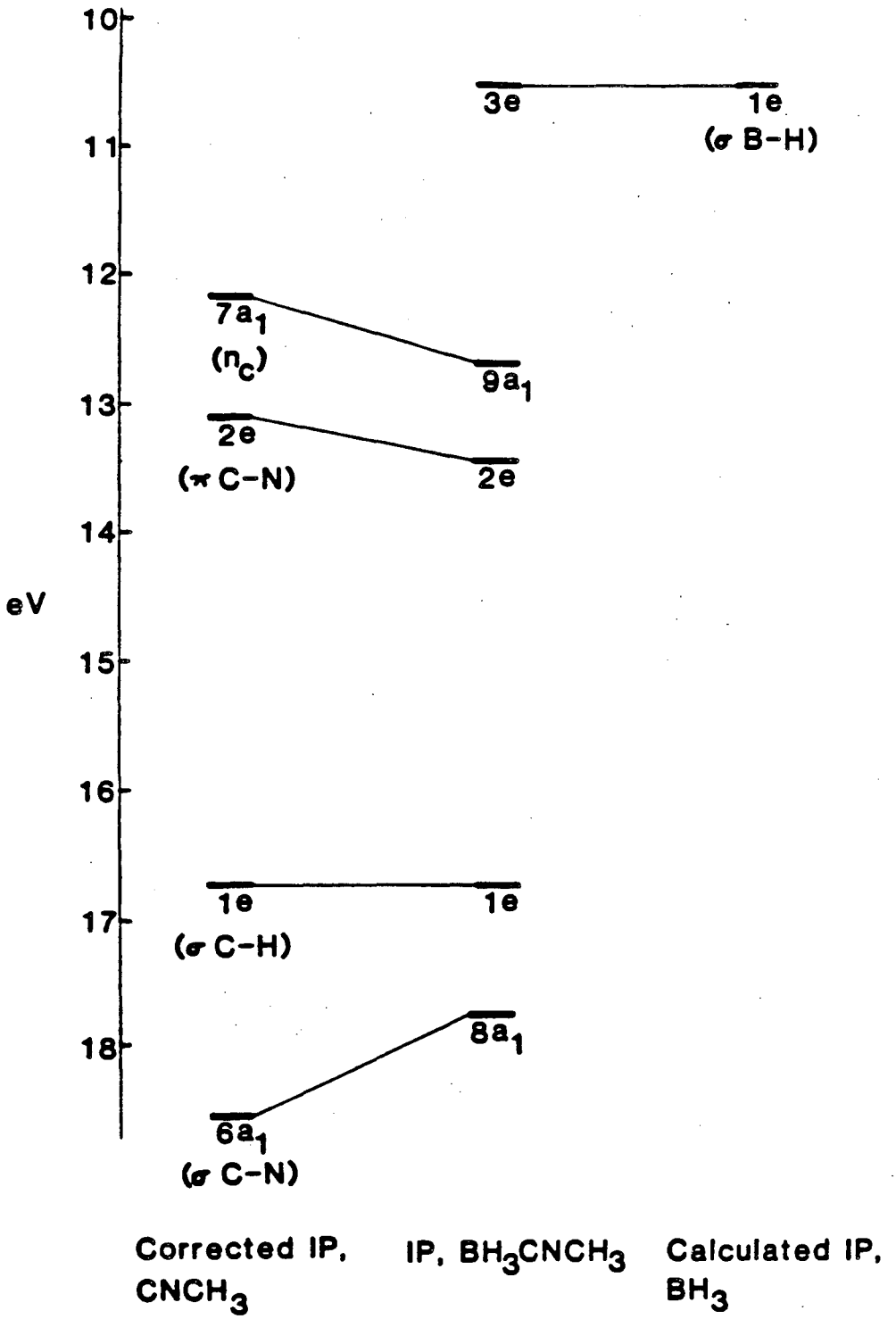

Figure 5.2. Energy level diagram for borane methyl isocyanide.

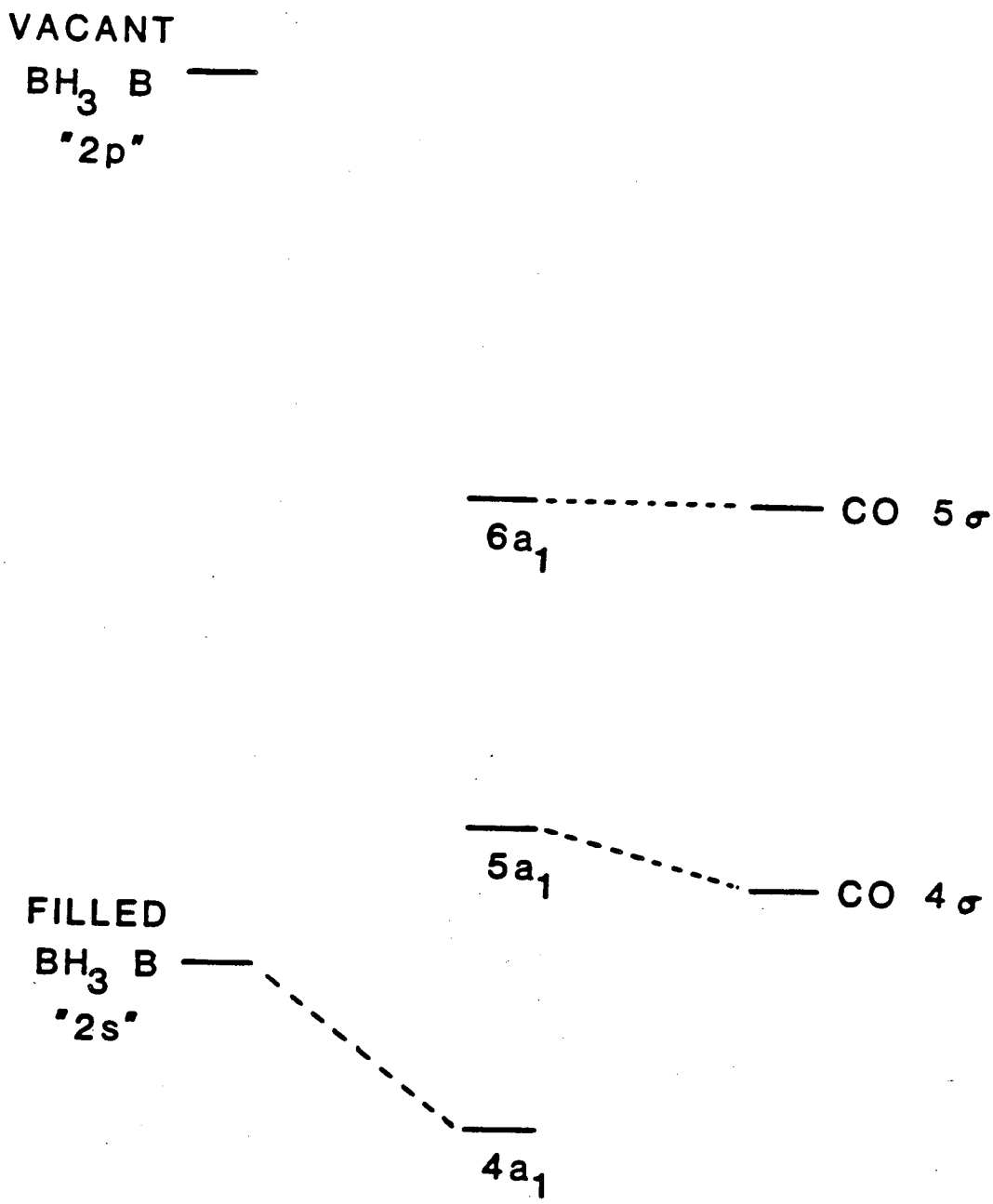

Figure 5.3. Sigma orbital interactions in BH_3CO.

CHAPTER VI. PHOTOELECTRON SPECTROSCOPIC STUDIES OF OLEFIN-TRANSITION METAL BONDING

A. Introduction

The chemistry of olefins bound to transition metals is an important area of research in organometallic chemistry,[1] particularly in the field of catalysis.[2] In an effort to better understand the details of metal-olefin bonding, we have undertaken this photoelectron study of coordinated olefins.

The theory developed to explain the bonding of olefins to metals is the Dewar-Chatt-Duncanson scheme,[3,4] in which the C-C pi bond donates electron density in a sigma bond to the metal, and the C-C antibonding pi orbital accepts electron density through a pi bond to the metal. This theory has been quite successful in explaining why the majority of metal olefin complexes have been late-transition metal complexes in low formal oxidation states, (filled, accessible d pi orbitals) and in explaining the coordination geometry adopted by the olefin (for example, the unusual geometry of Zeise's salt).[5]

The olefin complexes studied in this Chapter are all iron tetracarbonyl adducts. The olefin group of these compounds occupies an equatorial position with the C=C bond in the equatorial plane. These compounds were chosen for this study because they are well characterized and their UPS spectra have been reported.[6-10] In addition, the iron tetracarbonyl adducts of axially coordinating strong sigma

donors pyridine and trimethylphosphine were also studied, for comparison to the olefin complexes.

B. Experimental

1. Preparation of Compounds

The $Fe(CO)_4$ complexes of acrolein, methyl acrylate, and dimethyl maleate, trans-1,2-dichloroethylene, 1,1-dichloroethylene, and pyridine were prepared by procedures in the literature[11-13] which utilize the reaction of $Fe_2(CO)_9$ with the appropriate ligand. Diiron enneacarbonyl was prepared by the photolysis of $Fe(CO)_5$ in acetic acid.[14] The $Fe(CO)_4$ complexes of acrolein and of the dichloroethylenes were sufficiently volatile that it was possible to purify these compounds by fractional condensation on the vacuum line. The other $Fe(CO)_4$ complexes mentioned above were purified by vacuum sublimation.

Tetracarbonyl(trimethylphosphine)iron was prepared by the sealed tube reaction of equimolar amounts of $Fe(CO)_5$ and $P(CH_3)_3$. The tube was held at 70°C for 48 h, and the unreacted material was pumped off at 0°C. The residue was sublimed at 30°C under vacuum to give the desired product.

Tetracarbonyl(ethylene)iron was prepared by the method of Murdoch and Weiss,[15] in which $Fe_2(CO)_9$ was reacted with C_2H_4 under high pressure. The purification of the product required that it be separated from the large amount of $Fe(CO)_5$ produced in the reaction, a compound with very similar physical properties. Tetracarbonyl(ethylene)iron has been

reported to decompose on standing at room temperature[15] and on vacuum transfer from one vessel to another.[9] Van Dam and Oskam[8] suggested that the $Fe(CO)_4C_2H_4$ sample used in the UPS study of Baerends et al.[16] was contaminated with $Fe(CO)_5$ because of decomposition in the spectrometer. However, we have observed that the thermal and photochemical decomposition of $Fe(CO)_4C_2H_4$ results only in the formation of $Fe_3(CO)_{12}$ and C_2H_4. It is possible that the sample of Baerends et al. had not been originally free of $Fe(CO)_5$, as was also the case in the XPS study of Xiang et al.[17] Because of these prior difficulties in the preparation and handling of this important compound, the synthesis and characterization of $Fe(CO)_4C_2H_4$ are described in some detail below.

Diiron enneacarbonyl in pentane was treated with C_2H_4 at 50 atm for 48 h. The excess ethylene was vented, and the mixture of $Fe(CO)_5$ and $Fe(CO)_4C_2H_4$ was separated from the solvent by fractional condensation on a vacuum line at -63°C. The $Fe(CO)_5/Fe(CO)_4C_2H_4$ mixture was separated by reduced-pressure fractional distillation with a 15-cm Vigreux column, a 0°C condenser, and a four-arm fraction collector cooled to 0°C. It would have been desirable to use a more efficient distillation column, but because the product decomposes relatively rapidly above 0°C, a short column with minimal hold-up was used. Nitrogen was bled into the still pot to prevent bumping and to maintain the pressure at 12 mm. The majority of the material distilled in the range 19-26°C and was primarily $Fe(CO)_5$ contaminated with a small

amount of $Fe(CO)_4C_2H_4$. Tetracarbonyl(ethylene)iron was collected at 31-34°C. The middle portion of this fraction (bp 33-34°C) was distilled into a vial and stored in vacuo at -78°C in the dark prior to obtaining the XPS spectra. The absence of $Fe(CO)_5$ in the sample was confirmed by gas-phase infrared spectroscopy. The metal-ligand stretching regions of $Fe(CO)_5$ and $Fe(CO)_4C_2H_4$ are shown in Figure VI.1. The absence of bands at 610, 467, and 421 cm^{-1} in the infrared spectrum and the narrowness of the boiling range are our principal evidence that the $Fe(CO)_4C_2H_4$ sample was free of $Fe(CO)_5$.

2. Obtaining X-ray Photoelectron Spectra

All of the compounds in this study were introduced into the spectrometer by direct sublimation through the large diameter inlet system. Flow of vapor into the spectrometer was controlled by cooling the sample reservoir. The following temperatures were maintained around the sample reservoir: $Fe(CO)_4L$, where L = ethylene, -25°C; acrolein, -15°C; methyl acrylate, -15°C; dimethyl maleate, -5°C; 1,2-dichloroethylene, -10°C; 1,1-dichloroethylene, -10°C; pyridine, 25°C; trimethylphosphine, 20°C.

C. Results and Discussion

1. Core Binding Energies

The core binding energies of the $Fe(CO)_4$-olefin complexes, the $Fe(CO)_4$ complexes of pyridine and trimethylphosphine, and $Fe(CO)_5$ are given in Table VI.1 The assign-

ment of the spectra of the $Fe(CO)_4L$ compounds is discussed below.

i) L = Ethylene, 1,2-Dichloroethylene, 1,1-Dichloroethylene

The assignment of the spectra of these compounds is straightforward. The deconvoluted C 1s spectra of the ethylene complex is shown in Figure 6.2. The peak at lower binding energy is due to the CH_2 carbons, and the ratio of the intensity of the CH_2 peak relative to the CO peak is 0.68 ± 0.19. The deconvoluted C 1s spectra of the dichloroethylene complexes are shown in Figures 6.3 and 6.4. The binding energy of the CHCl carbon atoms of the trans-1,2-dichloroethylene complex is exactly the average of the CH_2 and CCl_2 binding energies of the 1,1-dichloroethylene complex. The chlorine 2p spectra were deconvoluted assuming the theoretical 2:1 ratio for the $2p_{3/2}$ and $2p_{1/2}$ peaks.

ii) L = Acrolein, Methyl Acrylate, Dimethyl Maleate

The carbon 1s spectra of all three complexes contain a broad peak at 293.5 eV and a well-resolved narrower peak at 290.4 eV. The area ratios of the higher binding energy peak to the lower binding energy peak are acrolein, 5:2; methyl acrylate, 6:2; dimethyl maleate, 8:2. No appreciable shake-up was observed in any of the spectra, so that the area ratios may be used in the assignment of the peaks. It may be reasonably concluded that the peak at lower binding energy is due to the olefinic C=C carbon atoms, and that the peak at higher binding energy is due to the metal carbonyl carbon atoms and to olefin carbon atoms attached to oxygen

atoms.

The oxygen 1s spectrum of the acrolein complex shows two peaks of area ratio 4:1, with the metal carbonyl oxygen peak at higher binding energy. The O 1s spectra of the methyl acrylate and dimethyl maleate complexes are similar in appearance to that of the acrolein complex, but the methoxy oxygen peaks overlap the metal carbonyl oxygen peaks so that the area ratio is 5:1 in the case of the methyl acrylate complex, and 6:2 in the case of the dimethyl maleate complex. The lower O 1s binding energy of the organic carbonyl oxygen atom is due to the large relaxation energy of these carbon atoms.

iii) L = Trimethylphosphine, Pyridine

The carbon 1s spectrum of the trimethylphosphine complex contains two well-resolved peaks with the expected 4:3 area ratio. The carbon 1s spectrum of the pyridine complex is broad and essentially featureless, and could not be meaningfully deconvoluted. The O 1s spectra of both complexes are distinctly asymmetric, with extra intensity on the low binding energy sides of the peaks. This low binding energy intensity is probably due to the trans carbonyl oxygens, which have more negative charges than the equatorial oxygens. The iron $2p_{3/2}$ binding energies of these two compounds are a full electronvolt lower than those of the other compound of Table VI.1. This result is consistent with the strong donor ability of the trimethylphosphine and

pyridine ligands, which causes a significant increase in the negative charge on the iron atom.

2. Atomic Charges in $Fe(CO)_4C_2H_4$

In comparing the the donor/acceptor properties of ethylene and carbon monoxide, it would be advantageous to determine the atomic charges of $Fe(CO)_4C_2H_4$ and compare them to the atomic charges of $Fe(CO)_5$. This can be done by using the core binding energy differences between $Fe(CO)_4C_2H_4$ and $Fe(CO)_5$, and between $Fe(CO)_4C_2H_4$ and the structurally related compound $c\text{-}C_3H_6$ using the equation[18]

$$\Delta E_B(A) = k_A \Delta q_A + \Delta V - \Delta E_R(A)$$

where $\Delta E_B(A)$ is the binding energy difference of atom A, k_A is a constant for that atom determined by the expectation value of the inverse of the radius of atom A,[19] ΔV is the difference in potential felt by atom A due to the charges of the other atoms, and $\Delta E_R(A)$ is the difference in the electronic relaxation energy of atom A. By the use of the binding energy data for $Fe(CO)_4C_2H_4$ and $Fe(CO)_5$, equations for $\Delta E_B(Fe)$, $\Delta E_B(C(CO))$, $\Delta E_B(O)$ were obtained. Atomic charges for $Fe(CO)_5$ were taken from an ab initio calculation (in which the Fe, C, and O atomic charges were calculated to be +1.039, +0.174, and -0.381, respectively).[20] A fourth equation, for $\Delta E_B(CH_2)$, was obtained from the C 1s binding energy difference of $Fe(CO)_4C_2H_4$ and $c\text{-}C_3H_6$. Atomic charges for $c\text{-}C_3H_6$ were assumed to be -0.1 for the carbon atoms and +0.05 for the hydrogen atoms.[21] A fifth equation was obtained by requiring the sum of all of the charges in

$Fe(CO)_4C_2H_4$ to be zero. Electron relaxation energies were calculated by the transition-state method,[22] using the equivalent cores approximation.[23] Valence potentials for the relaxation calcualtions were obtained using CNDO/2 wave functions.[24] The experimental geometry of $c\text{-}C_3H_6$[25] and symmetric idealized geomentries for $Fe(CO)_4C_2H_4$[26] and $Fe(CO)_5$[27] were used. It was found that the calculated differences in the relaxation energy of the Fe, C(CO), and O atoms in $Fe(CO)_4C_2H_4$ and $Fe(CO)_5$ were less than 0.1 eV and thus insignificant. The difference in CH_2 carbon relaxation energy between $Fe(CO)_4C_2H_4$ and $c\text{-}C_3H_6$ was calculated to be 1.13 eV. The five equations were solved by using for $\Delta E_R(CH_2)$ the calculated value, half the calculated value (a value previous studies have shown to give the best results), and zero. From the results, given in Table VI.2, it can be seen that the calculated charges are insensitive to the assumption regarding $\Delta E_R(CH_2)$.

The results indicate that each CH_2 group bears a charge of -0.2 electrons. In addition, it can be seen that the Fe atom of $Fe(CO)_4C_2H_4$ has a slightly higher positive charge than in $Fe(CO)_5$, even though a qualitative interpretation of the Fe binding energy alone would indicate the opposite. The observed decrease in Fe binding energy on going from $Fe(CO)_5$ to $Fe(CO)_4C_2H_4$ is mainly a result of replacing a carbonyl group, in which the negative charge is on the relatively distant oxygen atom, by the negatively charged

C_2H_4 group, in which the negative charge is relatively near the iron atom. Our calculations indicate that the CO ligands have essentially the same charge in $Fe(CO)_4C_2H_4$ as in $Fe(CO)_5$ and that the C_2H_4 group is more negatively charged than the carbonyl group it replaces.

3. LOIP Analysis Transition Metal-Olefin Bonding

The UPS spectra of all of the $Fe(CO)_4L$ complexes of this study have qualitatively similar features in the low ionization potential region. The band at lowest ionization potential is due to the Fe $d_{x^2-y^2}$, d_{xy} orbitals, which are also engaged in sigma and pi bonding to the equatorial ligands. The next band at about 1 eV higher ionization potential is due to the Fe d_{xz}, d_{yz} orbitals which are primarily pi orbitals. The next higher lying ionization potential is due the metal-ligand sigma bonding level of the ligand, L. By comparing the shifts in these ionization potentials to the parent compound, $Fe(CO)_5$, one obtains direct information about the bonding properties of L relative to CO.

Before discussing the olefin complexes, the method of analysis is illustrated here for the metal orbitals of the axially substituted complex $Fe(CO)_4P(CH_3)_3$. The iron core binding energy difference between $Fe(CO)_4P(CH_3)_3$ and $Fe(CO)_5$ is -1.05 eV. The correction term is thus -0.8 eV. The first ionization potentital of $Fe(CO)_5$ is 8.6 eV, so that the LOIP of the Fe $d_{x^2-y^2}$, d_{xy} orbitals of $Fe(CO)_4P(CH_3)_3$ is 0.8 eV lower, or 7.8 eV. The experimental ionization poten-

tial, 7.77 eV, is in excellent agreement with the LOIP. Indeed, these values should be the same because the replacement of an axial CO with a $P(CH_3)_3$ should not have any effect on the equatorial metal orbitals beyond the effects of changes in charge and relaxation energy. The LOIP value for the Fe d_{xz}, d_{yz} orbitals of $Fe(CO)_4P(CH_3)_3$ is 9.1 eV. The experimental ionization potential is 8.85 eV, corresponding to a destabilization of approximately 0.3 eV. This destabilization is quite reasonable, because $P(CH_3)_3$ is a poorer back-bonder than the CO it replaces. The results of similar analyses for all of the $Fe(CO)_4L$ compounds are represented in Table VI.3.

The results for the axially coordinated pyridine complex are essentially identical with those obtained for the trimethylphosphine complex. It is important to note that, although the core binding energy differences are large for these axially coordinated ligands, the method of analysis nevertheless correctly predicts the ionization potentials of the equatorial orbitals. In the case of the olefin complexes, the binding energy differences will be smaller, and any error associated with the correction term will be even smaller.

The simplest of the olefin complexes, $Fe(CO)_4C_2H_4$, is the next compound to be considered. The results of the LOIP analysis for the Fe $d_{x^2-y^2}$, d_{xy} orbitals (Table VI.2) show that this orbital has essentially the same bonding character

as in $Fe(CO)_5$, implying that ethylene and carbon monoxide have about the same sigma + pi effect on these orbitals. If we assume that the sigma donor character of ethylene is the same as carbon monoxide, it is concluded that the extent of back-bonding from the Fe $d_{x^2-y^2}$, d_{xy} orbitals is the same in ethylene as in carbon monoxide. If we more reasonably assume that the sigma donor character of ethylene is greater than that of CO (indeed, the IP of the donor orbital of C_2H_4 is 2.5 eV lower than in CO, and the proton affinity of ethylene is higher than that of carbon monoxide), it is reasonably concluded that the back-bonding from the Fe $d_{x^2-y^2}$, d_{xy} orbitals is greater to C_2H_4 than to CO. Greater back-bonding to C_2H_4 is consistent with our finding that the Fe atom of $Fe(CO)_4C_2H_4$ is more positively charged than that in $Fe(CO)_5$, and that the C_2H_4 group accepts more electron density than the CO group it replaces.

The data for the substituted olefin complexes can be analyzed similarly. The stabilization of the Fe $d_{x^2-y^2}$, d_{xy} orbitals increases to ~0.2 eV in the case of the acrolein and the methyl acrylate complexes, which have electron-withdrawing aldehyde and methyl ester groups, respectively, replacing a hydrogen atom of ethylene. On substituting two methyl ester groups, as in the dimethyl maleate complex, the stabilization increases to ~0.4 eV.

The stabilization of the equatorial orbitals in the dichloroethylene complexes is about the same as in the acrolein and methyl acrylate complexes. This is contrary to

the CNDO results of Van Dam and Oskam,[8] which indicated that the dihalogenated olefins should be better electron acceptors than olefins with aldehyde and ester groups. Notice that the naive interpretation of the Fe 3d orbital ionization potentials, ignoring the effects of charge, leads to the conclusion that the dichloroethylene ligands stabilize the metal orbitals to a greater extent than does dimethyl maleate.

The results of the LOIP analysis for the Fe d_{xz}, d_{yz} orbitals show that this orbital is destabilized by ~0.4 eV on going from $Fe(CO)_5$ to $Fe(CO)_4C_2H_4$. This is due to the orthogonality of these metal orbitals to the pi* C=C orbital of the equatorially coordinated ethylene. In fact, for all of olefin complexes studied, the Fe d_{xz}, d_{yz} orbitals were destabilized by ~0.3 eV. This was also the amount of destabilization observed in the axially coordinated complexes. The value of ~0.3 eV would appear to be the amount of destabilization attributable to the loss of one CO ligand.

The final interaction to consider is the interaction of the filled C=C pi orbital with the metal. The results of these analyses are presented in Table VI.4. If one were to compare the C=C pi ionization potentials of the free olefins with those of the coordinated olefins, without considering core binding energies, it might be concluded that this orbital is essentially unaffected by complex formation. This line of reasoning ignores the fact that, in the com-

plex, the olefin acquires a negative charge because of its attachment to an electropositive metal center. On the other hand, by comparing the ionization potential of the complex with the LOIP value, it is found that the C=C pi orbital is stablized to the extent of ~0.6 eV by complexation to the metal carbonyl fragment, corresponding to significant sigma donation by this orbital.

Summary

The gas-phase core binding energies of several iron tetracarbonyl olefin complexes were obtained. Atomic charge calculation for $Fe(CO)_4C_2H_4$ based on binding energy shifts indicate that the ethylene group accepts more electron density than the carbon monoxide group it replaces. Detailed analysis of metal-olefin orbital interactions using the LOIP method indicate that the equatorial metal orbitals of the $Fe(CO)_4$ fragment are stabilized to the same or a greater extent by olefins than by CO, while the Fe d_{xz}, d_{yz} orbitals are destabilized because they are orthogonal to the pi acceptor orbitals of the olefin. This leads to the conclusion that, in one dimension, olefins are better pi acceptors than carbon monoxide.

References

(1) Manojilovic-Muir, L.; Muir, K. W.; Iber, J. A. Discuss. Faraday Soc. 1969, 47, 84.

(2) Wilke, G. Pure Appl. Chem. 1978, 50, 677.

(3) Dewar, M. J. S. Bull. Soc. Chim. Fr. 1951, 18, c79.

(4) Chatt, J.; Duncanson, L. A. J. Chem. Soc. 1953, 2939.

(5) Love, R. A.; Koetzle, T. F.; Williams, G. J. B.; Andrews, L. C.; Bau, R. Inorg. Chem. 1975, 14, 2653.

(6) Van Dam, H.; Oskam, A. J. Electron Spectrosc. Relat. Phenom. 1979, 17, 357.

(7) Flamini, A.; Semprini, E.; Stefani, F.; Cardaci, G.; Bellachioma, G.; Andreocci, M. J. Chem. Soc., Dalton Trans. 1978, 695.

(8) Van Dam, H.; Oskam, A. J. Electron Spectrosc. Relat. Phenom. 1979, 16, 307.

(9) Hill, W. E.; Ward, C. H.; Webb, T. R.; Worley, S. D. Inorg. Chem. 1979, 18, 2029.

(10) Daamen, H.; Oskam, A. Inorg. Chim. Acta 1978, 26, 81.

(11) Weiss, E.; Stark, K.; Lancaster, J. E.; Murdoch, H. D. Helv. Chim. Acta 1963, 46, 288.

(12) Gravels, F. W.; von Gustorf, E. K. Justus Liebigs Ann. Chem. 1973, 11, 1821.

(13) Schubert, E. H.; Sheline, R. K. Inorg. Chem. 1966, 5, 1071.

(14) Jolly, W. L. "The Synthesis and Characterization of Inorganic Compounds"; Prentice-Hall: Englewood Cliffs, NJ, 1970, p 472.

(15) Murdoch, H. D.; Weiss, E. Helv. Chim. Acta, 1963, 46, 1588.

(16) Baerends, E. J.; Oudshoorn, C.; Oskam, A. J. Electron Spectrosc. Relat. Phenom. 1975, 17, 357.

(17) Xiang, S. F.; Chen, H. W.; Eyermann, C. J.; Jolly, W. L.; Smit, S. P.; Theopold, K. H.; Bergman, R. G.; Hermann, W. A.; Pettit, R. Organometallics 1982, 1, 1200.

(18) Gelius, U. Phys. Scr. 1974, 9, 133.

(19) Estimated from the Slater exponents of the valence shell orbitals.

(20) Baerends, E. J.; Ros, R. J. J. Electron Spectrosc. Relat. Phenom. 1975, 7, 69.

(21) Stevens, R. M.; Switkes, E. A.; Laws, E. A.; Lipscomb, W. N. J. Am. Chem. Soc. 1971, 93, 2603.

(22) Davis, D. W.; Shirley, D. A. J. Electron Spectrosc. Relat. Phenom. 1974, 3, 137.

(23) Jolly, W. L. In "Electron Spectroscopy: Theory, Techniques, and Applications"; Brundle, C. R.; Baker, A. D., Eds.; Academic Press: London, 1977; Vol. I, pp 119-149.

(24) Sherwood, P. A. M. J. Chem. Soc., Faraday Trans. 2 1976, 72, 1791, 1805.

(25) Bastiansen, O.; Fritsch, F. N.; Hedberg, K. Acta Crystallogr. 1964, 17, 538.

(26) Davis, M. I.; Speed, C. S. J. Organomet. Chem. 1970, 21, 401.

(27) Beagley, B.; Cruichshank, D. W. J. Acta Crystallogr., Sect. B. 1969, B25, 737.

Table VI.1. Core Binding Energies (eV) of $Fe(CO)_4L$ Compounds

	Fe $2p_{3/2}$		C 1s		O 1s	
L	E_B	fwhm	E_B	fwhm	E_B	fwhm
CO[a]	715.79(4)	1.25(9)	293.71(5)	1.27(13)	539.96(2)	1.38(5)
ethylene	715.40(2)	1.39(7)	293.53(3)[b]	1.41(7)	539.81(2)	1.62(7)
			290.32(3)[c]	1.32(11)		
acrolein	715.63(2)	1.31(6)	293.63(3)[d]	1.65(9)	539.97(3)	1.57(7)
			290.44(3)[c]	1.30(10)	537.20(6)[e]	1.32(22)
methyl acrylate	715.44(3)	1.37(9)	293.49(4)[f]	2.14(13)	539.61(2)[g]	1.76(6)
			290.34(4)[c]	1.37(12)	537.20(6)[e]	1.43(27)
dimethyl maleate	715.42(2)	1.35(7)	293.59(8)[f]	2.61(21)	539.56(4)[g]	1.83(15)
			290.52(10)[c]	1.27(35)	537.37(5)[e]	1.25(15)
trans-1,2-dichloro-ethylene	715.62(2)	1.28(6)	293.83(3)	1.49(7)	540.13(2)	1.48(5)
			291.57(3)[c]	1.26(8)		

(continued on next page)

Table VI.1. (continued)

L	Fe $2_{p3/2}$		C 1s		O 1s	
	E_B	fwhm	E_B	fwhm	E_B	fwhm
1,1-dicloro-ethylene	715.63(2)	1.28(5)	293.78(4)[b]	1.36(12)	540.10(2)	1.50(6)
			292.73(9)[j]	1.22(15)		
			290.36(4)[i]	1.24(14)		
pyridine	714.64(4)	1.39(12)	291.92(3)[j]	2.84(43)	538.82(2)	1.72(16)
trimethyl-phosphine	714.74(2)	1.25(6)	292.42(5)[b]	1.66(15)	538.81(2)	1.52(7)
			290.77(4)[k]	1.16(11)		

[a] Chen, H. W.; Jolly, W. L.; Kopf, J.; Lee, T. H. J. Am. Chem. Soc. 1979, 101, 2607. [b] Metal carbonyl carbon. [c] Olefin carbon. [d] Metal carbonyl and organic carbon. [e] Organic carbonyl oxygen. [f] Metal carbonyl, organic carbonyl, and methoxy carbon. [g] Metal carbonyl and methoxy oxygen. [h] CCl_2 carbon of olefin. [i] CH_2 carbon of olefin. [j] All carbons. [k] Methyl carbons.

Table VI.2 Calculated Atomic Charges in $Fe(CO)_4C_2H_4$

	using $\Delta ER(CH_2)$	using $1/2\Delta ER(CH_2)$	assuming $\Delta ER(CH_2) = 0$
q_{Fe}	+1.15	+1.16	+1.17
$q_{C(CO)}$	+0.16	+0.16	+0.16
q_O	-0.38	-0.38	-0.38
$q_{C(CH2)}$	-0.26	-0.31	-0.36
q_H	+0.06	+0.08	+0.10

Table VI.3. Experimental Ionization Potentials and Calculated LOIPs (eV) of $Fe(CO)_4L$ Compounds

L	$d_{x^2-y^2}$, d_{xy}			d_{xz}, d_{yz}		
	IP[a]	LOIP	IP - LOIP	IP	LOIP	IP - LOIP
CO	8.6	(8.6)	0.0	9.9	(9.9)	0.0
ethylene	8.38	8.3	0.1	9.23	9.6	-0.4
acrolein	8.69	8.5	0.2	9.42	9.8	-0.4
methyl acrylate	8.50	8.3	0.2	9.28	9.6	-0.3
dimethyl maleate	8.68	8.3	0.4	9.31	9.6	-0.3
trans-1,2-dichloroethylene	8.72	8.5	0.2	9.49	9.8	-0.3
1,1-dichloroethylene	8.82	8.5	0.3	9.51	9.8	-0.3
pyridine	7.65	7.7	0.0	8.65	9.0	-0.4
trimethylphosphine	7.77	7.8	0.0	8.85	9.1	-0.3

[a] Ionization potential data from Ref. 7 and Ref. 8.

Table VI.4. Experimental Ionization Potentials and Calculated LOIPs (eV) of the C=C π Orbital in $Fe(CO)_4$-Olefin Compounds

olefin	E_B(C 1s) of the free ligand[a]	IP of the free ligand[b]	IP of the complex[b]	LOIP	IP(complex) - LOIP
ethylene	290.88	10.51	10.56	10.1	0.5
acrolein	291.32	10.94	10.76	10.2	0.5
methyl acrylate	290.99	10.74	10.80	10.2	0.6
trans-1,2-dichloro-ethylene	292.41	9.8	9.7-9.9	9.1	0.7
1,1-dichloroethylene	292.28	9.96	9.98	9.4	0.6

[a] Binding energy data from: Jolly, W. L.; Bomben, K. D.; Eyermann, C. J. At. Nuc. Data Tables 1984, 31, 433. [b] Ref. 7.

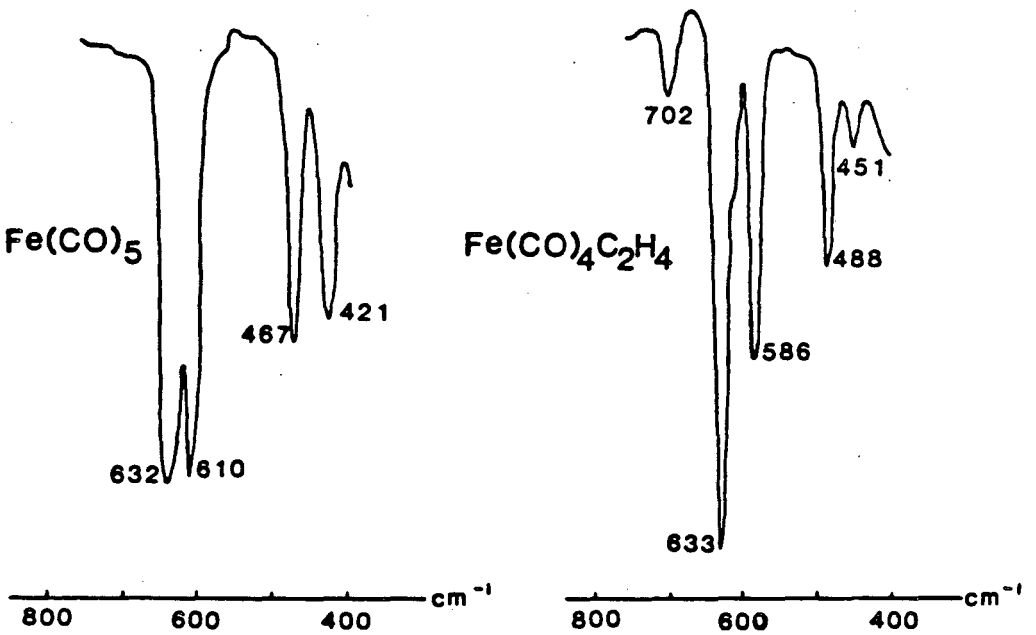

Figure 6.1. Metal-ligand stretch region of the infrared spectra of $Fe(CO)_5$ and $Fe(CO)_4C_2H_4$.

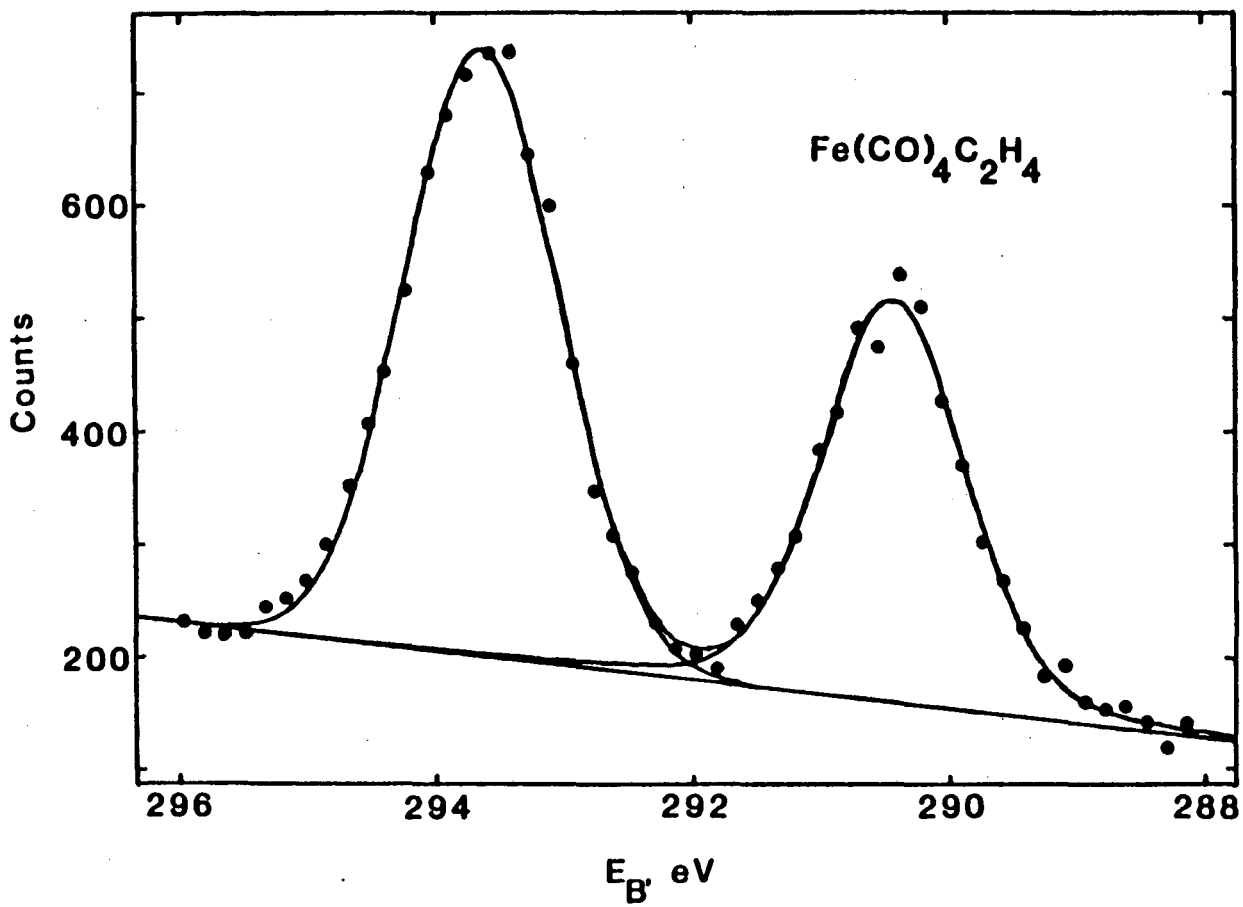

Figure 6.2. Carbon 1s spectrum of tetracarbonyl(ethylene)iron.

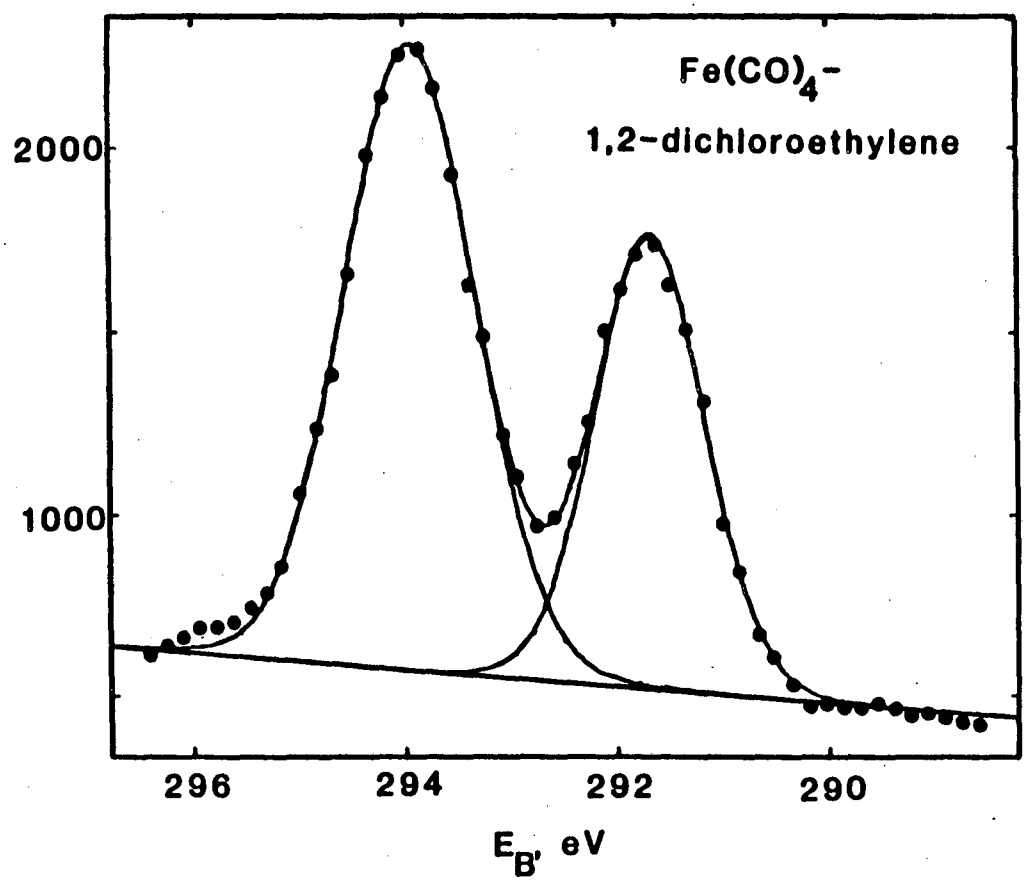

Figure 6.3. Carbon 1s spectrum of tetracarbonyl(1,2-dichloroethylene)iron.

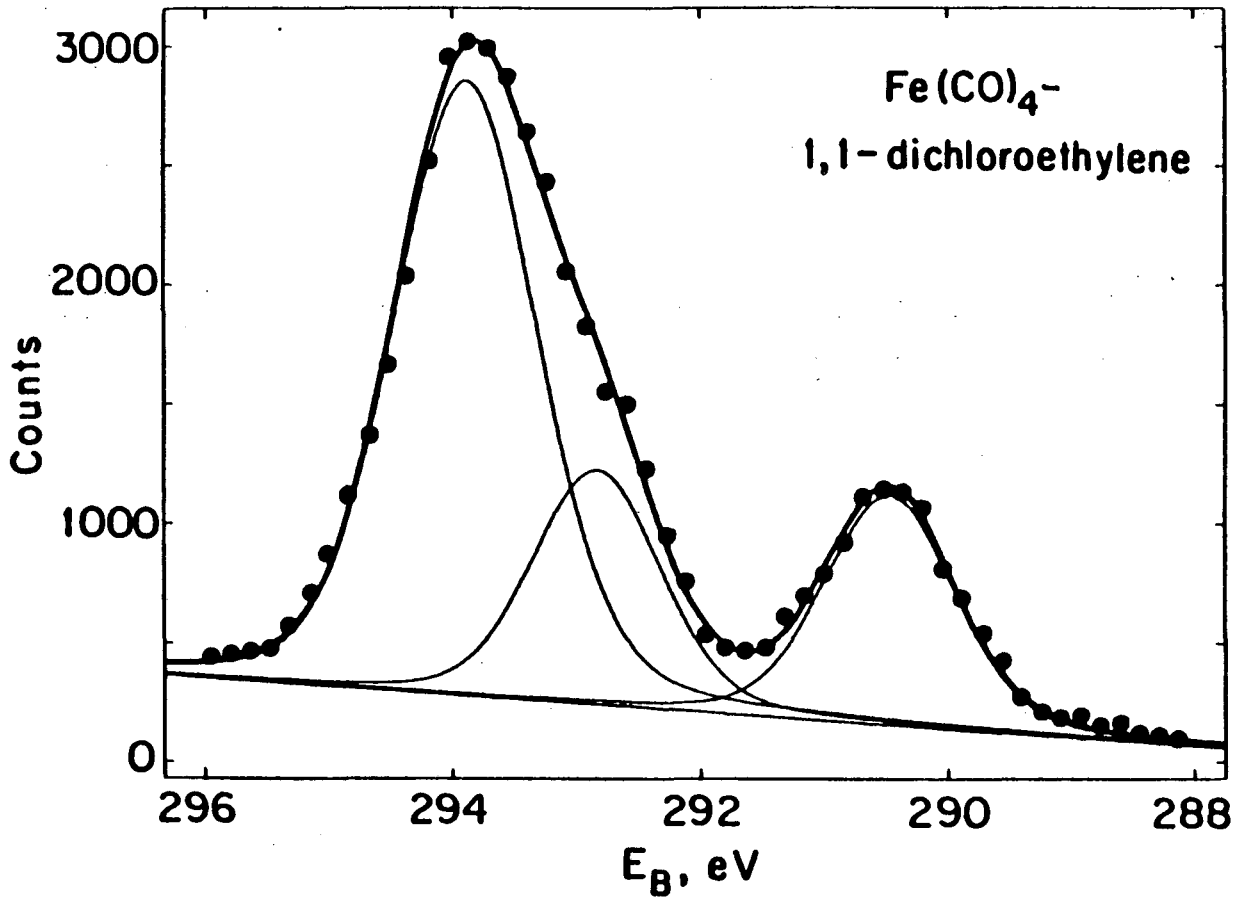

Figure 6.4. Carbon 1s spectrum of tetracarbonyl(1,1-dichloroethylene)iron.

CHAPTER VII. A PHOTOELECTRON SPECTROSCOPIC STUDY OF TRANSITION METAL-ISOCYANIDE COMPLEXES

A. Introduction

Considerable research has been done in recent years on the chemistry of transition metal-isocyanide complexes. The chemistry of transition metal-isocyanide complexes through 1969 has been reviewed by Malatesta and Bonati.[1] Subsequent developments in the field have been reviewed by Treichel[2] in 1973 and by Singleton and Oosthuizen[3] in 1983. The subject of zero-valent isocyanide complexes has been reviewed by Yamamoto[4] in 1980.

In spite of the activity in this field, the details of the bonding in these compounds have received relatively little attention. Sarapu and Fenske have published an approximate molecular orbital study of transition metal-isocyanide bonding,[5] and a structural study of $Mn(CO)_3(CNCH_3)_2Br$[6] in which they concluded that the metal-isocyanide bond had significant multiple bond character.

The only previously reported gas-phase UPS spectra of isocyanide complexes of transition metals were the He(I) spectra of $Cr(CO)_5CNCH_3$,[7] $Mn(CO)_4CNCH_3Br$,[8] and several iron tetracarbonyl isocyanide complexes.[9] The valence[10,11] and core[12] spectra of several free isocyanides have been reported.

In order to better understand the interaction of metal and isocyanide orbitals on bond formation, this Chapter describes studies of the X-ray photoelectron spectra of free

isocyanides, combined core and valence photoelectron studies of iron tetracarbonyl isocyanide complexes, and X-ray photoelectron studies of the novel isocyanide $CNCF_3$[13] and its transition metal complexes.[14] The transition metal complexes studied in this Chapter are all monosubstituted metal carbonyls. By studying the changes caused by the substitution of a CO ligand by a CNR ligand, one can obtain direct information about relative bonding properties of CO and CNR.

B. Experimental

1. Preparation of Compounds

Methyl isocyanide was prepared by the dehydration of N-methyl formamide,[15] and was purified by reduced pressure fractional distillation. Phenyl and t-butyl isocyanide were prepared from aniline and t-butyl amine using the modified Hoffmann carbylamine synthesis of Ugi et al.[16] Both isocyanides were purified by fractional distillation at reduced pressure. Trimethylsilyl cyanide was prepared by the reaction of $(CH_3)_3SiBr$ and AgCN,[17] and was purified by distillation at atmospheric pressure.

The iron tetracarbonyl complexes of methyl, t-butyl, trimethylsilyl, and phenyl isocyanide were prepared by condensing $Fe(CO)_5$ and the appropriate isocyanide (or cyanide) into a heavy-walled reaction tube which was sealed under vacuum.[18-20] The tubes were held at 70°C for 24h. Tetracarbonyl(methyl isocyanide) iron was purified by fractional

condensation on the vacuum line, with the desired product collected in a 0°C trap. The other products were purified by sublimation, and the melting points and infrared spectra of all of the products agreed with the literature.[1]

Pentacarbonyl(methyl isocyanide) chromium was prepared by the reaction of $[N(CH_3CH_2)_4][Cr(CO)_5I]$ with $[(CH_3CH_2)_3O][BF_4]$ in the presence of $CNCH_3$.[21] The compound was purified by sublimation, and its melting point, 68°C, agreed with the literature value.[22]

Trifluoromethyl isocyanide was prepared by the reduction of CF_3NCCl_2 over Mg.[13] The vapor pressure at -126°C (methylcyclohexane slush) was 66.1 mm and did not vary with the quantity of sample vaporized. The infrared spectrum agreed with the literature.[13]

The chromium and tungsten pentacarbonyl adducts of trifluoromethyl isocyanide[14] were prepared by Dr. D. Lentz, and were used without further purification.

2. Obtaining X-ray Photoelectron Spectra

The flow of vapor into the spectrometer from all of the free isocyanides was regulated using a micrometer type needle valve. Trifluoromethyl isocyanide was held at -126°C (methylcyclohexane slush) during data collection to prevent polymerization. The organometallic compounds were sublimed directly into the the spectrometer through the large diameter inlet system. Flow of vapor into the spectrometer was regulated by cooling the samples held in an exterior sample reservoir. The following temperatures were used: $Fe(CO)_4$-

$CNCH_3$, -10°C; $Fe(CO)_4CNC(CH_3)_3$, 0°C; $Fe(CO)_4CNSi(CH_3)_3$, 0°C; $Fe(CO)_4CNC_6H_5$, 25°C; $Cr(CO)_5CNCH_3$, 25°C; $Cr(CO)_5CNCF_3$, 10°C; $W(CO)_5CNCF_3$, 10°C.

C. Results and Discussion

1. Core Binding Energies

i) Free Isocyanides

The core binding energies of methyl, t-butyl, phenyl, and trifluoromethyl isocyanide are given in Table VII.1.

The deconvoluted C 1s spectra of methyl, t-butyl, and phenyl isocyanide are shown in Figures 7.1-7.3. The C 1s spectrum of methyl isocyanide (Figure 7.1) shows an unusual two-peak line shape. This is due to the difference in the half-width of the two peaks, with the the peak due to the isocyano carbon being broader than the methyl carbon peak. The peak due to the isocyano carbon of $CNCF_3$, which is well resolved, is significantly broader than the peak due to the trifluoromethyl carbon, indicating greater vibrational broadening for the ionization of an isocyano carbon. This is consistent with a large change in the equilibrium geometry when the carbon atom of the isocyano group undergoes core ionization:

$$CH_3-\overset{+}{N}\equiv\overset{-}{C} \xrightarrow{h\nu} [\ CH_3-\overset{+}{N}\equiv N \longleftrightarrow \overset{+}{H}CH_2=\overset{+}{N}=\overset{-}{N}\ ]$$

The C 1s spectrum of t-butyl isocyanide (Figure 7.2) was deconvoluted into three peaks of intensity 1:1:3. Clearly, the peak at lowest binding energy is due to the three methyl carbons. Because a methyl group is more elec-

tron releasing than a hydrogen atom, it would be reasonable to assume that the peak due to the isocyano carbon of t-butyl isocyanide would be at lower binding energy than the peak due to the isocyano carbon of methyl isocyanide, so the peak at 291.83 eV is assigned to the isocyano carbon, leaving the peak at 292.84 eV as the peak due to the carbon atom attached to the nitrogen atom of the isocyano group.

The C 1s spectrum of phenyl isocyanide (Figure 7.3) was deconvoluted into three peaks of intensity 1:1:5. The peak at lowest binding energy is the peak due to five of the carbons of the phenyl ring, and we are left with a choice of assignments for the other two peaks. Because of the similarities in the inductive effect of a phenyl group and a methyl group, we have assigned the peak at 292.53 eV to the isocyano carbon by analogy to methyl isocyanide. This leaves the the peak at 291.84 eV as the peak due to the phenyl ring carbon attached to the nitrogen atom of the isocyano group.

The N 1s binding energies also reflect the difference in the inductive effect of the methyl, t-butyl, and phenyl groups of the isocyanides. The N 1s binding energy of t-butyl isocyanide is 0.62 eV lower than the N 1s binding energy of methyl isocyanide, while the binding energy for phenyl isocyanide is only 0.17 eV lower, again indicative of the electron releasing ability of the methyl groups of t-butyl isocyanide and the similarity of the inductive effect

of methyl and phenyl groups.

ii) Iron Tetracarbonyl Isocyanide Complexes

The core binding energies of the iron tetracarbonyl complexes of methyl, t-butyl, trimethylsilyl, and phenyl isocyanide and iron pentacarbonyl are given in Table VII.2.

The fact that the Fe $2p_{3/2}$ binding energies of the isocyanide complexes are almost 1 eV lower than that of $Fe(CO)_5$ indicates a large decrease in the positive charge on the iron atom when an axial CO group is replaced by an isocyanide. This charge decrease indicates that the net electron acceptor character of an isocyanide is considerably less than that of carbon monoxide. The magnitude of the decrease in Fe binding energy on going from $Fe(CO)_5$ to the isocyanide complexes is slightly less than that seen on going to $Fe(CO)_4P(CH_3)_3$ and $Fe(CO)_4NC_5H_5$,[23] indicating that isocyanides have acceptor properties slightly greater than those of trimethylphosphine and pyridine.

The C 1s spectra were not clearly resolved, and only limited meaningful deconvolution was possible. The C 1s spectrum of $Fe(CO)_4CNCH_3$ shows only one band, with a slight shoulder on the low binding energy side (Figure 7.4). Deconvolution of this band gave two peaks of relative intensity 5:1 at 292.9 and 292.2 eV, respectively, with an uncertainty of at least 0.1 eV in the peak positions. The peak at lower binding energy is reasonably assigned to the donor carbon atom of the isocyanide group, and the peak at higher binding energy is assigned to the methyl carbon atom and the

carbonyl groups. This assignment indicates that the binding energy of the donor carbon atom of the isocyanide group decreases only slightly on coordination and implies that the electron flow from the isocyanide ligand is balanced by a flow of electron density back into the isocyanide and by an increase in the relaxation energy. The carbon binding energy of the methyl group of the isocyanide decreases by about 0.5 eV on going from the free ligand to the complex, a reasonable change when one considers that the nitrogen atom to which it is attached decreases in binding energy by 0.7 eV. The binding energy of the carbonyl carbon atoms in $Fe(CO)_4CNCH_3$ is 0.8 eV lower than in $Fe(CO)_5$, because of the lower Fe charge (potential effect), and because of the lower negative charge on the CO groups (increased back-bonding to CO because of relatively weak back-bonding to the $CNCH_3$ ligand). In the case of the t-butyl and phenyl isocyanide complexes, two peaks of relative intensity 6:3 and 6:5, respectively, were observed in the C 1s spectra. In both cases, the four carbonyl carbons and the two carbons attached to the N atom of the isocyanide group formed one band, and the three methyl or five phenyl carbons formed the other band. The C 1s spectrum of $Fe(CO)_4CNSi(CH_3)_3$ showed two peaks of relative intensity 5:3, with the isocyano carbon underneath the CO carbon peak, and the three methyl carbons well resolved at lower binding energy.

In general, the O 1s binding energy decreases about 0.9

eV on going from $Fe(CO)_5$ to $Fe(CO)_4CNR$. This decrease can be interpreted in the same way as the carbonyl carbon binding energy, i.e., in terms of relatively weak back-bonding to the isocyanide ligands. The decrease in O 1s binding energy on going from $Fe(CO)_5$ to $Fe(CO)_4P(CH_3)_3$ and $Fe(CO)_4NC_5H_5$ is about 1.2 eV, again indicating that the isocyanides are slightly better pi acceptors than trimethylphosphine and pyridine.

The N 1s binding energy decreases on going form the free ligands to the complexes. This decrease may be partly due to an increase in relaxation energy on coordination, but it is probably mainly due to a flow of electron density from the iron atom to the isocyanide. When methyl isocyanide is coordinated by a BH_3 group to form BH_3CNCH_3 (in which we have previously found little net pi interaction),[24] the N 1s binding energy <u>increases</u> by 0.5 eV. Thus the <u>decrease</u> of 0.7 eV in the N 1s binding energy on going from $CNCH_3$ to $Fe(CO)_4CNCH_3$ is strong evidence for some back-bonding in the iron complex.

<u>iii) Chromium and Tungsten Pentacarbonyl Isocyanide Complexes</u>

The core binding energies of the pentacarbonyl(trifluoromethyl isocyanide) complexes of chromium and tungsten, pentacarbonyl(methyl isocyanide)chromium, and chromium and tungsten hexacarbonyl are given in Table VII.3.

The binding energy of all of the atoms of the $CNCF_3$ ligand are lower in the chromium and tungsten complexes than

in the free ligand. In the case of the carbon atom of the isocyanide, this might have been expected because of an increase in relaxation energy associated with coordination by a polarizable $M(CO)_5$ fragment, but the marked decreases in the binding energies of the other atoms of the $CNCF_3$ ligand constitute clear evidence for very strong back-bonding in these complexes. The decrease of 2.2 eV in the N 1s binding energy on coordination suggests that the nitrogen atom may be aquiring significant lone pair character:

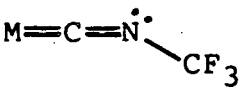

Recent electron diffraction studies[25] show that the C-N-C angle is 142° in the $CNCF_3$ ligand of $Cr(CO)_5CNCF_3$, consistent with the formation of a lone pair on nitrogen. The decrease of more than 1 eV in the F 1s binding enrgies on coordination indicates that part of the back bonding may also be due to hyperconjugation as represented by the structure:

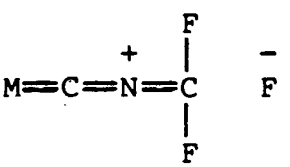

The N 1s data for $Cr(CO)_5CNCH_3$ provide more evidence that the N 1s binding energy is a reliable measure of back-bonding in isocyanide complexes. The N 1s binding energy of $Cr(CO)_5CNCH_3$ is 0.99 eV lower than $CNCH_3$, and 0.27 eV lower than $Fe(CO)_4CNCH_3$. Due to the lower nuclear charge of the chromium atom, there should be more back-bonding in the

chromium complex than in the iron complex, hence the lower N 1s binding energy of the isocyanide ligand. (The C 1s and O 1s binding energies of $Cr(CO)_6$ and $Fe(CO)_5$ also reflect this trend.) The decrease in N 1s binding energy on going from $CNCF_3$ to $M(CO)_5CNCF_3$ of more than 2 eV indicates that $CNCF_3$ is an extremely strong pi acceptor.

2. Comparison of the Bonding Properties of Methyl Isocyanide and Carbon Monoxide Using the LOIP Method

Using valence ionization potentials and core binding energies of $Fe(CO)_5$, $Fe(CO)_4CNCH_3$, CO and $CNCH_3$, the bonding properties of an isocyanide can be compared to carbon monoxide. The iron tetracarbonyl adduct of methyl isocyanide was chosen because all of the carbon binding energies are known, and methyl isocyanide is the simplest of the isocyanides.

The two lowest ionization potentials in $Fe(CO)_5$ and $Fe(CO)_4CNCH_3$ correspond to orbitals which are primarily Fe 3d atomic orbitals. The orbital that is primarily Fe $d_{x^2-y^2}$, d_{xy} in character (with significant σ^* Fe-CO character)[26] has the lower ionization potential and is assigned the symmetry designation e' in $Fe(CO)_5$ and e in $Fe(CO)_4CNCH_3$. The orbital of higher ionization potential is primarily Fe d_{xz}, d_{yz} in character, of e'' symmetry in $Fe(CO)_5$ and e symmetry in $Fe(CO)_4CNCH_3$. In order to compare the bonding characters of these orbitals in the complexes, it is necessary to use the Fe $2p_{3/2}$ binding energy difference to cor-

rect for decreased positive charge on the Fe atom and any change in the relaxation energy on going from $Fe(CO)_5$ to $Fe(CO)_4CNCH_3$. Eight-tenths of the Fe binding energy difference is 0.64 eV. When this quantity is subtracted from the ionization potentials of the e' and e'' orbitals of $Fe(CO)_5$, one obtains LOIP values that correspond to the ionization potentials that the e orbitals in $Fe(CO)_4CNCH_3$ would have if they had bonding character identical with that of the corresponding e' and e'' orbitals of $Fe(CO)_5$. When the calculated LOIP values are subtracted from the experimental ionization potentials of $Fe(CO)_4CNCH_3$, the magnitude and sign of the differences give a reliable measure of the change in bonding character of the metal orbitals caused by the substitution of a $CNCH_3$ ligand for a CO ligand. The results of these calculation for the metal orbitals of tetracarbonyl(methyl isocyanide)iron and the other iron tetracabony isocyanide complexes are presented in Table VII.4.

The metal orbitals of all of the isocyanide complexes are destabilized relative to $Fe(CO)_5$. This destabilization is probably due to interaction with a lower lying orbital of the same symmetry, in this case, the filled C-N pi bonding isocyanide orbital. In $CNCH_3$, the 2e C-N pi level (IP = 12.46 eV)[10] is energetically situated to have a much stronger interaction with the filled metal e orbitals than in CO 1π counterpart (IP = 16.91 eV).[10] In addition, the 2e orbital has greater electron density at the carbon atom than

does the CO 1π orbital.

This destabilization of the metal orbitals should be accompanied by a stabilization of the isocyanide C-N π orbital of the complex relative to the free isocyanide. In the case of $Fe(CO)_4CNCH_3$, the stabilization of the methyl isocyanide C-N π orbital can be determined, because the appropriate C 1s binding energies are known. This orbital is located mainly on the isocyano carbon and nitrogen atoms, so that the average of the C 1s and N 1s binding energy differences between $CNCH_3$ and $Fe(CO)_4CNCH_3$ should provide the necessary correction for differences in charge and relaxation energy. Eight-tenths of the average C-N binding energy difference is 0.37 eV, and when this amount is subtracted from the ionization potential of the free ligand, an LOIP of 12.1 eV is obtained. Comparison of the LOIP value with the observed C-N π ionization potential of $Fe(CO)_4CNCH_3$ indicates a stabilization of 0.8 eV. Although the C 1s binding energy of the isocyano carbon is not known with great certainty, we do not believe that it increases on coordination (the only result which could change the conclusion that this orbital is significantly stabilized on coordination). In previous X-ray photoelectron studies, we have always observed that the binding energies of all of the atoms in a ligand shift in the same direction when the ligand is coordinated to a metal atom. Because the N 1s binding energy of $CNCH_3$ decreases on forming $Fe(CO)_4CNCH_3$, it is reasonable

to assume that the isocyano C 1s binding energy also decreases. In either case, the C-N π orbital would be expected to have a larger contribution from the N 2p atomic orbitals than from the C 2p atomic orbitals, so that it would probably be acceptable to use only the N 1s binding energy when calculating the LOIP; such a calulation gives a stabilization of 1.0 eV for the C-N π orbital of the complex.

The filled orbital pi interactions that occur when an $Fe(CO)_4$ fragment bonds to a $CNCH_3$ ligand are shown in an energy level diagram in Figure 7.5. The metal orbital ionization potentials of $Fe(CO)_5$ are corrected for the differences in charge and relaxation energy on forming the isocyanide complex. Similarly, the C-N π oribital ionization potential of $CNCH_3$ is corrected for differences in charge and relaxation energy. Comparison of the LOIP values with the actual ionization potentials of the complex allows one to assess quantitatively the destabilization of the metal orbitals and the stabilization of the isocyanide C-N orbital. The equatorial metal orbital of $Fe(CO)_4CNCH_3$, which is Fe $d_{x^2-y^2}$, d_{xy} and M-CO σ in character, is destabilized less than the metal orbital which is d_{xz}, d_{yz} in character, as would be expected from the orientation of these orbitals relative to the axial isocyanide group. The amount of the destabilization of the d_{xz}, d_{yz} is 0.3 eV and is the same amount in all of the isocyanide complexes (Table VII.4). This is also the amount of destabilization observed

for this orbital in equatorially coordinated olefins, where the d_{xz}, d_{yz} orbital is orthogonal to the olefin π^* acceptor orbital.[23] Also, in our earlier study of the iron tetracarbonyl complexes of trimethylphosphine and pyridine, we concluded that these ligands were not acting as pi acceptors, because they caused a destabilization of 0.3 eV of the d_{xz}, d_{yz} orbital.

However, in this case, the destabilization cannot be taken as evidence that the isocyanides are not engaged in any back-bonding, because the observed destabilization may be the resultant of a stabilizing interaction with the π^* and an even greater destabilizing interaction with the π orbital. In view of the net electron acceptor character of the isocyanide group in $Fe(CO)_4CNR$ complexes as shown by the binding energy shifts, we believe that the isocyanides do act as pi acceptors, even in competition with carbon monoxide, but that the filled orbital pi interactions are relatively greater for isocyanides than for carbon monoxide. In this respect isocyanides are similar in their ligating properties to CS and NS, which Hubbard and Lichtenberger[27] have shown to have relatively strongly interacting filled pi orbitals.

Finally we consider the relative sigma bonding capabilities of isocyanides and carbon monoxide. Once again, this is only possible in the case $Fe(CO)_4CNCH_3$, for which we know the isocyano carbon binding energy. Using the isocyano

C 1s binding energy difference between $CNCH_3$ and $Fe(CO)_4$-$CNCH_3$, an LOIP of 11.1 eV is obtained for the carbon lone pair orbital of $CNCH_3$ in the complex. Comparison with the ionization potential of the Fe-CNR sigma orbital indicates a stabilization of 1.2 eV. An analogous calculation for CO in $Fe(CO)_4CNCH_3$ gives an LOIP of 11.4 eV for the CO carbon lone pair orbital in the complex. Comparison with the ionization energy of the Fe-CO sigma orbital is difficult because the bands due to the ionization of this orbital overlap bands due to the ionization of the CO π orbitals. These overlapping bands extend from 13 to 15 eV. If one conservatively choses an ionization potential on the low ionization potential side of this band, say 13.5 eV, for the ionization potential fo the Fe-CO sigma orbital, comparison with the LOIP value gives a lower limit for the stabilization of the CO lone pair orbital of 2.1 eV. A molecular orbital energy diagram illustrating the stabilization of the CO and $CNCH_3$ sigma lone pair orbitals in $Fe(CO)_4CNCH_3$ (corrected for potential and relaxation energy effects) is shown in Figure 7.6. This diagram graphically illustrates the greater net stabilization of the CO lone pair relative to the $CNCH_3$ lone pair.

The greater sigma donor character of CO relative to $CNCH_3$ in $Fe(CO)_4CNCH_3$ is undoubtedly a result of the sigma/pi synergism of the Fe-CO bond. The proton affinities of CO and $CNCH_3$ and our earlier study of borane adducts (Chapter V) indicate that, in non-transition metal com-

plexes, methyl isocyanide is a stronger sigma donor than carbon monoxide. Clearly, our results confirm the common picture of transition metal-carbonyl bonding, in which the removal of negative charge by the π^* orbitals of CO is so great that a very strong sigma bond is formed between the metal atom and carbon monoxide, a ligand generally thought of as a weak sigma donor.

Summary

The X-ray photoelectron spectra of free isocyanides, iron tetracarbonyl complexes of isocyanides, trifluoromethtyl isocyanide, and chromium and tungsten pentacarbonyl complexes of trifluoromethyl isocyanide were obtained. Analysis of the core binding energy data showed that isocyanides accept electron density from a metal atom in complexes, even in competition with CO, but that they accept less electron density than does a CO. Trifluoromethyl isocyanide was shown to be a strong pi acceptor ligand, comparable to CO. Use of the core binding energies of $Fe(CO)_4CNCH_3$ and $Fe(CO)_5$ allowed direct comparison of the bonding properties of $CNCH_3$ relative to CO. It was found that filled orbital pi repulsion is more significant for $CNCH_3$ than for CO, and that in $Fe(CO)_4CNCH_3$, CO is a stronger sigma donor than $CNCH_3$, presumably due to the sigma/pi synergism of the Fe-CO bond.

References

(1) Malatesta, L.; Bonati, F. "Isocyanide Complexes of Metals"; Wiley-Interscience: London, 1969.

(2) Treichel, P. Adv. Organomet. Chem. 1973, 11, 21.

(3) Singleton, E.; Oosthuizen, H. E. Ibid. 1983, 22, 209.

(4) Yamamoto, Y. Coord. Chem. Rev. 1980, 32, 193.

(5) Sarapu, A. C.; Fenske, R. F. Inorg. Chem 1975, 14, 247.

(6) Sarapu, A. C.; Fenske, R. F. Ibid. 1972, 11, 3021.

(7) Higginson, B. R.; Lloyd, D. R.; Burroughs, D. M.; Gibson, D. M.; Orchard, A. F. J. Chem. Soc. Faraday Trans. 2 1974, 70, 1418.

(8) Lichtenberger, D. L.; Sarapu, A. C.; Fenske, R. F. Inorg. Chem 1973, 12, 702.

(9) Beach, D. B.; Bertoncello, R.; Granozzi, G.; Jolly, W. L. Organometallics 1985, 3, 311.

(10) Turner, D. W.; Baker, C.; Baker, A. D.; Brundle, C. R. "Molecular Photoelectron Spectroscopy"; Wiley-Interscience: London, 1977.

(11) Young, V. Y.; Cheng, K. L. J. Electron Spectrosc. Relat. Phenom. 1976, 9, 317.

(12) Brant, P. Ibid, 1984, 33, 153.

(13) Lentz, D. J. Fluor. Chem. 1984, 24, 523.

(14) Lentz, D. Chem. Ber. 1984, 117, 415.

(15) Cassanova, J.; Schuster, R. E.; Werner, N. D. J. Chem. Soc. 1963, 4280.

(16) Weber, W. P.; Gokel, G. W.; Ugi, I. W. Angew. Chem., Int. Ed. Engl. 1972, 11, 530.

(17) McBride, J. J.; Beachell, H. C. J. Am. Chem. Soc. 1952, 74, 5247.

(18) Hieber, W.; von Pigenot, D. Chem. Ber. 1956, 89, 193.

(19) Seyferth, D.; Kahlen, N. J. Am. Chem. Soc. 1960, 82, 1080.

(20) Cotton, F. A.; Parish, R. V. J. Chem. Soc. 1960, 1440.

(21) Higginson, B. R.; Lloyd, D. R.; Burroughs, D. M.; Gibson, D. M.; Orchard, A. F. J. Chem. Soc. Faraday Trans. 2 1973, 69, 1659.

(22) Connor, J. A.; Jones, E. M.; McEwen, G. K.; Lloyd, M. K.; McCleverty, J. A. J. Chem. Soc. Dalton Trans. 1971, 12, 1246.

(23) Chapter VI.

(24) Chapter V.

(25) Oberhammer, H.; Lentz, D., private communication.

(26) Rossi, A. R.; Hoffmann, R. Inorg. Chem. 1975, 14, 365.

(27) Hubbard, J. L.; Lichtenberger, D. L. J. Chem. Phys. 1981, 75, 2560.

Table VII.1. Core Binding Energies (eV) of the Free Isocyanides

	C 1s		N 1s	
	E_B	fwhm	E_B	fwhm
$CNCH_3$	292.37(10)[a]	1.48(20)	406.67(4)	1.33(7)
	293.35(10)	1.30(20)		
$CNC(CH_3)_3$	291.83(16)[a]	1.55(20)	406.05(2)	1.13(9)
	292.84(8)[b]	1.33(14)		
	291.06(3)	1.20(9)		
CNC_6H_5	292.53(6)[a]	1.35(15)	406.50(2)	1.24(6)
	291.84(8)[b]	1.10(20)		
	290.84(3)	1.26(8)		
$CNCF_3$[c]	294.28(4)[a]	1.74(15)	407.97(3)	1.26(7)
	301.35(3)	1.27(10)		

[a] Isocyano carbon. [b] Other carbon atom attached to nitrogen. [c] F 1s binding energy: 695.53(3), fwhm 1.83(8)

Table VII.2. Core Binding Energies of Iron Tetracarbonyl Isocyanide Complexes and Related Compounds

	Fe $2p_{3/2}$		C 1s	
	E_B	fwhm	E_B	fwhm
$Fe(CO)_4CNCH_3$	714.98(4)	1.40(12)	292.83(3)[a]	1.88(10)
$Fe(CO)_4CNC(CH_3)_3$	714.81(2)	1.37(7)	292.53(7)	1.85(15)
			291.05(7)[b]	1.21(14)
$Fe(CO)_4CNSi(CH_3)_3$[c]	714.84(2)	1.34(8)	292.52(3)	1.73(10)
			290.40(3)[b]	1.65(12)
$Fe(CO)_4CNC_6H_5$	714.85(2)	1.29(6)	292.50(3)	1.61(8)
			290.79(3)[d]	1.29(7)
$Fe(CO)_5$[e]	715.79(4)	1.25(9)	293.71(5)	1.27(13)
	O 1s		N 1s	
$Fe(CO)_4CNCH_3$	539.14(5)	1.63(13)	405.95(4)	1.53(7)
$Fe(CO)_4CNC(CH_3)_3$	539.03(4)	1.81(16)	405.54(2)	1.45(8)
$Fe(CO)_4CNSi(CH_3)_3$	539.03(2)	1.65(6)	404.88(4)	1.35(9)
$Fe(CO)_4CNC_6H_5$	539.05(2)	1.54(6)	406.02(3)	1.33(8)
$Fe(CO)_5$	539.96(2)	1.38(5)		

[a] All carbon (see text). [b] Methyl carbon. [c] Si 2p binding energy: 107.59(3), fwhm 1.61(10). [d] Phenyl carbon. [e] All data from: Jolly, W. L.; Bomben, K. D.; Eyermann, C. J. At. Nucl. Data Tables 1984, 31, 433.

Table VII.3. Core Binding Energies (eV) of $Cr(CO)_5CNCF_3$, $W(CO)_5CNCF_3$, and Related Compounds

	Metal		C 1s	
	E_B	fwhm	E_B	fwhm
$Cr(CO)_5CNCF_3$[a]	581.74(2)[b]	1.25(8)	292.89(2) 299.09(7)[c]	1.58(6) 3.30(46)
$W(CO)_5CNCF_3$[d]	37.72(3)[e]	1.23(6)	292.95(2) 299.13(10)[c]	1.50(10) 2.97(44)
$Cr(CO)_5CNCH_3$	581.20(2)[b]	1.19(9)	292.51(3)[f]	1.74(10)
$Cr(CO)_6$[g]	581.87b		293.21	
$W(CO)_6$[g]	37.84e		293.15	

	O 1s		N 1s	
$Cr(CO)_5CNCF_3$	539.49(2)	1.57(5)	405.73(4)	1.56(9)
$W(CO)_5CNCF_3$	539.43(3)	1.54(9)	405.62(6)	1.50(16)
$Cr(CO)_5CNCH_3$	538.85(2)	1.59(7)	405.68(5)	1.58(18)
$Cr(CO)_6$	539.49			
$W(CO)_6$	539.27			

[a] F 1s binding energy: 694.40(2), fwhm 1.95(5). [b] Cr $2p_{3/2}$. [c] CF_3 carbon + CO shake up. [d] F 1s binding energy: 694.49(2), fwhm 2.00(6). [e] W $4f_{7/2}$. [f] All carbon. [g] Data from: Jolly, W. L.; Bomben, K. D.; Eyermann, C. J. At. Nucl. Data Tables 1984, 31, 433.

Table VII.4. Experimental Ionization Potentials (eV) and Calculated LOIPs of the Metal Orbitals of Iron Tetracarbonyl Isocyanide Complexes

	$d_{x^2-y^2}$, d_{xy}		
	IP[a]	LOIP	IP - LOIP
$Fe(CO)_5$	8.53	(8.53)	0.0
$Fe(CO)_4CNCH_3$	7.68	7.88	-0.20
$Fe(CO)_4CNC(CH_3)_3$	7.58	7.75	-0.17
$Fe(CO)_4CNSi(CH_3)_3$	7.60	7.77	-0.17
$Fe(CO)_4CNC_6H_5$	7.63	7.78	-0.15
	d_{xz}, d_{yz}		
	IP	LOIP	IP - LOIP
$Fe(CO)_5$	9.85	(9.85)	0.0
$Fe(CO)_4CNCH_3$	8.89	9.20	-0.31
$Fe(CO)_4CNC(CH_3)_3$	8.74	9.07	-0.33
$Fe(CO)_4CNSi(CH_3)_3$	8.74	9.09	-0.35
$Fe(CO)_4CNC_6H_5$	8.83	9.10	-0.27

[a] IP data from Ref. 9.

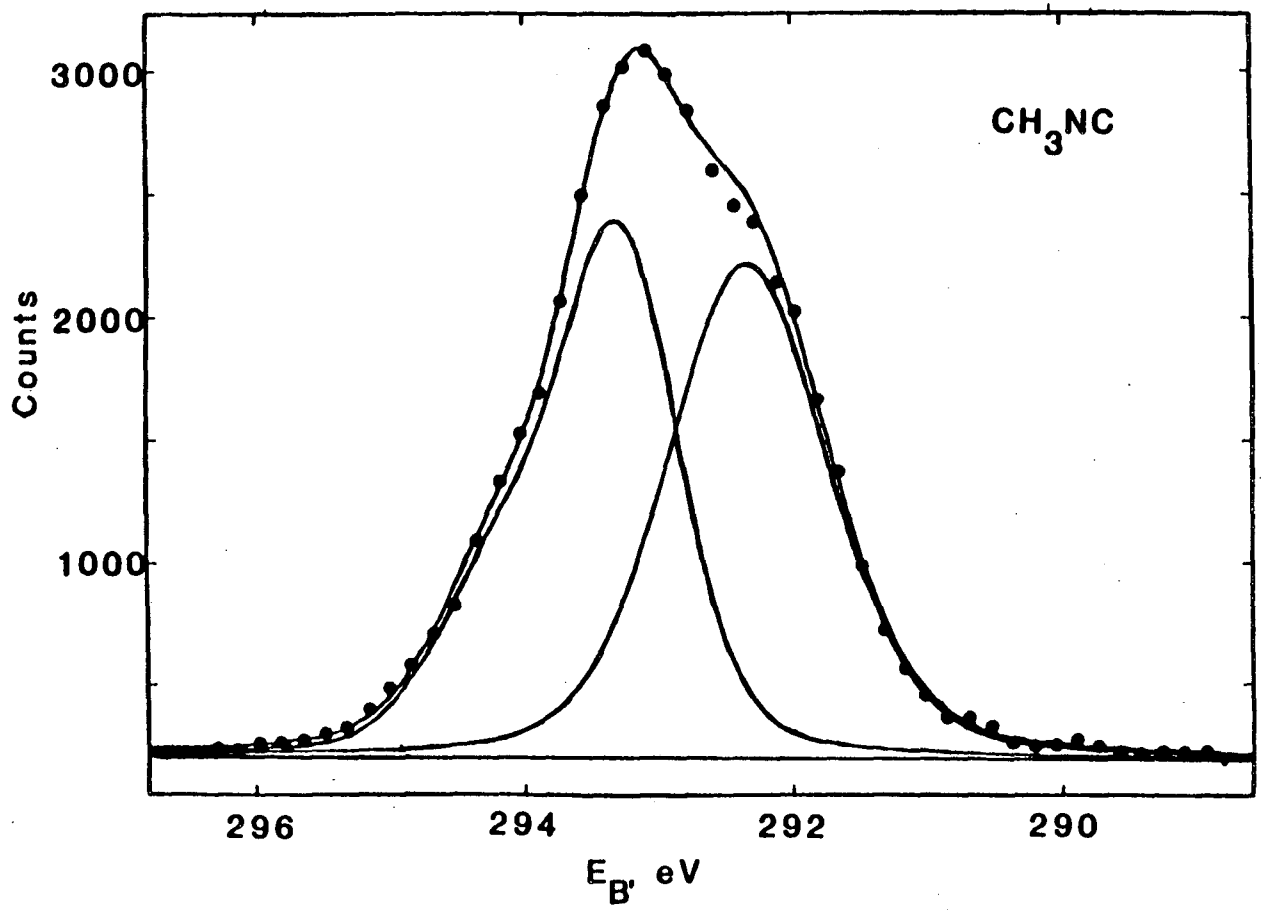

Figure 7.1. Carbon 1s spectrum of methyl isocyanide.

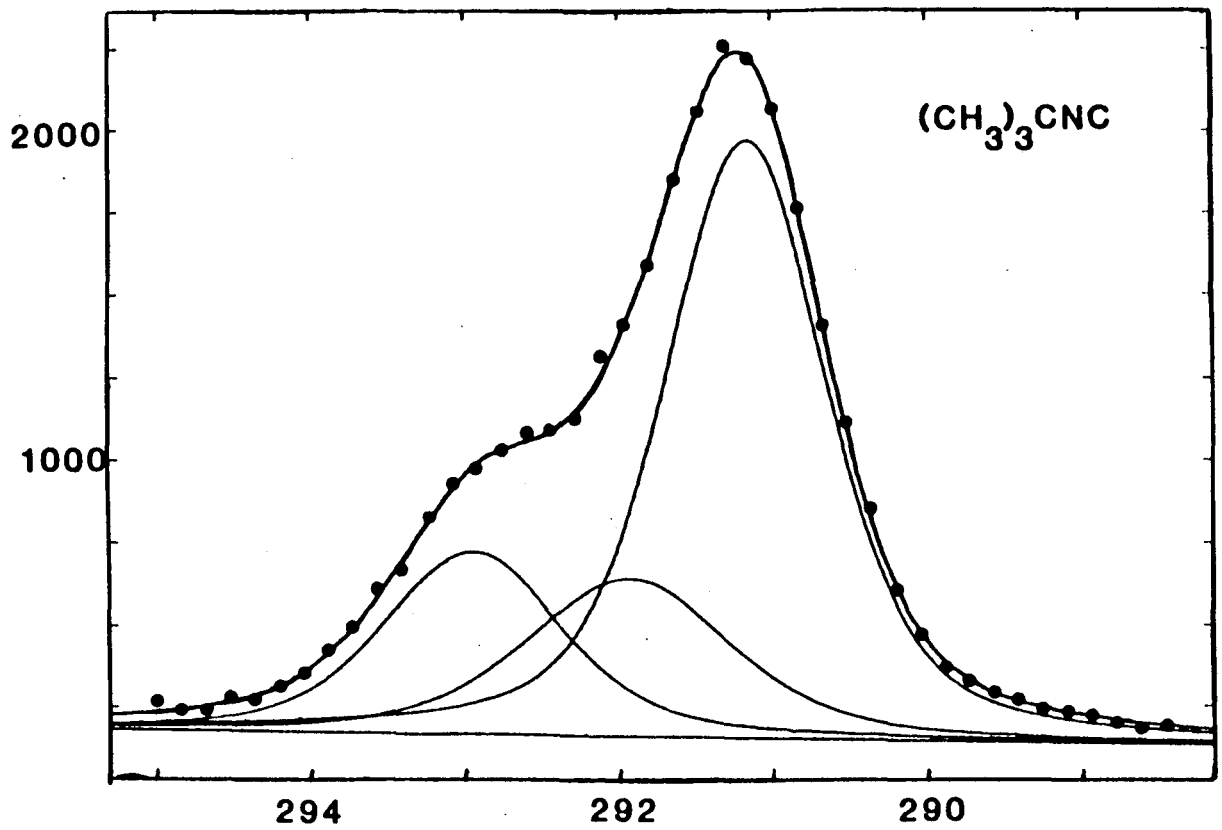

Figure 7.2. Carbon 1s spectrum of t-butyl isocyanide.

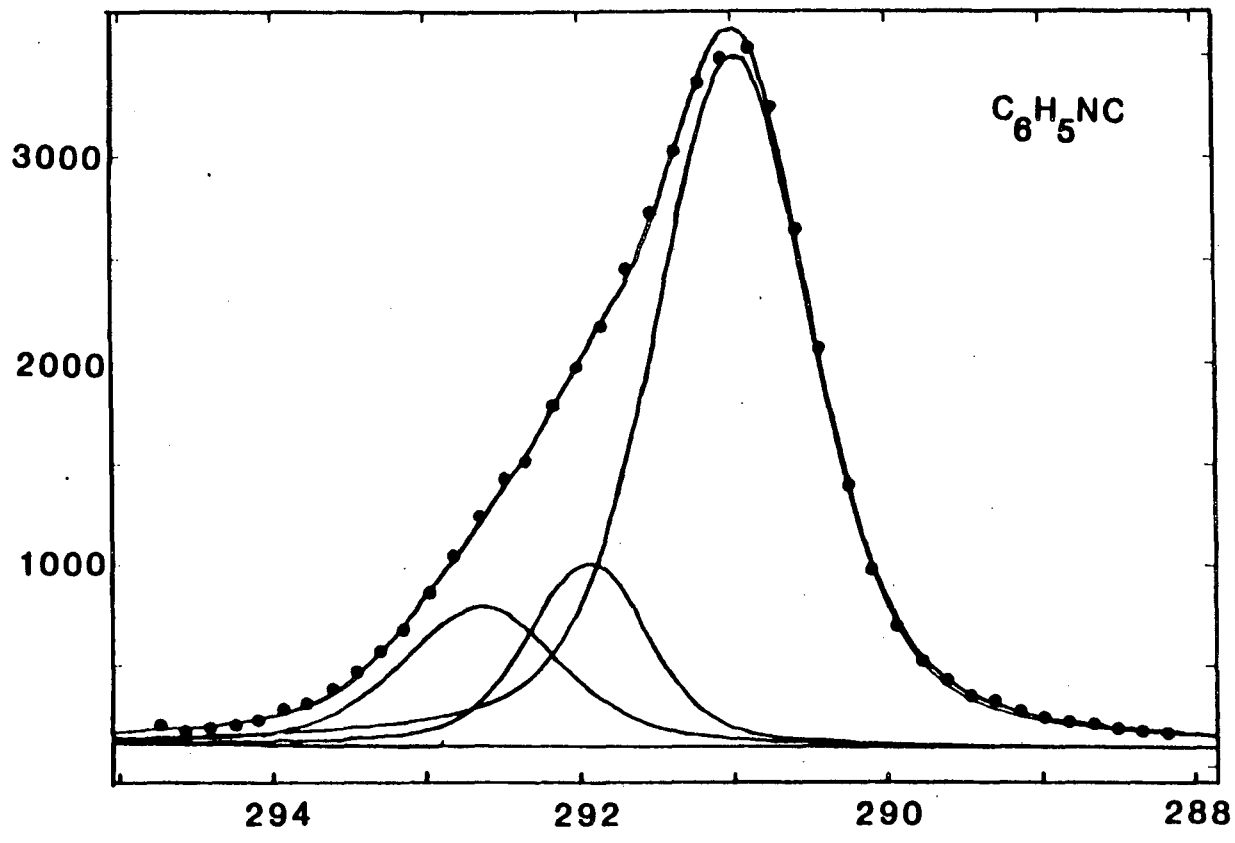

Figure 7.3. Carbon 1s spectrum of phenyl isocyanide.

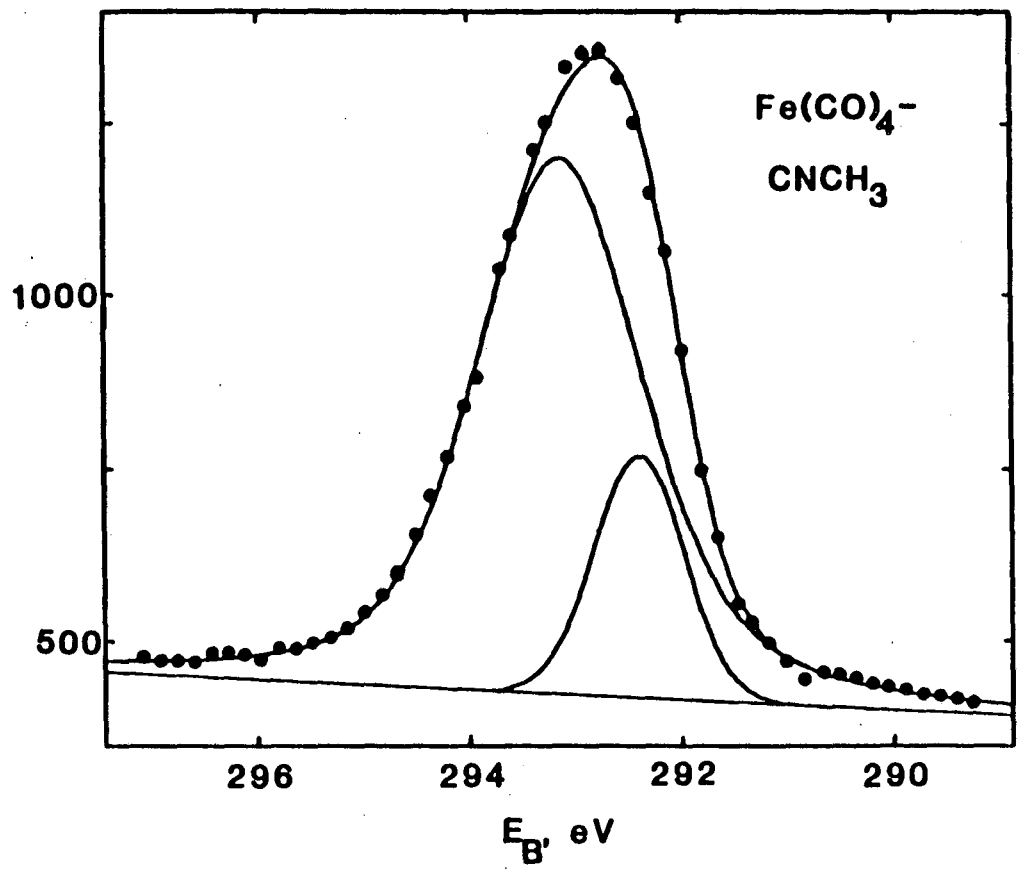

Figure 7.4. Carbon 1s spectrum of tetracarbonyl(methyl isocyanide)iron.

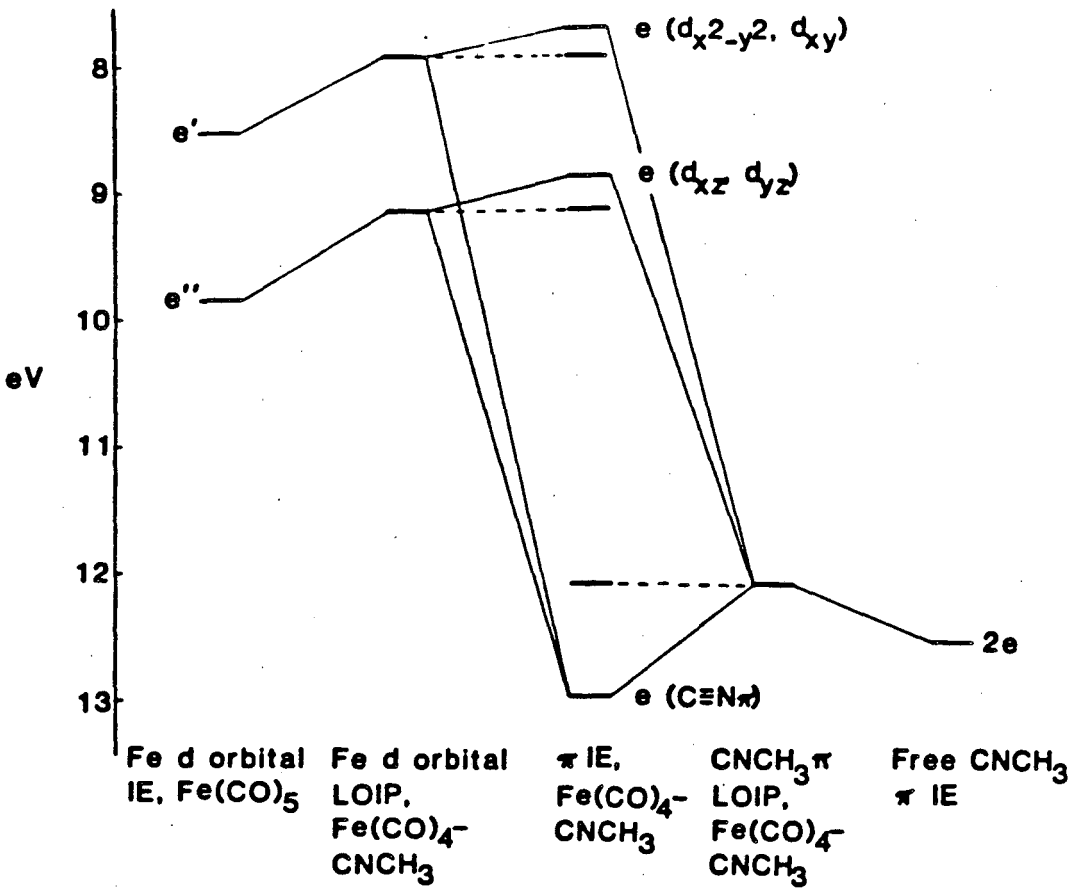

Figure 7.5. Pi orbital interactions in $Fe(CO)_4CNCH_3$.

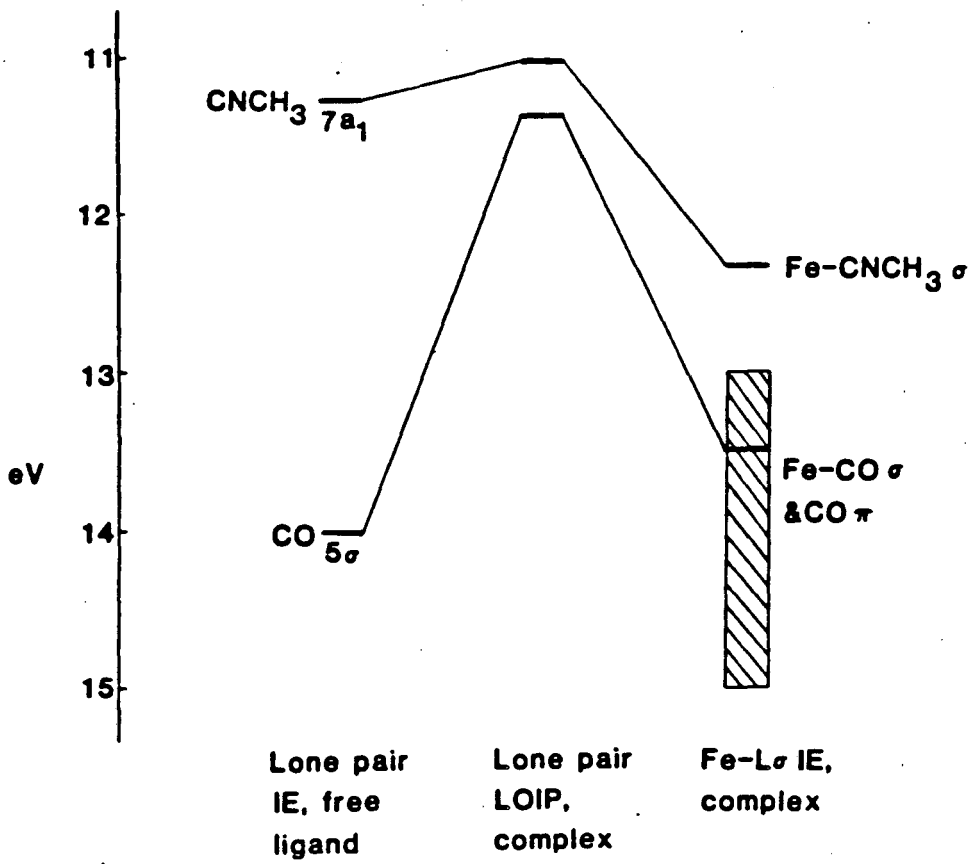

Figure 7.6. Sigma orbital interactions in $Fe(CO)_4CNCH_3$.

APPENDIX

Construction of a Heated Gas Cell for XPS

In order to expand the number of substances which could be studied in the gas-phase using XPS, a heated gas cell was constructed. Because the vast majority of organometallic compounds and some inorganic compounds are sensitive to oxygen and/or moisture, it was desirable to introduce the samples in a manner which would minimize their exposure to the atmosphere.

The heated gas cell is shown in Figure 1. The design is basically the gas cell supplied by McPherson with the addition of a sample reservoir and heater. The entire apparatus was constucted from stainless steel. The heater is a 42 w resistive heating element from a Weller soldering iron. The temperature was controlled using an Omega Series 4200 Temperature Controller. The tempertaure was measured at the base of the sample reservoir using a platinum resistor temperature sensor. The resistance of the sensor was used both to control the heater and provide a read-out of the temperature on a digital display. The desired temperature was set at the controller and the the flow of current was regulated by turning the heater off and on using a Triac. Over-shoot was minimized by decreasing the voltage applied to the heater with a Variac.

The calibrant gas inlet tube was insulated from the gas cell with a Teflon spacer. To prevent material from blocking the electron slit, the slit was made part of the gas

cell instead of part of the nose piece. The gas cell was insulated from the nose piece with a Teflon spacer.

The general procedure for using the heated cell was as follows. Thin all-glass sample bulbs were blown from 6-mm o.d. glass tubing. The sample bulbs were filled with sample in the glove box and evacuated and sealed on the vacuum line. The filled sample bulbs were placed in the sample reservoir, and the sample chamber was evacuated. After the X-ray tube had been outgassed, the sample bulb was broken by tightening the large screw on the side of the sample reservoir. In this way, relatively large amounts (several hundred milligrams) of sample could be introduced into the spectrometer with minimal decomposition. The temperature was raised slowly until a spectrum of the strongest line in the compound was observed. The controller was then set to this temperature and the spectra were run in the usual manner.

Thus far, the device has been tested on several organometallic compounds at temperatures as high as 110^{o}C with excellent results.

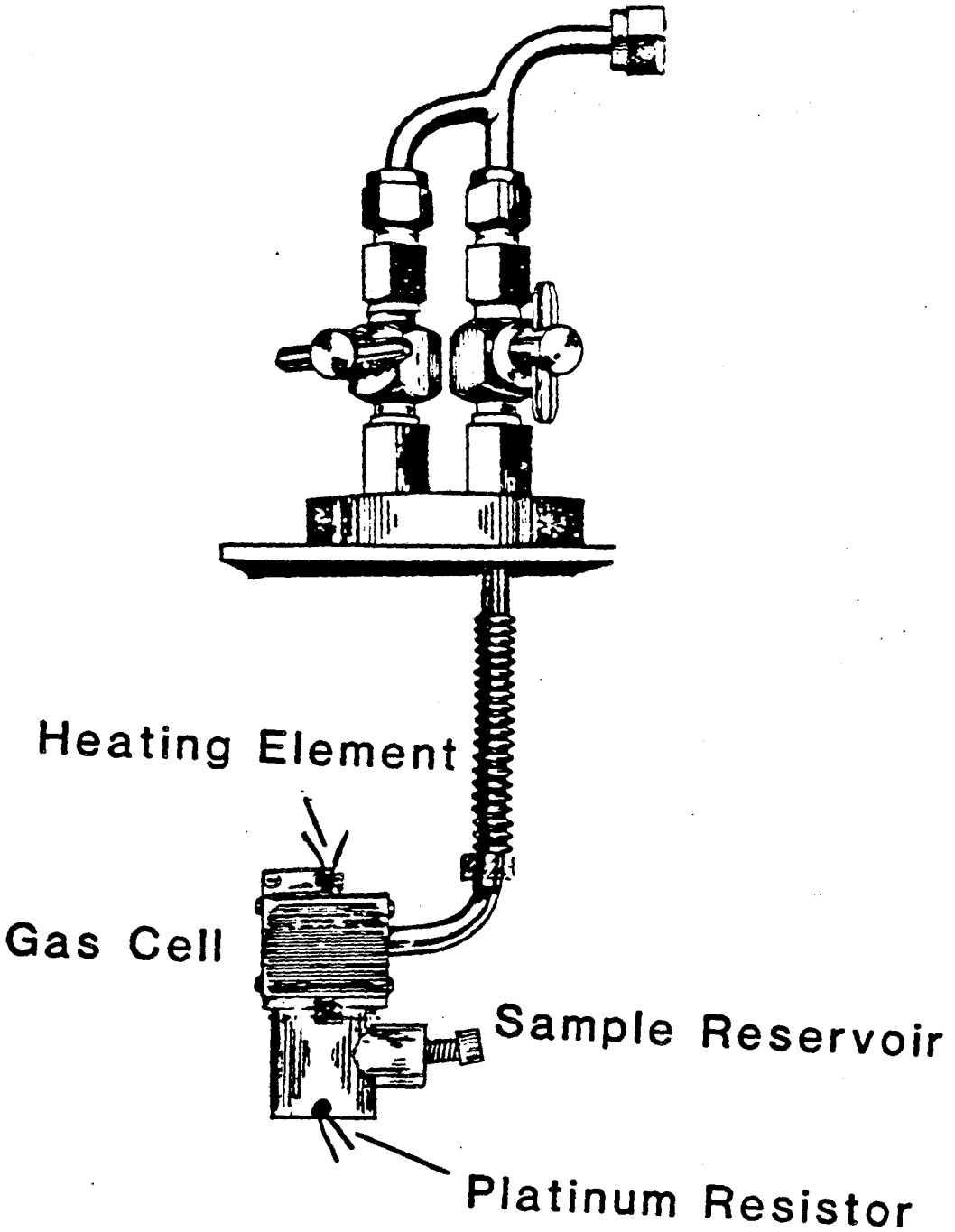

Figure 1. Heated gas cell.

This report was done with support from the Department of Energy. Any conclusions or opinions expressed in this report represent solely those of the author(s) and not necessarily those of The Regents of the University of California, the Lawrence Berkeley Laboratory or the Department of Energy.

Reference to a company or product name does not imply approval or recommendation of the product by the University of California or the U.S. Department of Energy to the exclusion of others that may be suitable.

TECHNICAL INFORMATION DEPARTMENT
LAWRENCE BERKELEY LABORATORY
UNIVERSITY OF CALIFORNIA
BERKELEY, CALIFORNIA 94720